INVESTIGATION OF THE ROLE OF THE K_{ATP} CHANNEL IN VASCULAR HYPOREACTIVITY IN SEPSIS

James Francis Buckley

A thesis submitted to University College London,

in part fulfilment for the degree of

DOCTOR OF PHILOSOPHY

Centre for Clinical Pharmacology

Department of Medicine

University College, London

July 2012

Declaration of Work

I, James Francis Buckley, confirm that the work presented in this thesis is my own. Where information has been derived from other sources, I confirm that this has been indicated in the thesis.

Abstract

The lack of responsiveness of vascular smooth muscle cells (VSMCs) to vasopressor catecholamines is termed vascular hyporeactivity. Vascular hyporeactivity is an important component of sepsis. ATP-sensitive potassium channels (K_{ATP}) play a fundamental role in vascular hyporeactivity in long-term (>20hrs) sepsis. These channels remain in the open state, leading to membrane hyperpolarisation and subsequent relaxation of VSMCs. However, the precise mechanism of K_{ATP} activation in sepsis has yet to be elucidated. Disruption of the actin cytoskeleton, the direct effect of nitric oxide and the metabolic state of the cell all activate K_{ATP} channels and are possibilities. Therefore, three hypotheses were investigated: 1). Disruption of the actin cytoskeleton alters K_{ATP} channel function 2). Nitric oxide exerts a direct effect on the K_{ATP} channel. 3). Metabolic derangement is responsible for altered K_{ATP} channel function.

Using confocal microscopy and biochemistry, it was demonstrated that the actin cytoskeleton of VSMCs was not disrupted in sepsis, and is therefore an unlikely mechanism for K_{ATP} channel activation. There was, however, a functional impairment of vascular function, indicating a lack of correlation between structure and function in the context of the model investigated. That NO has a direct effect on the K_{ATP} channel, and is subsequently responsible for its altered function in sepsis was also inconclusive. Finally, using HPLC techniques, no evidence to suggest that altered levels of adenosine nucleotide phosphates cause dysregulation of the K_{ATP} channel in either *in vitro* or *in vivo* models of sepsis (despite evidence of functional impairment) was observed.

Therefore, in the context of the models used, none of the afore-mentioned mechanisms were shown to be responsible for the altered K_{ATP} channel observed in vascular tissue in sepsis.

Commonly used Abbreviations

ABC	ATP-binding Cassette
ADP	adenosine 5’ diphosphate
AMP	adenosine 5’ monophosphate
AOI	area of interest
ATP	adenosine 5’ triphosphate
ATP_i / $[ATP]_I$	intracellular adenosine triphosphate
BKCa	large conductance calcium activated potassium channels
BSA	bovine serum albumin
cAMP	cyclic adenosine 3’, 5’ monophosphate
cGMP	cyclic guanosine 3’, 5’ monophosphate
CO_2	carbon dioxide
COX-2	cyclooxygenase-2
Deta NO	nitric oxide donor
DMEM	Dulbecco’s modified Eagle’s medium
DMSO	dimethylsulphoxide
F actin	filamentous actin
G actin	globular actin

GFP	green fluorescent protein
HBSS	Hanks Balanced Salt Solution
HEPES	hepes (4-(2hydroxyethyl) piperazine-1(4-(2-hydroxyethyl)-1-piperizineethanesulphonic acid)
HPLC	high performance liquid chromatography
hrs	hours
IC_{50}	half maximal inhibitory concentration
IL	interleukin
iNOS	inducible nitric oxide synthase
K^+	potassium
K_{ATP}	ATP sensitive K^+ channel
KCB	potassium channel blocker
KCL	potassium chloride
KCOs	potassium channel openers
kDa	kilodaltons
kg	kilograms
Kir	inwardly rectifying K^+ channel
K_{NDP}	NDP sensitive K^+ channel

K_V	voltage-gated K^+ channels
KZ method/technique	Kallman Z-stack acquisition method
LPS	lipopolysaccharide
LTA	lipoteichoic acid
mg	milligrams
Mg^{2+}	magnesium (divalent cation)
mins	minutes
ml	millilitres
MOF	multi-organ failure
mV	millivolts
NBFs	nucleotide binding folds
NDPs	nucleotide diphosphates
NFκB	nuclear factor kappa B
nM	nanomolar
NO	nitric oxide
NO synthase	nitric oxide synthase
NTPs	nucleotide triphosphates
PBS	phosphate buffered saline solution
PE	phenylephrine
pH	potential of hydrogen
PKA	protein kinase A

PNU37883A	4-morpholinecarboximide-N-1-adamantyl-N'-cyclohexylhydrochloride
pS	pico siemens
ROS	reactive oxygen species
SEM	standard error of the mean
SR	sarcoplasmic reticulum
SUR	sulphonylurea receptor subunit
TLR	toll-like receptors
TNFα	tumour necrosis factor α
uM	micromolar
VSM	vascular smooth muscle
W_A	walker A motif
W_B	walker B motif

Acknowledgements

I would like to give thanks to the following:

To my primary supervisors, Professor Lucie Clapp and Professor Mervyn Singer for their guidance, tolerance and patience throughout my studies;

Prof. Andy Tinker, Dr. Sue Hall and Dr. David Kelly for their help, support and advice with confocal microscopy. Dr. Rita Jabr, Dr. Andrew Wilson and Dr. Jon Giblin for their help with laboratory techniques, positive feedback and constructive criticism. Dr. Alain Rudiger for help with HPLC. Valerie Taylor and Raymond Stidwell for all of their help and hard work with the *in vivo* model;

To Drs Emilia Falcetti and Brian Tennant, previous members of the Clapp laboratory, for their friendship and advice;

To my long-suffering partner, Dr Tabasum Farzaneh, who has been a pillar of support and encouraged throughout;

Special thanks to the British Heart Foundation, who sponsored this work, and without whom this work would not have been possible.

Contents

List of Tables and Figures

Chapter One

Chapter Two

Chapter Three

Chapter Four

Chapter Five

Chapter One

Introduction

1.1 General introduction

Sepsis (derived from the Greek for decay) is an infection-induced syndrome currently responsible for approximately 10% of all deaths worldwide (Tsiotou, 2005). It is defined as a systemic response to infection, with an abnormal temperature (>38 ^{o}C or < 35 ^{o}C), deranged leukocyte count (> 12.10^{9} or < 4.10^{9} cells/ml). It was first coined as a separate clinical syndrome by Bone and colleagues in 1989 (Bone, 1989), and has an annual incidence of 51 per 100,000 population in the UK (Padkin, 2003). Despite decades of research, significant outcome improvements, particularly in the high mortality (40-60%) syndromes of shock (BP < 90 mmHg systolic or a drop of > 20 mmHg, despite adequate fluid resuscitation) and multi-organ failure (MOF: failure or more than two organ systems, i.e. cardiovascular, pulmonary, hepatic, renal or haematological) (Padkin, 2003; Brun-Buisson, 2004), have yet to be made. Numerous clinical trials have been conducted using agents that modulate inflammatory pathways; despite promising Phase II studies, these have generally failed to show any survival benefit (Angus, 2000; Eskandari, 1992; Petros, 1994).

A novel therapeutic target is the ATP-sensitive (K_{ATP}) potassium channel; a channel that is critical in the adaptive response to stress. Indeed, pharmacological opening of these channels (e.g. with nicorandil) is already used therapeutically to treat angina pectoris while inhibitors (e.g. glibenclamide) are used in type II diabetes. Excessive activation of the K_{ATP} channel is becoming increasingly recognised as a major cause of hypotension and vascular hyporeactivity to catecholamines in septic shock. This has led some researchers to advocate that blocking these channels will be beneficial in shock (Landry, 1992; Vanelli, 1995;

Salzman, 1997). However, recent advances in the K_{ATP} channel field could suggest otherwise (Warrillow et al. 2006). Not only may the effectiveness of these inhibitors be substantially impaired in sepsis, but channel opening may actually represent a protective mechanism against the development of cellular dysoxia, mitochondrial dysfunction and decreased energy production, all common features in MOF.

1.2 Pathophysiology of sepsis

Genetic (Arcaroli, 2005), cellular (Tracey, 1986) and patient factors (e.g. co-morbidities) can cause an infectious insult to trigger an inappropriately exaggerated and systemic inflammatory response. Various constituents of the micro-organism (e.g. cell wall components and DNA) bind to endothelial and white cell membrane-bound proteins as well as soluble proteins within the plasma, leading to a brisk innate and adaptive immune response (Shelley, 2003). This also leads to activation of endothelium, platelets and coagulation pathways (Levi, 1993). A comprehensive review of this topic has been published by various groups (Annane, 2005; Bochud, 2003) and (Hotchkiss, 2003). One such family of proteins which bind a host of pathogens are the Toll-like receptors (TLRs), which, when activated, lead to activation of nuclear transcription factors, including NF-κB (Reviewed in (Akira, 2003) and (Liu, 2006).

1.2.1 Toll-like receptors as pattern-recognition molecules for the innate immune system

Originally studied in the *Drosophila* embryo, eleven different Toll-like Receptors (TLR 1-11) have now been identified in mammalian cells and they form part of

the interleukin 1 super family of receptors (Akira, 2003). At least seven of these receptors interact with microbial motifs, suggesting these receptors are important regulators of innate immunity. TLR4 recognises lipopolysaccharide (LPS or endotoxin), a gram-negative wall constituent (Cartwright, 2007), whilst TLRs 2 and 6 recognise lipoteichoic acid (LTA), a gram-positive wall constituent (Cartwright, 2007). However, components of vertebrate cells are not recognised by TLRs, indicating their ancient origins and importance in the innate immune system. Toll-like receptors are expressed in human cells and importantly, TLR4 mRNA and protein is found in vascular smooth muscle cells obtained from human saphenous veins (Sasu, 2001). Thus TLR4 may be an important target in the development of septic shock. There is a growing realisation that Gram-positive bacteria are an equally important cause of sepsis, with both peptidoglycan and LTA involved in the underlying pathophysiology (Wang, 2003). However, in this thesis I will concentrate almost exclusively on Gram-negative infections, where LPS has been extensively used as an experimental tool to mimic sepsis and elucidate cellular mechanisms of inflammation.

Lipopolysaccharide, in order to stimulate TLRs, must either bind to the membrane bound CD14-receptor (Leturcq, 1996) and/or soluble CD14 in the plasma before forming a complex with TLR 4 and other adapter molecules (Cartwright, 2007). Once formed, it triggers various kinase signalling pathways, including IL-1 receptor associated kinases (IRAKs), transforming growth factor β associated kinases (TRAKs) and the adapter protein MyD88, the combination of which leads to the upregultation of NF-κB and the transcription of a multitude of pro-inflammatory genes (Cartwright, 2007; Liu, 2006; Akira, 2003).

1.2.2 Pro-inflammatory and anti-inflammatory signalling in sepsis

TLRs up-regulate expression of a wide range of genes encoding for numerous pro-inflammatory cytokines (e.g. tumour necrosis factor α (TNFα) and interleukins-1 and -6), mediators, receptors and enzymes (e.g. the inducible isoform of nitric oxide synthase (iNOS) and cyclooxygenase-2 (COX-2) that increase production of nitric oxide (NO) and prostaglandins, respectively (Cartwright, 2007; Reddy, 2001; Tunctan, 2003; Oettinger, 1987). Stimulation of the arachidonic acid cascade generates pro-inflammatory prostaglandins, thromboxanes (Oettinger, 1987) and leukotrienes (Petrak, 1989). Activation and degranulation of neutrophils release reactive oxygen species (Kantrow, 1997; Singer, 1999) and proteases.

This inflammatory response also includes an up-regulation of anti-inflammatory cytokines (e.g. IL-10) and mediators that attempt to suppress inflammation (Gerard, 1993), however a severe imbalance between pro- and anti-inflammatory cytokine production can lead to the clinical picture of the systemic inflammatory response syndrome (SIRS) (Annane, 2005; Bochud, 2003). This is defined as the clinical features of sepsis, but without evidence of infection.

1.3 Septic shock and multi-organ failure

The exaggerated inflammatory response results in increased vascular permeability with enhanced passage of fluid, plasma proteins, activated macrophages and neutrophils to extravascular compartments, a microcoagulopathy (Levi, 1993) and alterations in microvascular tone (Annane, 2005; Hotchkiss, 2003). A synergistic

effect between pro-inflammatory mediators and tissue hypoxia consequent to myocardial depression, hypovolaemia, interstitial oedema and blood flow redistribution will result in decreased mitochondrial energy production and a metabolic shutdown which, if severe enough, becomes clinically apparent as organ dysfunction (Singer, 1999).

The septic process can affect most organ systems within the body. The most severe cardiovascular manifestation is septic shock, a condition defined as organ dysfunction with perfusion abnormalities plus hypotension (or a drop in systolic blood pressure of more than 40 mmHg) that does not respond to adequate fluid resuscitation. This results from a combination of excessive vasodilatation, vascular hyporeactivity (i.e. decreased responsiveness to catecholamines) and variable degrees of myocardial depression (Danner, 1991).

1.3.1 Current management of septic shock

Better knowledge of the mechanisms underlying shock will enable a more focused therapeutic strategy. Current management consists of adequate fluid resuscitation, inotropic and pressor support (e.g. norepinephrine) and adjuvant treatments such as corticosteroids (Annane, 2002). In the event of failure of norepinephrine to maintain an adequate blood pressure (e.g. mean arterial pressure > 60 mmHg), alternatives such as vasopressin can be tried (Russell, 2008). However, in certain cases, these are either not appropriate (e.g. because of pre-existing cardiac failure or mesenteric ischaemia), or patients fail to respond.

A number of mechanisms are known to mediate vascular hyporeactivity and hypotension. These include the nitric oxide (NO) pathway (Thiemermann, 1990;

Petros, 1991; Hotchkiss, 1992) excess activation of potassium (K^+) channels (Landry, 1992; Hall, 1996) and a relative reduction in the circulating levels of vasopressin (Landry, 1997). Large dose infusions of catecholamines can often be significantly reduced or even stopped after administration of a NO synthase (NOS) inhibitor (Petros, 1991) or vasopressin (Landry, 1997; Russell, 2008). These actions are likely to be mediated in part by closure of the vascular smooth muscle ATP-sensitive (K_{ATP}) channel (O'Brien, 2005; Wilson, 2002; Wakatsuki, 1992), giving rise to membrane depolarisation and, ultimately, vasoconstriction. However, it is likely that K_{ATP} opening itself represents an independent mechanism underlying hypotension and vascular hyporeactivity (O'Brien, 2005; Wilson, 2002).

1.4 Potassium Channels

Potassium (K^+) channels are membrane-spanning proteins that selectively allow movement of K^+ ions across cells through a water-filled permeation pathway (pore) (reviewed in (Nelson, 1995). A gating mechanism (driven by a voltage change or ligand binding) switches the channel between open and closed conformations. Channel opening normally promotes K^+ loss from the cell, resulting in membrane hyperpolarisation. Key roles for K^+ channels include maintenance of the cellular resting membrane potential, regulation of neuronal excitability, neurotransmitter release, control of heart rate and smooth muscle tone, hormone secretion and epithelial electrolyte transport. Several hundred genes encoding for K^+ channels have been identified; genetically, these broadly fall into three families; voltage-gated (including Kv and calcium-activated channels), inward rectifiers (Kir1-7.0) and twin pore K^+ channels (Shieh, 2000). I

will concentrate on the role of the K_{ATP} channel and, specifically, its role in vascular hyporeactivity and hypotension in septic shock. Large conductance, calcium-activated K^+ (BK_{Ca}) channels are also thought to play a role in vascular hyporeactivity in sepsis (Miyoshi, 1994) and this will be briefly discussed.

1.4.1 Molecular biology of K_{ATP} channels

The K_{ATP} channel is an integral membrane protein, ligand-gated, ATP-sensitive potassium channel which links the metabolic state of the cell to membrane potential. The K_{ATP} channel was first discovered in cardiomyocytes by Noma in 1983 (Noma, 1983) and shown to be a channel inhibited by ATP. Structurally, the channel consists of two proteins; a central pore-forming subunit (Kir6.1/6.2), which is responsible for ion conduction and an associated sulphonylurea receptor subunit (SUR) (Fig 1.1). The pore of the K_{ATP} channel is a member of the inward rectifying family of potassium channels, allowing the efflux of potassium to repolarise the cell following membrane depolarisation. It exists in two isoforms; Kir6.1, encoded by the gene Kcnj8 in humans (Inagaki, 1995) and Kir6.2, encoded by Kcnj11 (Inagaki, 1995). Expression of Kir6.1 and Kir6.2 isoforms shows tissue variation conferring an element of tissue specificity as well as dictating biophysical characteristics. The ion channel protein is dependent on co-expression with an SUR subunit to form a functional K_{ATP} channel (Inagaki, 1995; Yamada, 1997). An *–RKR-* motif on the C terminus of the Kir6.2 is crucial for the normal trafficking of the Kir subunit to the membrane (Tucker, 1997) and a similar *–RKQ-* motif exists on the SUR (Bryan, 1999). The SUR is a member of the ATP-binding cassette (ABC) protein family and consists of 17 transmembrane domains with two intracellular nucleotide binding fold domains (Bryan, 1999).

The SUR subunit exists as two genes SUR1 (ABCC8) (Aguilar-Bryan, 1995) and SUR2 (ABCC9), though two major splice variants exist for SUR2, giving rise to either SUR2A (Inagaki, 1996) or SUR2B (Isomoto, 1996) proteins. SUR subunits also display tissue variability and pharmacology (Fig 1.2). For instance, the SUR1 subunit is expressed in pancreatic β cells and has a greater affinity for the sulphonylurea agent, glibenclamide (an inhibitor of the K_{ATP} channel) than the SUR2B isoform, which is expressed in vascular smooth muscle (Fujita, 2000). The SUR also dictates responses to drugs that open the K_{ATP} channel (KCOs); diazoxide is able to activate pancreatic but not cardiac K_{ATP} channels (Fujita, 2000).

The stoichiometry of the two subunit proteins is not precisely known, but is thought to consist of a hetero-octameric complex, with a tetramer of the pore-forming subunit surrounded by four SUR subunits, having a combined molecular mass estimated at 950 kD (Shyng, 1997). This combination was originally suggested because of the stoichiometry seen with other types of potassium channels, namely voltage-dependent potassium channels (K_v) and G-protein-activated potassium channels (GIRK) (Fujita, 2000). This has been confirmed by studying current-voltage relationships of heteromeric mutant mouse Kir6.2 ion channels, along with expression of dimeric hamster SUR1-mouse Kir6.2 constructs in COSm6 cells (Shyng, 1997). As outlined in the table, different compositions of Kir6.0/SUR will give rise to tissue-specific types of K_{ATP} channels. Broadly speaking, Kir6.2/SUR1 channels represent the main K_{ATP} channel in pancreatic β-cells and neurons, while Kir6.2/SUR2A is the major composition of channels in cardiac and skeletal muscle. Kir6.1/SUR2B constitutes

the 30-40 pS vascular channel (termed K_{NDP}) that is relatively insensitive to ATP, but is activated by nucleotide diphosphates (NDPs) and inhibited by glibenclamide (see (Seino, 2003; Rodrigo, 2005) for review).

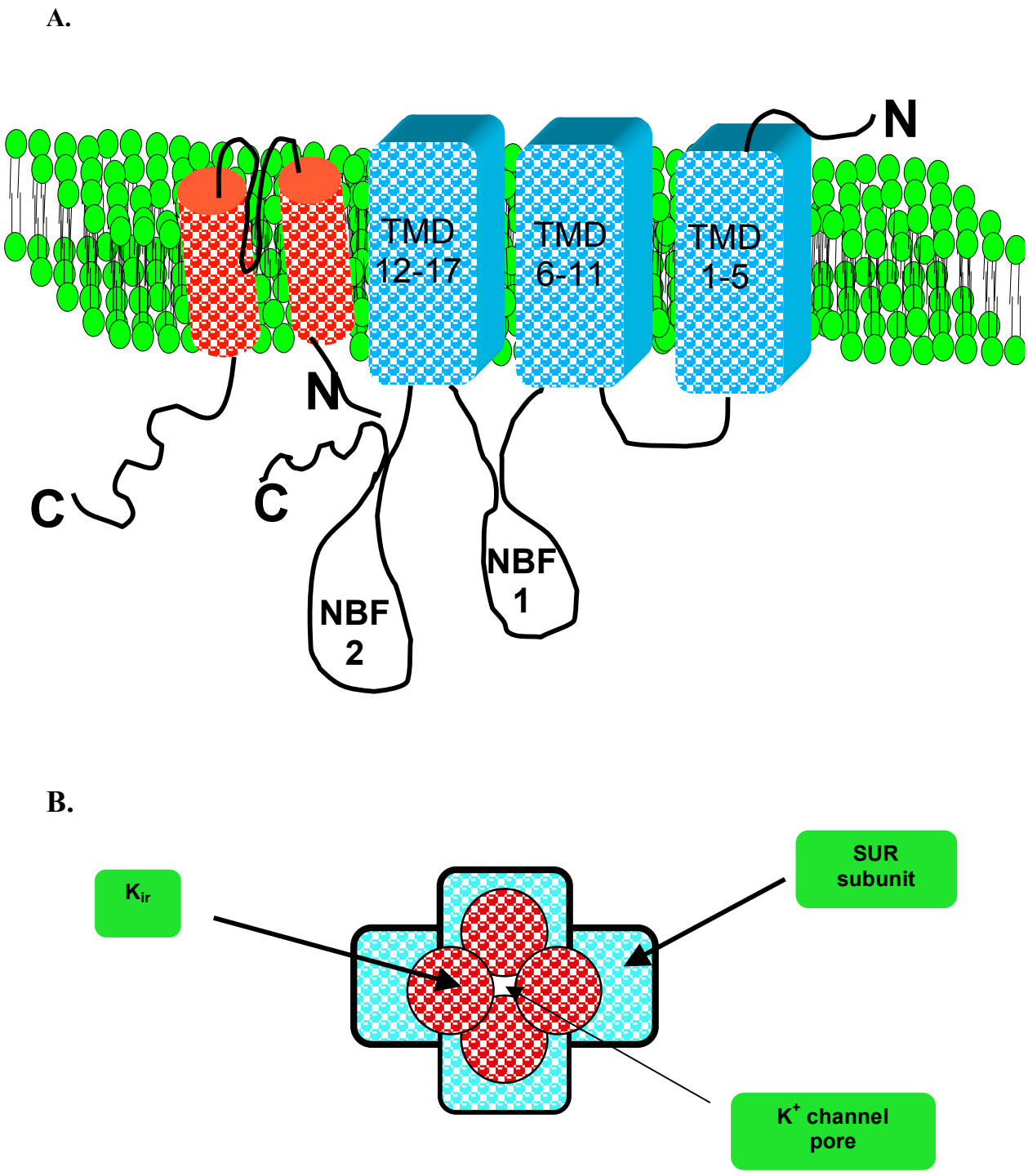

Figure 1.1: Molecular structure of the K_{ATP} channel subunits: Transverse view (A) and cross-sectional view (B). The channel consists of two proteins: the ion-channel pore protein Kir, shown in red and the sulphonylurea receptor subunit (SUR) in blue. Mass = 950 kD (Shyng,1997). The Kir protein consists of two

transmembrane domains, with an intra-membrane loop. Both N and C terminals are intracellular. The SUR consists of a 17 transmembrane domain (TMD) protein, with an extracellular N terminus and an intracellular C terminus. There are two additional intracellular loops, known as nucleotide binding folds 1 (NBF1) and 2 (NBF2), which bind ADP and Mg^{2+} ADP. This alters the ATP sensitivity of the ion channel pore.

Tissue	Subtype	Function	Pathophysiology	Openers	Closers
Brain (see Ref [a, b, c] for review)	Kir6.1/SUR2A (neurones) (Kir6.2/SUR2B) sunstantia nigra (Kir6.2/SUR2) astrocytes	Neuronal activity Neurotransmitter release Hypoglycaemic-induced glucagon secretion	Ischaemic preconditioning Ischaemic reperfusion Epilepsy & propagation of seizures	Diazoxide Insulin, Leptin [d] Isoflurane,	Glibenclamide Tolbutamide
Heart (see Ref [a, c] for review)	Kir6.2/SUR2A (Kir6.2/SUR2B)	Low open probability in normal physiological states	Ischaemic preconditioning/reperfusion injury [f, g] Action potential shortening during metabolic stress Ventricular fibrillation	Pinacidil, Nicorandil (coronary arteries, cardiomyocytes) Adenosine, insulin	Glibenclamide HMR1098 HMR1883 Vasopressin [h] Endothelin, Angiotensin II
Vascular smooth muscle (see Ref [a, i, j] for review)	Kir6.1/SUR2B most blood vessels *(Kir6.2/SUR2B) portal vein & mesenteric artery?	Resting membrane potential in somoe vessels Regional tissue perfusion (e.g coronary & mesenteric circulation)	Increased flow to hypoxic and energy deplete tissues Ischaemic preconditioning/reactive hyperaemia Hyporeactivity & hypotension in sepsis & haemorrhage shock [k]	Levcromakalim Pinacidil Diazoxide Isoflurane (vasorelaxation & hypotension) CGRP, Adenosine PGI_2, VIP, NO [j]	Glibenclamide PNU 37883A Vasopressin Endothelin, Angiotensin II, Norepinephrine
Smooth muscle (non-vascular) (see Ref [a] for review)	(Kir6.2/SUR2B) §(Kir6.2/SUR2B) urethra	Modulation of contractility in colon, bladder & airway smooth muscle	Unknown	Levcromakalim, pinacidil	Glibenclamide
Pancreas (see Ref [b, e] for review)	Kir6.2/SUR1	Insulin release	Persistent hyperinsulinaemia of infancy Neonatal diabetes & some forms of adult diabetes Insulin resistance in sepsis? [o]	Diazoxide, Levcromakalim, Pinacidil	Glibenclamide Tolbutamide Gliclazide
Skeletal muscle (see Ref [a, b] for review)	Kir6.2/SUR2A (Kir6.2/SUR1)	Glucose uptake Contractility during fatigue & recovery after fatigue	Protection against ischaemic reperfusion injury K^+ channel syndrome [p] Insulin resistance in sepsis?	Diazoxide Insulin [q]	Glibenclamide
Subcellular Mitochondria Mito(K_{ATP}) (see Ref [a, f, r] for review)	Unknown	Matrix volume Metabolic regulation of mitochondrial membrane potential	Ischaemic preconditioning Organ failure in sepsis Apoptosis	Diazoxide Insulin	Glibenclamide 5-HD

Potential subunit configuration or limited tissue expression is shown in brackets. *May underlie metabolically-sensitive channels in these tissues. §One of the few tissues to show K_{NDP}-like current, but SUR1 may contribute.

Figure 1.2: Table of the molecular structure, pharmacology and function of K_{ATP} channels. References: [a](Rodrigo, 2005), [b](Miki, 2005), [c](Shi, 2005), [d](Mirshamsi, 2005), [e](Seino, 2005), [f](Hanley, 2005), [g](LaDisa, 2004), [h](Tsuchiya, 2002), [i](Clapp, 1998), [j](Quayle, 1997), [k](Landry, 1997), [l](Humphrey, 1996), [m](Wakatsuki, 1992), [n](Das, 2003), [o](Singer, 2005), [p](Tricarico, 1997), [q](Ardehali, 2005).

1.4.2 Basic properties of K_{ATP} channels

K_{ATP} channels containing Kir6.1/SUR2B subunits have single channel conductance of ~33pS (Yamada, 2000; Fujita, 2000) and are inhibited by intracellular ATP with an IC_{50} in the millimolar range. In contrast, Kir6.2/SUR1 subunits have single channel conductance of around 60-80 pS and are typically inhibited by intracellular ATP with an IC_{50} in the micromolar range (Inagaki, 1995; Fujita, 2000). This means that channel openings are relatively rare under normal physiological or resting conditions. However, substantial channel opening will occur in response to either a fall in ATP or a rise in Mg^{2+}ADP. Thus, the ratio of ATP to ADP within the cell is often considered the key determinant of basal activity (Seino, 2003). ATP inhibits the channel by binding to the interface between two Kir subunits within the tetramer, interacting with the C-terminus of one subunit and the N-terminus of another (Antcliff, 2005). ADP, while having an inhibitory effect on the pore, will bind as Mg^{2+}ADP to the Walker A motif of the nucleotide binding folds (NBFs) contained within the SUR, the net effect being to promote opening of the K_{ATP} channel (Gribble, 1997).

1.4.3 Pharmacological regulation

Pharmacologically, the channel is opened by a diverse group of drugs termed K^+ channel openers (KCOs, e.g. levcromakalim, pinacidil and diazoxide) and closed by sulphonylureas (e.g. glibenclamide, tolbutamide, gliclazide). However, tissue selectivity and differences in potency exist with respect to these K_{ATP} channel modulators. For example, cardiac K_{ATP} channels are capable of activation by pinacidil, but are relatively unresponsive to levcromakalim and diazoxide, whereas pancreatic and vascular channels respond well to all these agents (Fig

1.2). Likewise, tolbutamide and glibenclamide potently inhibit pancreatic channels in the low nanomolar range but higher concentrations (<100 fold) are required to inhibit the vascular channel (Fujita, 2000). The situation is still more complex since K_{ATP} channels have two binding sites for sulphonylureas, a low affinity site (IC_{50} > 1.5 mM) on the Kir and a high affinity site (IC_{50} 10-200 nM) on the SUR (Aguilar-Bryan, 1999; Fujita, 2000).

The mechanistic action of KCOs is to increase the open probability (P_o) of the channel, an effect that is triggered by a conformational change in the SUR upon binding of the drug. This conformational change requires that Mg^{2+}ADP be bound to the Walker A motif on the NBF (Gribble, 1997). On the other hand, glibenclamide inhibits the binding of KCOs to the SUR (Dickinson, 1997; Hambrock, 1998; Loffler-Walz, 1998; Schwanstecher, 1998). This, in turn, prevents binding of Mg^{2+}ADP to the NBF domains and allows the inhibitory effect of ATP on the Kir subunit to tip the balance in favour of K_{ATP} channel closure (Aguilar-Bryan, 1999).

1.4.4 Cellular functions of K_{ATP} channels

One of the functions of the K_{ATP} channel is to link the metabolic state of the cell to membrane excitability. Such a mechanism is responsible for insulin secretion in response to increasing levels of glucose in pancreatic ß cells (Eliasson, 2003). Activation of an intracellular signaling cascade culminates in mobilization of exocytotic cytoskeletal proteins (SNARE proteins), closure of the K_{ATP} channel, depolarization of the cell membrane and, ultimately, release of insulin (Nevins, 2003). Within the brain, heart and coronary vasculature K_{ATP} channels are

responsible for the phenomenon of ischaemic preconditioning (Kaneko, 2005; Otani, 2003), whereby a preceding, sub-lethal ischaemic episode protects against a subsequent lethal ischaemic event. Nicorandil is a therapeutically used KCO that causes dilatation of coronary vessels in ischaemic heart disease (Seino and Miki, 2003) (Rodrigo and Standen, 2005).

1.4.5 K_{NDP} channel

The K_{ATP} channels described in vascular smooth muscle exhibit a number of differences from the classical K_{ATP} channels described in other tissues. As already mentioned, the channel is relatively insensitive to the inhibitory effects of intracellular ATP [ATP]i, but is opened by NDPs including ADP, GDP and UDP (Matsuo et al. 2005). Given the dependence on these nucleotides not only for channel regulation but also for activation by KCOs, it has therefore been termed the K_{NDP} channel. More fundamentally, differences are seen in the single channel conductance of K_{ATP} channels in smooth muscle. These can vary from 10-50 pS to 100-250 pS, as opposed to the conductance of 70-80 pS consistently found in pancreatic and cardiac tissue (reviewed in (Clapp, 1998)). Typically, the K_{NDP} channel is said to have a conductance of 30-40 pS (Yamada, 2000). Despite this, there is a great deal of evidence that the pharmacological properties of this channel vary significantly, depending on the smooth muscle tissue studied, with IC_{50} for ATP_i varying from 350 μM in canine coronary arteries, to the millimolar range in porcine coronary arteries (Fujita, 2000).

1.4.6 K_{ATP} channels and vascular tone

The membrane potential is determined by a number of ionic pathways. Potassium ions play an important role, contributing about 70% of total membrane conductance (Nelson *et al.*, 1995). The normal resting membrane potential of a smooth muscle cell is between -50 and -70 mV. Depolarisation means shifting this potential in a positive direction towards the equilibrium potential for chloride (approximately –30 mV), whereas hyperpolarisation means shifting the membrane potential in a more negative direction, towards the equilibrium potential for K^+ being approximately -83 mV in most smooth muscle types (see (Brayden, 2002) for review). When K_{ATP} channels close, this prevents efflux of potassium out of the cell, causing depolarisation of the cell membrane. The opposite occurs when channels open.

In vascular smooth muscle, depolarisation activates voltage-dependent L-type calcium channels (VDCCs), leading to the influx of calcium into the cell. The relationship is steep around the resting potential, with a 3mV change in the membrane potential of a cell capable of more than doubling calcium influx through these channels (Nelson, 1995). Once in the cytosol, calcium can bind to ryanodine receptors on the sarcoplasmic reticulum (SR) causing a further release of calcium from the SR, a mechanism known as calcium-dependent calcium release. Once calcium is significantly elevated, it will activate myosin light chain kinase. The subsequent phosphorylation of myosin leads to actin-myosin cross-linkage and contraction of the vascular smooth muscle cell.

In vascular smooth muscle, K_{ATP} channels contribute to maintenance of resting membrane potential and local blood flow (Nelson, 1995). Evidence that K_{ATP} channels are open under resting conditions comes from studies in mesenteric and coronary vascular beds whereby application of glibenclamide not only caused membrane depolarisation of between 5-9 mV (Garland, 1992), but also increased arterial resistance and decreased blood vessel diameter (Nelson, 1995; Salzman, 1997). The extent to which K_{ATP} channels control blood pressure is unclear. On the one hand, SUR2 and Kir6.1 knockout mice are hypertensive (Miki, Suzuki et al. 2002; Chutkow, 2002), while there is an absence of a hypertensive effect in normal dogs given glibenclamide (Landry, 1992. The contribution to vascular tone is more evident during pathological states such as ischaemia (Thierfelder, 1994). Low levels of intracellular ATP, indicative of the poor cellular metabolic status, leads to channel opening and smooth muscle relaxation. Subsequent dilatation of the blood vessel increases blood supply to the energy-deplete tissue (Salzman, 1997). The same effect is seen with hypoxia (Thierfelder, 1994) and with hypercapnia, whereby rising CO_2 levels decrease intracellular pH, thereby opening K_{ATP} channels in mesenteric artery vascular smooth muscle cells (Wang, 2003).

1.4.7 Hormonal regulation of K_{ATP} channels

Angiotensin II, vasopressin, norepinephrine and endothelin all inhibit K_{ATP} channel opening, and this may contribute to their vasoconstrictor mechanism (Miyoshi, 1991; Miyoshi, 1992; Wakatsuki, 1992; Bonev & Nelson MT, 1996). Such vasoconstrictors act via G_q-protein coupled receptors that can close the K_{ATP} channels, given that agonist effects on K_{ATP} channel currents are dependent upon

phospholipase C-β (PLCβ) and protein kinase C-ε (PKCε) activity (Hayabuchi, 2001; Rodrigo and Standen 2005).

In sepsis, this pathway is inhibited, either directly by nitric oxide production or indirectly via opening of the K_{ATP} channel. Subsequent hyperpolarisation inhibits opening of the voltage-dependent calcium channels and thus inhibition of contraction. Vasodilators such as adenosine (acting on the A_2 receptor) or calcitonin gene-related peptide (CGRP) act via stimulatory G-protein coupled receptors to open K_{ATP} channels (Kleppish et al. 1995). This is a cyclic adenosine monophosphate (cAMP) and protein kinase A (PKA)-dependent process (see (Buckley, 2006), involving phosphorylation of Ser/Thr sites located on both SUR and Kir6.1 (Quinn et al. 2003; Quinn et al. 2004).

1.5 K_{ATP} channels in the pathophysiology of sepsis

The role of K_{ATP} channel activation in sepsis can be divided into its established role in vascular hyporeactivity (discussed below), and its potential role in mitochondrial dysfunction, which is further expanded upon in the discussion section.

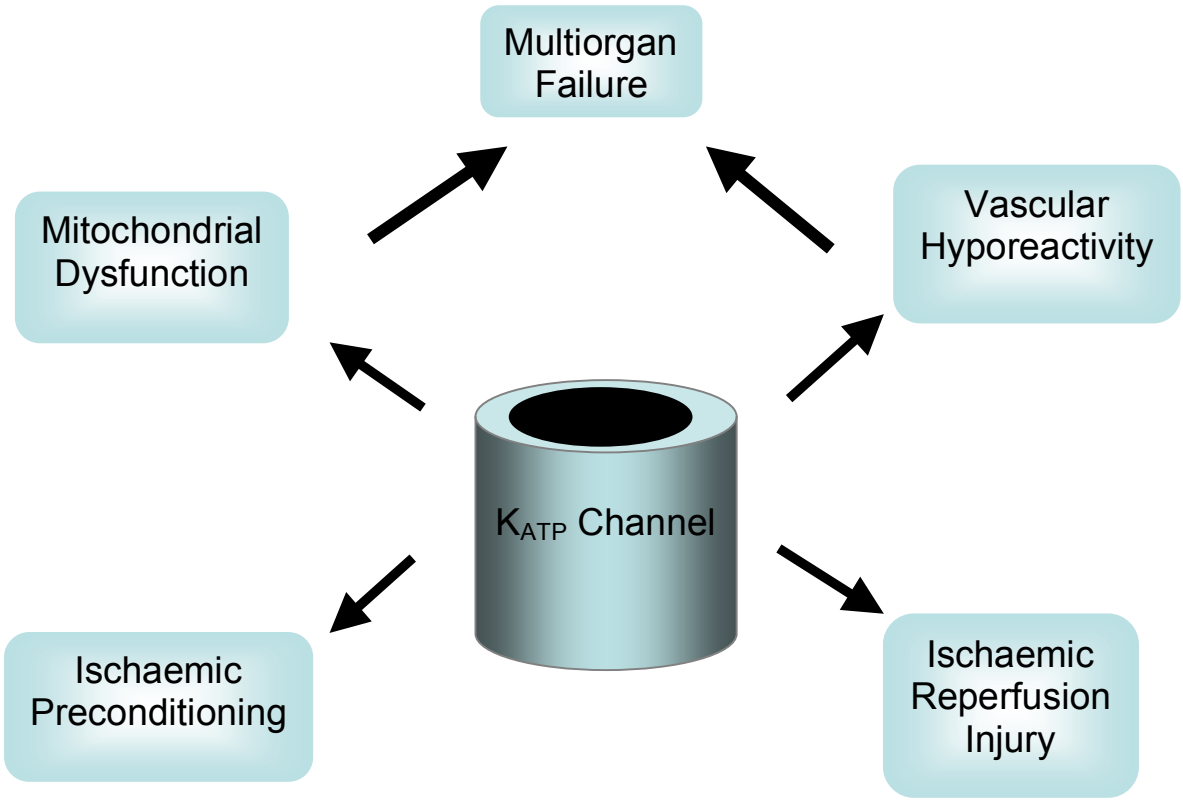

Figure 1.3: The K_{ATP} channel may be key to several pathophysiological processes in sepsis, including vascular hyporeactivity, mitochondrial dysfunction and MOF .

1.5.1 Vascular hyporeactivity

Electrophysiological data show that K^+ channels play a role in the control of vascular tone. Vascular tone refers to the degree of constriction of the vascular smooth muscle cells in blood vessels. In the arterial tree this is the determinant of

systemic vascular resistance (SVR) and, therefore, one of the determinants of blood pressure (BP). They are related by the equation:

$$BP = SVR \times CO$$

where CO is cardiac output. The constriction of vascular smooth muscle is dependent on an increase in intracellular calcium $[Ca]_i$ in response to vasoconstrictors.

However, the contribution of K_{ATP} channels to SVR and BP under normal conditions is probably minimal, as evidenced by the lack of hypertension in animals given glibenclamide (Landry, 1992). In the presence of pathology such as sepsis, hypoxia or haemorrhage, K_{ATP} channels have a more important role in the determination of SVR and BP (Landry, 1992; Landry, 2001).

The evidence for the role of K_{ATP} channels in sepsis can be divided primarily into studies that examine their role in either short-term (<6 hrs) or longer-term (>20hrs) laboratory models. Only one study has formally examined their role in human sepsis (Warrillow et al., 2006). However, by the time a patient displays symptoms and signs of overt septic shock they are likely to have had systemic inflammation for far longer than 6 hrs. Longer-term *in vivo* models are likely to be more relevant in this regard.

1.5.2 *In vivo* models of sepsis

The *in vivo* evidence for the role of K_{ATP} channels in sepsis consists of data from anaesthetised rats (Sorrentino, 1999; Wu, 1999), dogs (Landry, 1992) and pigs (Vanelli, 1995). Injection of LPS was found to consistently cause a drop in blood pressure in the animals 30-90 mins after administration (Landry, 1992; Wu, 1999) and was associated with vascular hyporeactivity to phenylephrine (Landry, 1992; Sorrentino, 1999). In most cases, both the hypotension and vascular hyporeactivity could be reversed by the administration of glibenclamide (Vanelli, 1995; Landry, 1992). The beneficial effect of glibenclamide was rapid, occurring within a few mins and lasting for up to 20-30 mins (Landry, 1992; Vanelli, 1995). The effect on blood pressure was via an increase in SVR and not from an increase in cardiac output (Landry, 1992; Vanelli, 1995). Interestingly, hypotension caused by the administration of glyceryl trinitrate (GTN) or nitroprusside was unaffected by glibenclamide, suggesting a more complex interaction of the iNOS pathway with the channel (Landry, 1992). In other studies, increased vasorelaxation to the potassium channel opener, cromakalim, was observed in septic animals; not surprisingly, glibenclamide reversed this effect (Sorrentino, 1999). These *in vivo* data confirm that over-activity of K_{ATP} channels in vascular smooth muscle is likely to contribute to hypotension in sepsis. Indeed, a Kir6.1 knockout mouse displayed a blunted vasodilator response when given LPS (Kane et al. 2006).

1.5.3 *In vitro* models of sepsis

Vascular hyporeactivity can be demonstrated *in vitro* using an organ bath model (Chen, 2000a; Chen, 2000b; Hall, 1996; O'Brien, 2001; Sorrentino, 1999; Wilson, 2002). Here, arterial rings (with or without an intact endothelium) bathed in media are mounted on a spring-loaded system to maintain them under tension; a concentration-response curve to increasing concentrations of vasoconstrictors is then generated.

The pathophysiological mechanisms underlying vascular hyporeactivity may change with time. Inhibition of NO production in *in vitro* models of <6 hrs' duration demonstrated almost complete reversibility of hyporeactivity (Chen, 2000; O'Brien, 2001; Sorrentino, 1999; Wilson, 2002), whereas this was only partial in longer-term (>20 hrs) models (O'Brien, 2001). Potential underlying mechanisms to explain these differences are discussed in detail later.

In vitro studies can be performed in arteries extracted from septic/endotoxic animals, or in vessels taken from healthy animals that are subsequently incubated with endotoxin for varying durations (Hall, 1996; Sorrentino, 1999; Chen, 2000a; Chen, 2000b; O'Brien, 2001; Wilson, 2002). Decreased contractility, particularly to catecholamines, can be readily shown in septic/endotoxic rings as a depressed concentration-response curve (O'Brien, 2005). However, application of glibenclamide did not reverse this hyporeactivity (O'Brien, 2001). This may be indicative of altered channel pharmacology (Wilson & Clapp, 2002), irreversible damage to the contractile apparatus, or other mechanisms contributing to hyporeactivity. It is equally plausible that glibenclamide fails to depolarise

tissues in the range that will open a significant number of voltage-gated calcium channels to raise intracellular calcium levels and thus increase vascular tone.

In contrast, the increased ability of K_{ATP} channel openers (KCOs) to cause relaxation of vascular tissue in both *in vitro* and *in vivo* models of sepsis, could be viewed as further evidence for the role of K_{ATP} channels (Chen, 2000; d'Emmanuele di Villa Bianca, 2003; Sorrentino, 1999). This action can be exploited as another tool for examining contractility in control and septic tissues (Chen, 2000a; Chen, 2000b; Wilson, 2002). From a mechanistic standpoint it suggests that during sepsis the K_{ATP} channel is in a state more favourable to opening. A more stable binding of Mg^{2+}ADP to the nuclear binding folds on the cytosolic surface of the SUR protein would facilitate this type of interaction. Similarly, the SUR protein favouring the "open" conformation would have the same effect on channel function and characteristics.

The use of *ex vivo* models also enables the simultaneous assessment of membrane electrophysiology, enabling demonstration of membrane hyperpolarisation during vascular hyporeactivity (Chen, 2000; Wu et al., 2004). Using a 6 hour *in vivo* model, Chen et al demonstrated that LPS given intravenously to anaesthetised Wistar-Kyoto rats caused hypotension and vascular hyporeactivity to norepinephrine. Subsequent *ex vivo* studies demonstrated LPS-induced hyporeactivity in an organ bath model, and hyperpolarization measured using microelectrodes. This hyperpolarization was reversed using inhibitors of NO synthase (L-NAME) and partially reversed by glibenclamide, confirming a role of K_{ATP} channels.

1.6 Factors that might contribute to K_{ATP} channel opening

1.6.1 Nitric oxide and K_{ATP} channels in sepsis

Overwhelming evidence from animal models suggests that endotoxin-induced hypotension and vascular hyporeactivity is largely a consequence of over-production of iNOS-derived NO within the blood vessel wall (Thiemermann, 1994; Thiemermann, 1997). Increased production of NO, albeit at much lower levels, is recognised in patients with sepsis (Ochoa, 1991) and inversely correlates with mean arterial pressure and systemic vascular resistance (Bellissant, 2000).

Compared to animals, induction of iNOS appears restricted in humans, occurring mainly in blood vessels at the point of infection (Bellissant, 2000) or in infiltrating monocytes (Kobayashi, 1998). Taken together, this may suggest that NO derived from iNOS may not be the only source of NO in human sepsis (Vallance, 2001). However, iNOS may be present at levels below the limit of detection but still produced in sufficient quantity to have a significant effect on vascular tone in humans. In addition, although specific iNOS inhibitors have not been used in human sepsis, the use of non-specific NOS inhibitors resulted in potent elevation of BP (Petros, 1994).

Once formed, NO can activate soluble guanylate cyclase and increase cyclic GMP, or it can react with superoxide to form peroxynitrite ($ONOO^-$), a process that occurs more readily during systemic inflammation (Frost, 2005).

As previously mentioned, the NO/cyclic GMP pathway is likely to be responsible for K_{ATP} channel activation, at least in the short term (<6 hr) (O'Brien, 2001). NOS or guanylate cyclase inhibitors fully reversed endotoxin-induced hyporeactivity or membrane hyperpolarisation with effects of near-similar magnitude to that seen with K_{ATP} channel blockade (Hall, 1996; O'Brien, 2001; O'Brien, 2005; Wilson, 2002; Wu, 2004). NO can also potentiate KCO responses in cardiac myocytes (Shinbo, 1997). In septic models, potentiation of levcromakalim-induced hypotension or vascular relaxation can be largely reversed by NOS or guanylate cyclase inhibition (Chen, 2000; Sorrentino, 1999; Wilson, 2002).

1.6.2 Calcitonin Gene-Related Peptide and K_{ATP} channels in sepsis

Calcitonin gene-related peptide is a 37 amino acid vasoactive peptide contained in sensory neurones that plays a role in the regulation of local blood flow. It is a potent vasodilator. Increased levels of CGRP were reported in septic rats (Griffin, 1992), and administration of a CGRP receptor antagonist (hCGRP) transiently reversed tachycardia and hypotension (Huttemeier, 1993). In normal blood vessels, glibenclamide partially reversed the relaxation of mesenteric arteries when exposed to CGRP (Nelson, 1990). CGRP is thought to activate K_{ATP} channels via increased levels of cyclic AMP and subsequent activation of protein kinase A (PKA) (Quayle, 1994).

1.6.3 The actin cytoskeleton: not just scaffolding for K_{ATP} channels?

The actin cytoskeleton consists of the protein actin (molecular mass 42kDa), which represents 50% of total cellular protein content. It exists in α, β and γ isoforms, with the functional polymerised form (F actin) consisting of many monomers of globular (G actin) (Janmey, 1998). These are in a dynamic (Amann, 2000; Gokina, 2002), energy-dependent flux which is controlled by, amongst other things, small GTP proteins e.g. Rho kinases (Peck, 2002). The cytoskeleton plays a role not just as a scaffolding protein determining the shape of the cell, but also in cell division, cell motility, contraction (e.g. cardiac, skeletal & smooth muscle cells), as well as being implicated in the control of various ion channels. For example, disruption of the cytoskeleton increased Na^+ influx via Na^+ channels in the jejunum (Strege, 2003) and increased chloride efflux via Cl^- channels in renal cortical cells (Schwiebert, 1994). The cytoskeleton is also implicated in the trafficking of proteins from the nucleus to the cell membrane, and signal transduction from the membrane to the nucleus, including nuclear transcription induced by shear stress in endothelial cells (Numaguchi, 1999).

Interactions between the actin cytoskeleton and the K_{ATP} channel have mainly been shown in isolated cardiac myocytes (Brady, 1996; Terzic, 1996; Yokoshiki, 1997), vascular smooth muscle cells (Loffler-Walz, 1998) and other artificial cell lines. Disruption of the cytoskeleton with the fungal toxin cytochalasin D (Terzic, 1996), or with DNAse I (Brady, 1996) causes increased opening of the K_{ATP} channel. Such effects were accompanied by altered glibenclamide binding (Yokoshiki, 1997) and decreased efficacy of other closers of the channel (Brady, 1996; Yokoshiki, 1997).

Nitric oxide disrupts the actin cytoskeleton in various cell types, including the lamina propia of the small intestine (Banan, 2000; Chakravortty, 2000), the kidney (Sandau, 2001) and in liver and kidney tissue in a murine model of sickle cell disease (Aslan, 2003). This is likely to be secondary to nitration (Aslan, 2003; Banan, 2000) or nitrosylation (Dalle-Donne, 2000) of actin. In addition, disruption of the actin cytoskeleton secondary to LPS has been shown in bovine aorta endothelial cells (Chakravortty, 2000) and in pulmonary vascular endothelial cells (Goldblum, 1993).

Alternatively, this phenomenon of the cytoskeleton altering K_{ATP} channel activity may be a result of changes in the energy status of the cell. This may therefore be a phenomenon seen alongside increased K_{ATP} opening during ATP-deficient states. However, it is also possible that the cytoskeleton is required for the K_{ATP} channel to execute its conformational change from the open to the closed state, and that disruption of the cytoskeleton in sepsis inhibits this conformational change. This situation would then keep the K_{ATP} channel open, thus causing relaxation of the relevant muscle. Disruption of the actin cytoskeleton has a direct effect on the contractile apparatus of muscle cells; if this were the sole consequence of such disruption it may be sufficient to cause vascular hyporeactivity in sepsis. Furthermore, the increased protein turnover and decreased synthesis seen for many proteins during sepsis may also underlie any alteration in cytoskeletal function. Ultimately, the disruption of the cytoskeleton is likely to have an irreversible effect on vascular hyporeactivity in longer-term models of sepsis.

1.6.4 Changes in energy status in sepsis

K_{ATP} channels may be opened by a fall in $[ATP]_i$, pH or oxygen tension, or by a rise in intracellular lactate and NDPs (Clapp, 1998; Landry, 2001). These may facilitate NO activation of the channel or act independently. Many of these factors operate in sepsis though the extent to which these play a role will likely depend on the degree of perturbation of the individual variable, as well as the severity and duration of the septic insult. Lactic acidosis is consistently reported in animal and human sepsis (Landry, 1992; Fall, 2005; Revelly, 2005) although, paradoxically, tissue hypoxia is not found in the resuscitated patient/animal, with raised tissue oxygen tensions reported in skeletal muscle (Boekstegers, 1991), bladder epithelium (Rosser, 1996) and gut mucosa (VanderMeer, 1995). This finding, in conjunction with a decrease in global oxygen consumption, suggests adequate availability but decreased cellular utilisation of oxygen, giving rise to a state of 'cytopathic dysoxia' related to mitochondrial dysfunction, increased generation of NO and decreased production of ATP (Boveris, 2002; Brealey, 2004). The ensuing 'energy failure' is implicated in the pathophysiology of organ failure. Of note, ATP levels are preserved in the skeletal muscle of eventual survivors of septic shock but fall in non-surviving patients (Brealey, 2002). This fall in ATP with increasing sepsis severity has been replicated in other tissues in various animal models (Brealey, 2004; Hart, 2003). Thus, opening of K_{ATP} channels due to metabolic failure may only be significant in severe sepsis. In vascular smooth muscle, this is likely to depend to a greater extent on the change in NDP levels rather than on ATP itself because of the main subtype (Kir6.1/SUR2B) expressed in this tissue (Kantrow, 1997).

1.6.5 Altered K_{ATP} channel expression in sepsis

Increased expression of K_{ATP} channels may contribute to channel activation and vascular hyporeactivity in sepsis. Simultaneous administration of dexamethasone and LPS to rats completely abolished the hyporeactivity to phenylephrine observed after 24 hrs from LPS injection alone (d'Emmanuele di Villa Bianca, 2003). Dexamethasone treatment also significantly reduced, in a time-dependent manner, the increased hypotensive effect induced by cromokalim in LPS-treated rats. This effect was significantly reverted by the glucocorticoid receptor antagonist RU38486 (6.6 mg/kg i.p.). Glibenclamide-induced hypertension in LPS-treated rats was significantly inhibited by dexamethasone, if administered at the same time of LPS. (d'Emmanuele di Villa Bianca, 2003). Thus, the K_{ATP} channels were no longer activated (opened) by sepsis and therefore attempted closure by glibenclamide had no effect. This is akin to the effect of administering glibenclamide to normal, non-septic animals. Dexamethasone could also inhibit *de novo* K_{ATP} channel protein synthesis, which could also be involved in its effect. This suggests that the beneficial effect of corticosteroids in improving vascular tone in sepsis could be ascribed, at least in part, to its ability to interfere with K_{ATP} channel activation.

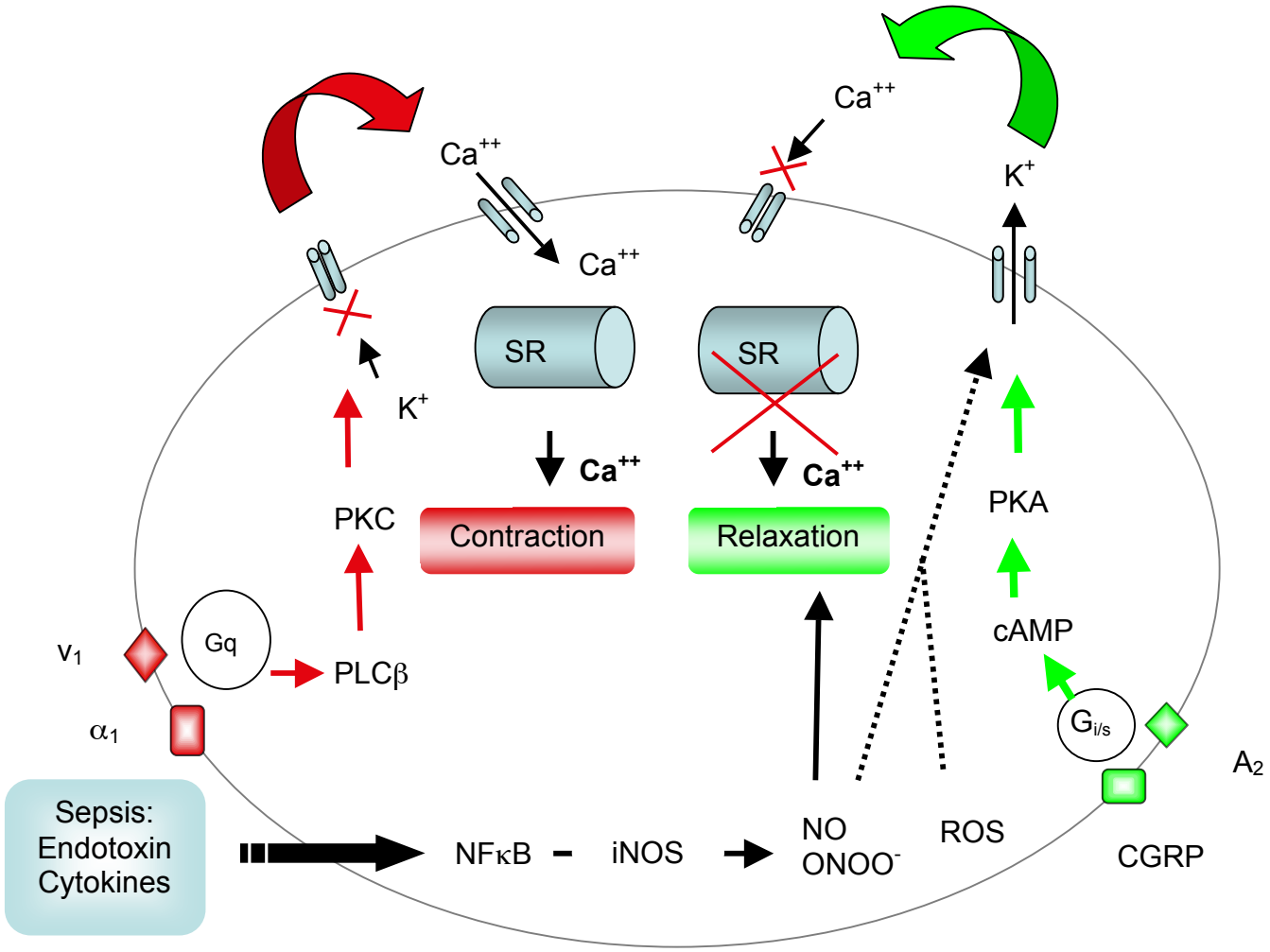

Figure 1.4: Mechanisms involved in vascular smooth muscle contraction (in red) and relaxation (in green). A_2: adenosine receptor, α_1: alpha-1 adrenoceptor, V_1: vasopressin receptor, CGRP: calcitonin gene-related peptide, G_i/G_s: inhibitory/ stimulatory G-protein coupled receptors, NFκB: nuclear transcription factor kappa B, NO: nitric oxide, $ONOO^{\bullet -}$: peroxynitrite, ROS: reactive oxygen species, PLC-β: phospholipase C β, PKC: protein kinase C.

1.7 Role of BK_{Ca} channels in sepsis

1.7.1 Vascular hyporeactivity

BK_{Ca} channels are found in the membranes of most cell types and are abundantly expressed in vascular smooth muscle cells (Nelson, 1995). BK_{Ca} channels, like K_{ATP} channels, alter the electrophysiological state of the membrane of vascular smooth muscle cells, regulating calcium entry into the cell and hence altering vessel wall tone (Nelson, 1995). NO directly activates BK_{Ca} channels in normal vessels (Mistry, 1998) and septic vessels. NO produced through iNOS can open BK_{Ca} channels (Miyoshi, 1994; Nameda, 1996), contributing to membrane hyperpolarisation induced by LPS in rat thoracic aorta (Chen, 2000a; Chen, 2000b). Conceivably, BK_{Ca} and K_{ATP} channels may work in concert in sepsis to produce changes in vascular reactivity.

1.7.2 Regulation of immune function

Circulating neutrophils play a pivotal role in the killing of a range of pathogens. In human neutrophils, microbial killing was elicited by BK_{Ca} channel activation. This functions to provide the K^+-rich environment necessary for activation of proteases within the phagocytic vacuole (Ahluwalia, 2004). In macrophages, endotoxin-induced cytokine release, particularly that of TNF-α, Il-6 and interferon-γ, requires prior K^+ channel activation. This involves a number of different types, including BK_{Ca}, inward rectifier and Kv channels (Haslberger, 1992; Blunck, 2001; Muller, 2003). Production of NO by activated macrophages is also an important cytotoxic function involved in the killing of micro organisms. Both K_V and K_{ATP} channels promote cytokine-induced NO production (Wu, 1995;

Lowry, 1998). Taken together, K^+ channels appear to be key players in the early activation of immune cells.

1.8 Cellular metabolism

The K_{ATP} channel links the metabolic state of the cell to its membrane potential; in VSMCs this channel influences contractile state and hence vascular tone. Like all cells in the body, vascular smooth muscle cells utilise ATP as an energy substrate. Energy is derived from hydrolysis of the high-energy phosphate bonds within ATP. Hydrolysis of ATP to ADP + P_i and ADP to AMP + P_i yields 30.5 Kj mol^{-1} per phosphate bond hydrolysed. This ATP is derived from glucose, free fatty acids and protein through glycolysis, β oxidation, oxidative phosphorylation and the phosphocreatine-phosphate transfer system. ATP and ADP levels are important for control of cellular metabolism (operating with negative feedback loops), and for control of the K_{ATP} channel. Therefore, understanding cellular metabolism helps in understanding the potential effects of sepsis on ATP and ADP levels and, hence, on K_{ATP} channel function.

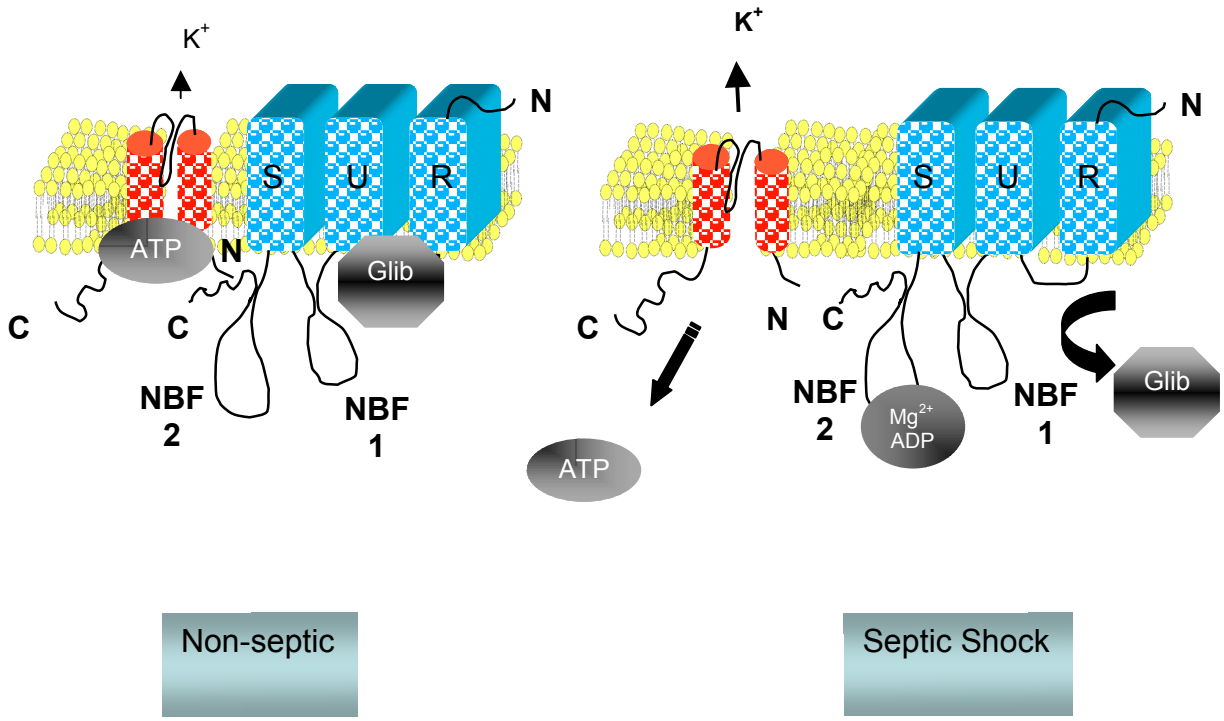

Figure 1.5: The K_{ATP} channel consists of two proteins, an ion-channel pore and a sulphonylurea receptor subunit (SUR). These interact at their N- and C- termini, respectively. On the left is a representation of the two subunits of the K_{ATP} channel under normal circumstances and, on the right, the K_{ATP} channel in sepsis where it is abnormally open in vascular smooth muscle cells. The diagram illustrates the various hypotheses as to underlying mechanisms. These include abnormal regulation of the channel by the sulphonylurea receptor subunit, altered binding of inhibitors of the channel and metabolic disregulation. The altered control of the pore by the SUR may be caused by disruption of the cytoskeleton or by nitration and/or nitrosylation of the proteins involved.

ATP: adenosine triphosphate, Mg^{2+}ADP: magnesium adenosine diphosphate, NBF-1 and NBF-2, nucleotide binding folds -1 and -2 respectively. Glib: glibenclamide.

Hypothesis:

During sepsis we observe vascular hyporeactivity due to altered function and subsequent opening of the K_{ATP} channel. It is hypothesised that the reasons for this channel opening are due to a combination of/one of the following effects:

a) Disruption of the actin cytoskeleton. The actin cytoskeleton has been shown to interact with the K_{ATP} channel (Brady, 1996; Terzic, 1996; Yokoshiki, 1997, Loffler-Walz, 1998). Disruption of F actin into G actin induces opening of the K_{ATP} channel (Brady, 1996; Terzic, 1996). Such effects were accompanied by altered glibenclamide binding (Yokoshiki, 1997) and decreased efficacy of other closers of the channel (Brady, 1996; Yokoshiki, 1997). This altered pharmacology is similar to that seen in sepsis (Wilson & Clapp, 2002; O'Brien et al., 2005). I hypothesised that this increased K_{ATP} channel opening and altered pharmacology in sepsis was due to disruption of F actin into G actin.

b) A direct NO effect. The role of NO in endotoxin-induced vascular reactivity is well established (Thiemermann & Vane, 1990) and this has been demonstrated to be due to K_{ATP} channel opening, via a cGMP pathway (O'Brien, 2001; O'Brien, 2005; Wilson, 2002). NO also causes disruption of the actin cytoskeleton (Banan, 2000; Chakravortty, 2000; Sandau, 2001; Aslan, 2003). I hypothesised that NO caused altered pharmacology via a direct NO effect on the channel.

c) Metabolic derangement. K_{ATP} channels are inhibited by intracellular ATP (Yamada, 2000; Fujita, 2000) and opened by intracellular NDP. Metabolic derangement, with altered ATP levels, has been demonstrated in sepsis (Brealey et al., 2002; Brealey et al., 2004). I hypothesised that altered

levels of ATP and ADP in rat thoracic aorta caused increased opening and altered pharmacology of K_{ATP} channels in sepsis.

Aims of Study:

1). To develop a technique for semi-quantifying the actin-cytoskeleton in rat aorta and mesenteric artery vascular smooth muscle using confocal microscopy and immunohistochemistry.

2). To semi-quantify levels of F and G actin in vascular smooth muscle using Western blotting techniques.

3). To assess the effects of sepsis on the actin cytoskeleton using an *in vitro* model of endotoxin incubation.

4). To compare results in 3) against those with a NO donor.

5). To assess parallel effects upon K_{ATP} channel function using specific activators and inhibitors of the sulphonylurea receptor and ion channel pore subunits.

6). To measure ATP, ADP & AMP levels in thoracic aorta taken from an *in vivo* model.

All work complied with the Animals (Scientific Procedures) Act 1986 and the Home Office Project License that gave authority for the work.

Chapter Two

Materials

&

Methods

2.1 Animal dissection

For the *in vitro* model of sepsis, rings of aorta and mesenteric artery were obtained from male Sprague Dawley rats (200-300g, Charles River, UK) sacrificed according to Schedule 1 of the Animals (Scientific Procedures) Act 1986 and the Home Office License for this project. The animals were stunned with a blow to the head and sacrificed *via* cervical dislocation. The abdomen was then opened, the retroperitoneal cavity identified and then opened. Following identification of the superior mesenteric artery, the superior portion of the mesentery was carefully dissected and a length of it was then removed from its origin at the aorta to its distal portion. The abdominal aorta was then identified, and dissected free from the vertebrae, starting distally at the bifurcation of the iliac arteries and proximally to the diaphragm.

Each of the vessels was then placed in physiological salt solution (PSS) containing in mM: NaCl 112, KCl 5, $MgCl_2$ 1, $NaHCO_3$ 25, NaH_2PO_4 0.5, KH_2PO_4 0.5, glucose 10, $CaCl_2$ 1.8. The vessels were then further cleaned and cut into rings, 3-4 mm in length. These rings were then washed twice in sterile Dulbecco's Modified Eagle Medium (DMEM, Invitrogen, Paisley, UK) containing penicillin/streptomycin (pen/strep, 50 $U.ml^{-1}$/50 $\mu g.ml^{-1}$ respectively).

2.2 *In vitro* model of sepsis

Rings of aorta or mesenteric artery were incubated for 24 hr or 48 hr in 2 ml of DMEM containing 0.1μg/ml LPS (*Salmonella typhosa*, Sigma-Aldrich, Dorset, UK) and pen/strep at 37^{o}C, in a humidified atmosphere of 5% CO_2. Control tissue was incubated in DMEM alone. The addition of pen/strep was required because

initial experiments showed there was a significant degree of hyporeactivity in all control tissue at 48 hr when antibiotics were not added to the culture medium (data not included). The concentration of LPS used was based on pilot data based on previous studies done by Wilson et al. (Wilson et al., 2000) and O'Brien et al. (O'Brien et al., 2001).

2.3 *In vivo* model of sepsis

The established conscious *in vivo* model of faecal peritonitis previously published by our laboratory (Brealey, 2004) was used. Raymond Stidwell and Valerie Taylor carried out this model. Male Wistar rats at 14 weeks old (approx 300-350g) were anaesthetised with inhaled isoflurane. A midline incision was made over the anterior chest wall and catheters were inserted into the carotid artery and external jugular vein. These lines were then tunnelled beneath the skin and exited the rat over the back of the animal. This was then connected to a mobile, pivoted tether (fig.2.1). The rat was allowed to recover from surgery and anaesthesia for 24 hr.

The rat was then fluid resuscitated at a rate of 10 $ml.kg^{-1}.hr^{-1}$ using a mixture of 0.9 % saline and 5% dextrose, in a 1:1 ratio. Animals assigned to the septic group were then injected with a solution of faeces (0.625 ml/ 100g body weight) obtained from another male Wistar rat (Brealey et al., 2004). Time of injection was assigned "Time 0". The animal continued to have free access to food and water for the duration of the experiment. The rats were then sacrificed at either 24 hr or 48 hr time points. Appropriate controls were animals that underwent the same surgical procedure, but were not injected with faeces. Before death at

predetermined time points, rats were scored as having mild, moderate, or severe sepsis. The scoring assessed appearance, alertness, and blood pressure (Brealey et al., 2004). Mildly affected animals were hunched, alert, displayed piloerection, with a blood > 90 mmHg. Moderately affected animals were hunched, with marked piloerection, a bloated abdomen, sunken eyes, depressed level of alertness, decreased mobility and a lower blood pressure of 75 – 90 mmHg. Animals with severe sepsis had marked piloerection, a markedly bloated abdomen, depressed level of consciousness, no movement and a significant drop in blood pressure, < 75 mmHg (see Brealey et al., (2004)) for a more detailed description.

Tissue was then removed under deep anaesthesia at either 24 hr or 48 hr time points. For measurement of ATP, ADP and AMP levels thoracic aorta was removed and immediately frozen in liquid nitrogen. This was then processed as described below. Abdominal aorta was removed for functional organ bath studies and placed in HBSS.

A

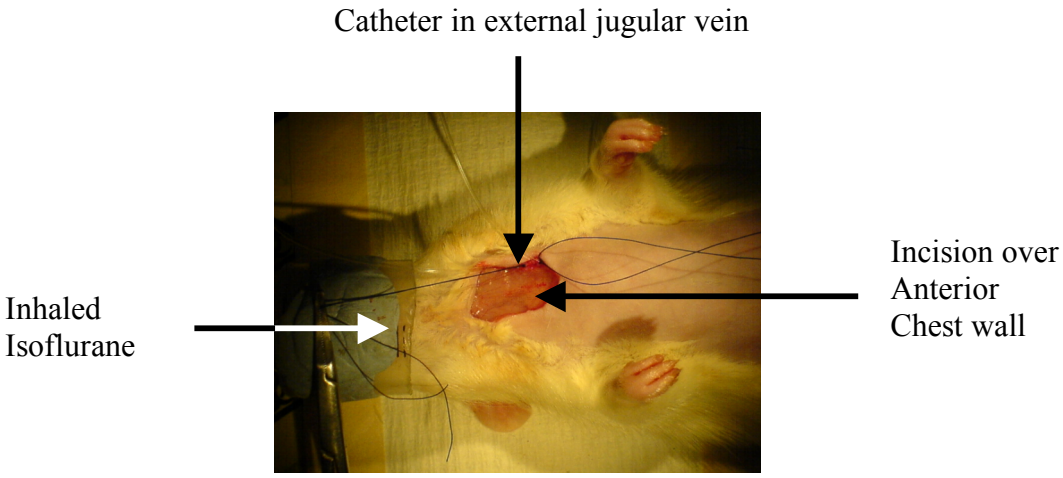

B

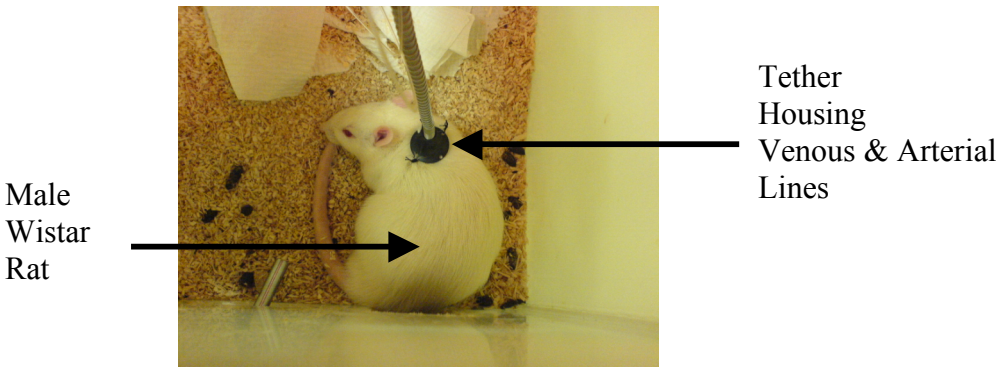

Fig. 2.1. A: Photograph of surgical insertion of venous line into the left external jugular vein in a male Wistar rat. The animal is deeply anaesthetised using inhaled isoflurane. **B:** Photograph of a male Wistar rat recovering from surgery, with the tunnelled lines exiting from the animals back. The lines are tethered to a pivoted arm above the cage, allowing the animal to move freely within its cage.

2.4 Organ bath Studies

Measurement of isometric tension in rat mesenteric artery and aortic rings was achieved using the classical organ bath method. Intact rings of artery were suspended between two tungsten wires in a jacketed organ bath (25 ml volume) containing physiological salt solution, maintained at 37 ^{0}C, gassed with 95% O_2 / 5% CO_2. One of the wires was fixed to an external platform; the other was connected to an isometric force displacement transducer (FT-03, Grass Instruments, Astro-Med UK, Slough, UK) for measurement of tension. Tension was recorded using Powerlab Chart (version 4), a data acquisition and analysis program for biological systems (ADInstruments, Oxfordshire, UK). The aorta from a single animal was cut into eight rings and set up in 8 individual organ baths. The rings were maintained at a resting tension of 1g and equilibrated for one hour.

2.4.1 Endothelium intact experiments

Phenylephrine (PE, 1 μM) was used to contract the tissue (O'Brien & Wilson, 2001). Once the contraction had reached a plateau, acetylcholine (5 μM) was added and only those tissues showing relaxation > 50%, was endothelium considered functional (O'Brien & Wilson, 2001). After wash off of acetycholine, the tissue was further primed by the addition of KCl (50 mmol) and following several washes, tissues were further contacted with 1 μM PE. This was again washed off before the main experiments were carried out (O'Brien & Wilson, 2001).

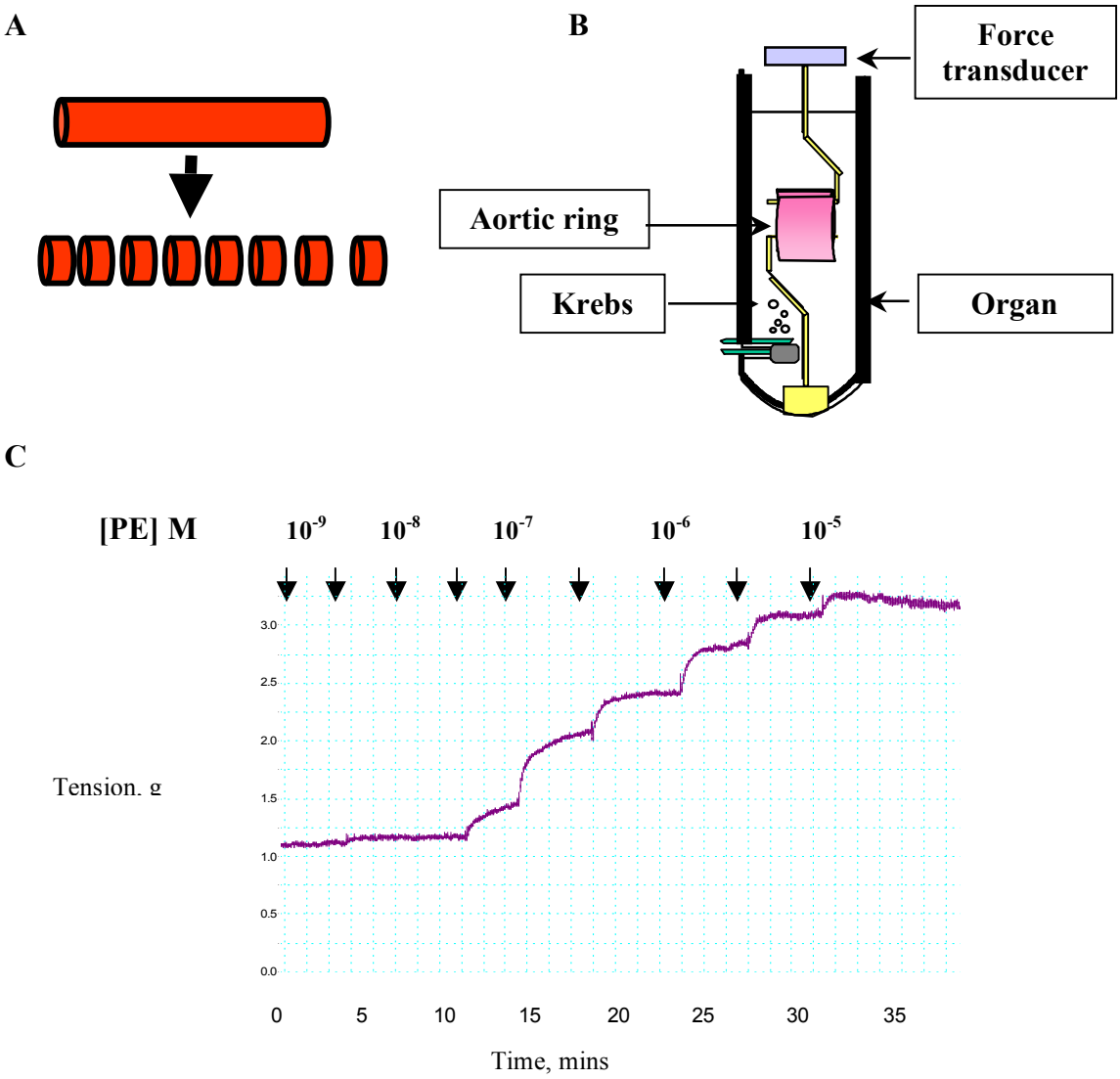

Fig 2.2: Schematic of a vessel (A) divided into rings, which were then mounted in the organ bath (B), where tension studies were carried out at 37°C in physiological salt solution (Krebs'). (C) A sample trace from a cumulative concentration-response curve to PE in a ring of mesenteric artery. The arrows indicate the time when each concentration of PE (10^{-9}-10^{-5} M) was added to the bath.

2.4.2 Functional assessment of blood vessels used in microscopy

Rings from the same vessels that were used in immunohistochemistry and confocal microscopy were examined in the organ bath. The tissue was set up and primed as described above and all experiments were performed in vessels where the endothelium remained intact. PE concentration-response curves were carried out (10^{-9} – 10^{-5} M) on fresh tissue and tissue from the 24 hr and 48 hr time points (± LPS, 1 μg.ml^{-1}) (O'Brien & Wilson, 2001). Therefore, the images obtained could be matched with known contractile responses in normal tissue (fresh tissue and 24 hr and 48 hr time controls) or from hyporeactive tissue (LPS treatment for 24 and 48 hr).

2.4.3 K_{ATP} channel pharmacology in an *in vitro* model of sepsis

Tissue obtained from the *in vitro* organ culture model of sepsis was placed in the organ bath, primed as described above, and then contracted with 1 μM PE. Once contractions had peaked, the K_{ATP} channel opener, levcromakalim (3 μM) was applied and when relaxation had reached a plateau, either PNU 37883A (10 μM) or glibenclamide (10 μM) were added to the organ bath (O'Brien & Wilson, 2001). Results were then displayed as percentage reversal of levcromakalim-induced relaxation. Concentrations of drugs used were based on pilot data (data not shown) and on previous studies done by Wilson et al. (Wilson et al., 2000) and O'Brien et al. (O'Brien et al., 2001).

2.4.4 Assessment of effects of Deta NO on K_{ATP} channel pharmacology

To investigate the direct effects of NO on the K_{ATP} channel, an NO donor (Deta NO) was used to replicate levels measured in an *in vitro* model of sepsis (O'Brien

et al., 2002). Tissue was incubated in DMEM (Invitrogen, Paisley, UK) with 10 μM Deta NO (Sigma Aldrich, Dorset, UK) for 20 hr. This concentration and time point was based on a calculation of the half-life of Deta NO at room temperature and pH 7.4 to be ~20 hr (Griffiths & Garthwaite, 2001) (fig.2.2). Previous data (O'Brien *et al*., 2002) suggested that the level of nitrite produced in the supernatant of a ring incubated with LPS for 20hr was 2 μM per mg of protein. Therefore, this was the desired level of nitrite in DMEM, reflecting the amount of NO that blood vessels would have been exposed to in organ culture with LPS. Levcromakalim (10^{-9} – 10^{-5} M) (O'Brien & Wilson, 2001) concentration-response curves were then carried out on abdominal aorta incubated for 20 hr in DMEM ± Deta NO (10 μM) to explore K_{ATP} channel pharmacology after exposure to a pure NO donor.

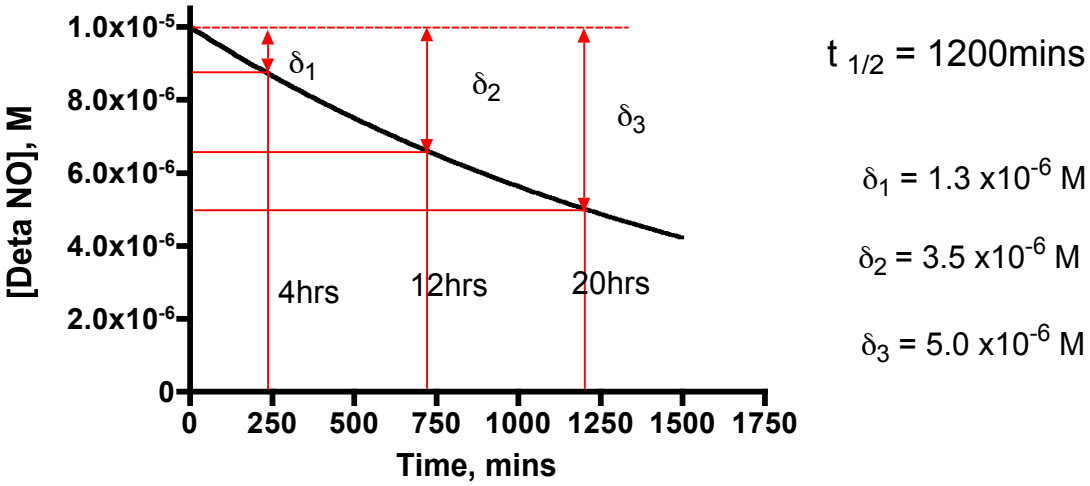

Fig 2.3: Theoretical decay curves for Deta NO, 37 °C, pH 7.4. At the 20 hr time point, an initial concentration of 10 µM Deta NO will break down by 50%, i.e. 5 µM. One mole of Deta NO releases 2 moles of NO. Therefore, the breakdown of 5 µmoles of Deta NO will release around 10 µmoles of NO.

2.4.5 K_{ATP} channel pharmacology in an *ex vivo* model of sepsis

Abdominal aorta from the male Wistar rats subjected to faecal peritonitis for 0, 24 and 48 hr were dissected out and placed in the organ bath and subjected to protocols as described in 2.4.1 above. Concentration-response curves were generated to PE and levcromakalim (10^{-9} – 10^{-5} M) to assess whether the tissue exhibited typical pharmacology seen in septic tissues (O'Brien *et al.*, 2002).

2.5 Immunostaining of frozen sections

My hypothesis states that sepsis decreases the polymerised (F) actin and may either increase or have no effect on the monomeric/dimeric (G) α actin. Immunohistochemistry was used to stain for F and G actin in abdominal aorta and mesenteric artery taken from male Sprague Dawley rats (250-300g, Charles Rivers, UK). These rings were placed in OTC embedding medium (Sakura, Berkshire, UK), snap frozen in liquid nitrogen and then cut at -20°C into 10 μm transverse sections using a cryotome (Model AS 620 SME, Thermo Shandon, Cheshire, UK). Sections were then placed on polysine-coated slides (BDH Laboratories, Poole, UK) and allowed to air-dry for 45 minutes. Following this, sections were outlined using a PAP Pentomark pen to provide a waterproof barrier for the immunostaining. These sections were then rehydrated in phosphate buffered saline (PBS) containing 0.02% bovine serum albumin (BSA) solution for three minutes. Subsequently they were permeabilised with PBS + 0.2% Triton X-100 for three minutes, followed by two successive 2 minute washes with PBS containing 0.02% BSA. So as to inhibit non-specific protein binding, the section was blocked with serum-free protein block (DAKO, California, USA) for 30 minutes. The surplus fluid was drained off (not washed) and either AlexaFluor

568 Phalloidin (1:40 dilution; 20 µl per section) or Texas Red-labeled DNAse I (20 µl per section) was applied to the sections and incubated for 45 minutes. Antibody concentrations were developed from pilot data (not shown). Following this, three successive 2 minute washes were carried out with PBS + 0.02% BSA. Finally, the sections were fixed using 5% formal-saline for five minutes, before being washed with distilled water and air-dried for 45 minutes. Once dried, a drop of Vectashield (Vector Laboratories, California, USA) was applied and a cover slip placed on the slide. This was then sealed using nail varnish.

2.6 Confocal microscopy

Confocal microscopy was used with a view to assess changes in the actin cytoskeleton using an image quantification method. This presented a number of methodological challenges. The majority of confocal imaging is performed on cells rather than tissue. In addition, confocal microscopy is normally utilised in a semi-quantitative fashion and my aim was to develop a reproducible, quantitative method of obtaining and analysing confocal images. Images were taken from transverse sections of aorta to determine the optimum laser and confocal settings to quantify both F and G actin. An initial problem was how to focus on tissue sections, and from which area of this tissue should one obtain images in a non-biased fashion. Focusing on the elastin layer of vessels solved this, which autofluoresces in the green spectrum (488 nm), most likely to be due to the presence of several fluorescent compounds, including a cross-linking tricarboxylic amino acid with a pyridinium ring (Deyl et al., 1980). Focusing on the elastin also helped to delineate the boundaries of the image. The initial experimental design had been to image F and G actin simultaneously in the same sections. However,

the majority of the commercially available actin flurophores emit light in the green (488nm) and red (568nm) spectra. Since elastin autofluorescence precludes the use of fluorophores emitting in the green spectrum, I was forced to look at F and G actin in separate sections because it was not possible to separate out signals from probes emitting in the red spectra.

Alexa Fluor-568 Phalloidin (Molecular Probes, Amsterdam, Europe) was used to stain for F actin. 20 μl of a 1:5 dilution of the fluorophore was used per section of tissue (concentration developed from pilot data, not shown). This was then stimulated using a green Helium/Neon laser at 543 nm. A long pass filter was set at 560 nm, with a short pass filter at 570/590 and all emission above this was captured. Images were obtained (x60 magnification with a water immersion lens) *via* a confocal microscope (Bio-Rad Radiance 2100) using Lasersharp 2000 image acquisition software (Bio-Rad, Hemel Hempstead, UK) and staining quantified using Laserpix software (Bio-Rad, Hemel Hempstead, UK). G actin was identified using Texas Red- labelled DNAse I (Molecular Probes, Amsterdam, Europe) with 20 μl of a 10 mg/ml stock used per tissue section and incubated for 45 min at room temperature (concentration developed from pilot data, not shown). The slides were then stimulated using the green Helium/Neon laser, using the same wavelengths and filters as above.

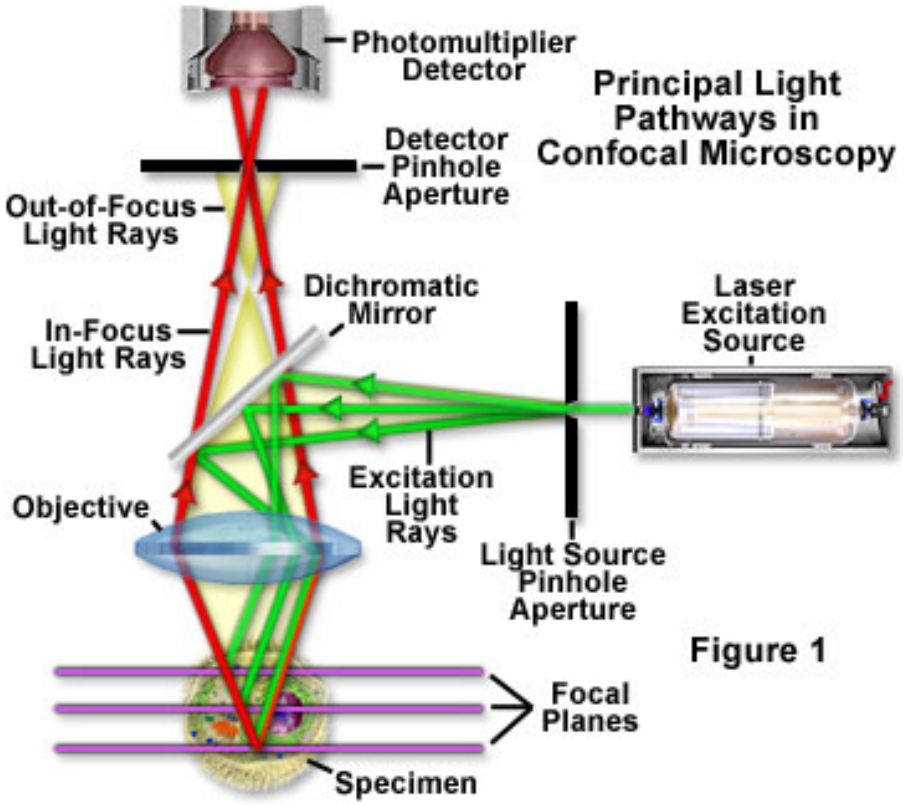

Fig 2.4: Light pathways used in confocal microscopy (Biorad). Only focused light is seen by the photomultiplier detector, as opposed to other microscopes, which allow unfocused light through. This enables tissue sections to be examined in steps of 1 μm thickness at a time if desired.

2.7 Tissue homogenisation and alpha actin separation

Biochemical quantification of the levels of F and G actin was carried out according to the detailed method previously published (Hall *et al.*, 2000). Briefly, the abdominal aortae from male Sprague Dawley rats were weighed, then finely chopped and placed in 10 ml of extraction buffer (100mM KCl, 2mM EGTA, 1mM $MgCl_2$, 0.5% Triton-X 100), which also contained one protease inhibitor tablets, (Complete mini, EDTA-free, Roche, UK). Phalloidin (10μg.ml^{-1}) (Sigma, Dorset, UK) was added to the cold (4 ^{o}C) extraction buffer and allowed to permeate the chopped tissue in order to stabilise the F actin content of the vessel thereby inhibiting seepage into the extraction buffer (Hall *et al.*, 2000). This sample was not homogenised, but allowed to sit in the phalloidin-containing buffer on ice. The supernatant, assumed to contain some F but mainly G actin, was decanted after a 4 hr incubation and spun at 350,000g at 4^{o}C at for 90 minutes. Following centrifugation, the secondary supernatant was removed and assumed to only contain G actin (Hall *et al.*, 2000). The remaining chopped tissue, post decanting of the supernatant, was blotted dry, weighed and placed in further extraction buffer (20 μl of buffer per mg of tissue) before being homogenised in a glass mini-homogeniser (Kontes, New Jersey, USA). This sample was taken to represent total F actin in the tissue sample. It was assumed that all G actin was extracted from the tissue, while all F actin was stabilised within the tissue during the 4hr incubation period. See fig. 2.5 for a summary of this method. Filamentous (F) actin consists of polymerised monomeric (G) actin, has a greater mass and can therefore be separated by centrifugation.

The final method used for separating F and G actin had an additional step of centrifuging the homogenised sample (theoretically F only) at 260,000g for one hour at 4 ^{o}C (fig.2.5). This step was added because the positive controls contained not just F actin in this sample, but additional G actin, indicating insufficient separation of F and G prior to homogenisation. Therefore, the additional centrifugation step was used to remove this contamination of the F actin pellet by G actin (see results section).

2.8 Western Blotting

Protein samples (normalised to volume) were run on an SDS-Page gel. This consisted of a resolving gel (7.5% acrylamide, 1.5 M Tris base, 10% SDS, 10% ammonium persulphate (APS), TEMED, pH 6.8) and a stacking gel (5.36% acrylamide, 1.0 M Tris base, 10% SDS, 10% APS, TEMED, pH 8.8). The gels were run on ice, at 200 V, for one hour in high-salt running buffer (SDS 3.5 mM, Tris base 24.8 mM, glycine 193 mM). These gels were then cold-transferred electrophoretically to nitrocellulose membranes (Hybond, Amersham Biosciences, Buckinghamshire, UK) at 4^{o}C for 3 hours, in transfer buffer (SDS 1.3 mM, Tris base 48 mM, glycine 39 mM, methanol (20% v/v)). Blots were then blocked overnight with blocking buffer (PBS, 0.1% Tween, 400 μg I-Block (Tropix, MA, USA)), washed with PBS, and stained with mouse monoclonal antibody (1:50,000 in blocking buffer) to α actin (mouse monoclonal anti-actin, alpha smooth muscle; Sigma-Aldrich, Dorset, UK) for one hour (antibody concentration developed from pilot data, not shown). These were then washed four times with washing buffer (PBS, 0.1% Tween) for 15 minutes each. Secondary anti-mouse antibodies, at a 1:5000 dilution (peroxidase-labelled,

Amersham Biosciences, Buckinghamshire, UK) were then applied for one hour. This was again washed with washing buffer, as above. All antibodies were dissolved in blocking buffer. The gels were stained using the ECL Western Blotting chemiluminescence immunoblot detection system (Amersham Biosciences, Buckinghamshire, UK). These were then exposed to Hybond ECL photosensitive films (Amersham Biosciences, Buckinghamshire, UK) and then developed. Typical exposure times were from 5 secs to 1 min 30 secs.

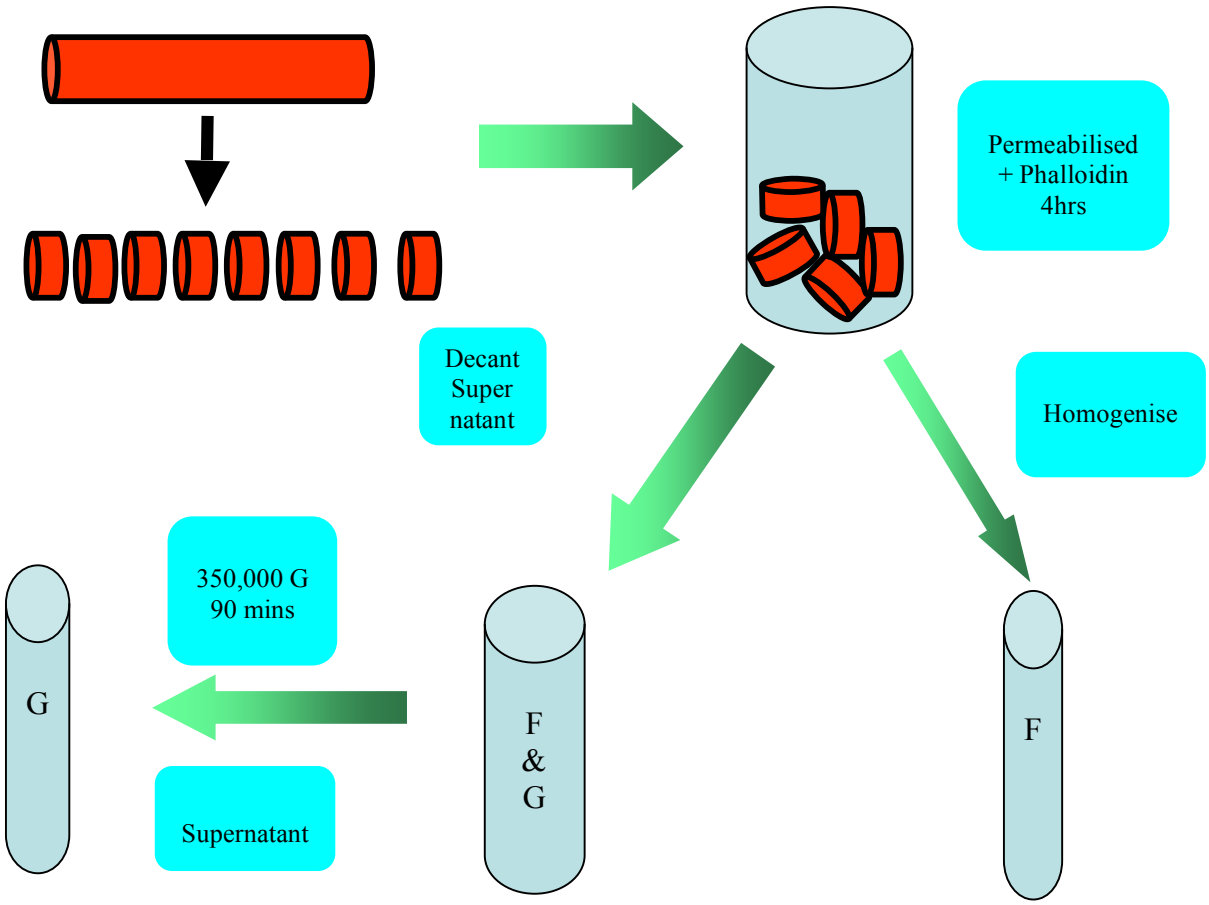

Fig 2.5: Separation of F & G Actin: Schema demonstrating the method for separating F and G actin, as per protocol published by Hall et al (2000) (Hall *et al.*, 2000). The vessel is finely chopped and incubated in phalloidin for 4 hr. The supernatant is then decanted; this represents F and G actin. G is further extracted by centrifugation. The finely chopped vessel is then homogenised, representing the F actin fraction.

2.9 Griess Assay

The Griess assay is a method for the quantification of nitrite (NO_2^-) in a variety of solutions, including cell culture media. NO is unstable therefore NO_2^- is used as a marker of its production. The Griess reaction is based on a diazotisation reaction, with the production of a coloured azo compound. This is concentration-dependent and hence colorimetric measurement of the azo compound allows quantification of nitrite, which is then used as a surrogate marker for NO production.

Nitrite measurements were carried out on culture media using the Griess assay (Alexis Corporation, Nottingham, UK) (method as per O'Brien & Wilson, 2001). Briefly, 100 µl of media was placed in a 96 well plate. 50 µl of Griess assay solution 1 (0.1% naphthylethylenediamine dihydrochloride in distilled water) was added, with 50 µl of Griess assay solution 2 (1% sulfanilic acid in 5% concentrated H_3PO_4). This was carried out in triplicate, with an appropriate series of standards (1 µM- 100 µM) produced by the serial dilution of sodium nitrite solution (fig.2.6). The samples were mixed on a rotating plate and left for 15 mins. The plate was then placed in a spectrophotometer (Opsys MR, Dynex Technologies, Worthing, UK) and absorbance measured at 540 nm.

Deta NO was used as a direct NO donor to assess the effects of NO on the pharmacology of the K_{ATP} channel. For the Deta NO experiments, 10 µM Deta NO was dissolved in DMEM and rings of endothelium-intact rat aorta were placed in 2 ml of media in 6 well plates for 20 hr. After this time period, the supernatant was then taken and analyzed as described above.

Nitrite quantification was also carried out on the supernatant from tissues used in the *in vitro* organ culture model of sepsis. The aim was to quantify nitrite levels produced by that model, thus validating 10 μM Deta NO as producing a similar amount of NO. This is demonstrated in fig.3.10.

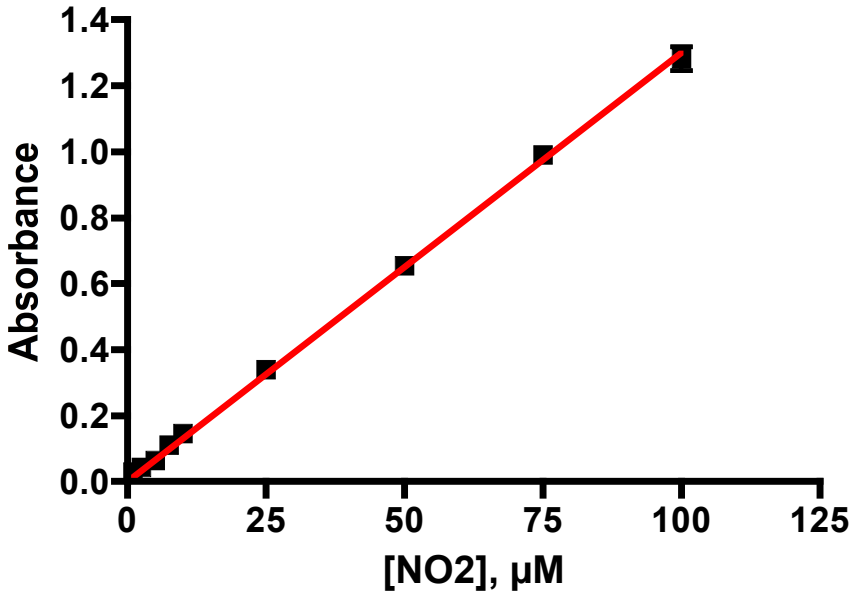

Fig 2.6: Example standard curve of nitrite concentration against absorbance at 540 nm, mean ± SEM, samples are in triplicate.

2.10 Protein assay

Protein assays were carried out using the Lowry Method, with the BioRad DC protein assay solutions and carried out according to manufacturer's guidelines (BioRad, Hemel Hempstead, UK). Measurements were carried out on tissue homogenised using a glass homogeniser (Kontes, New Jersey, USA). The tissue was placed in a buffer, containing protease inhibitors (Complete Mini Protease Inhibitor Cocktail, without EDTA, Roche, Hertfordshire, UK) and homogenised on ice. The homogenate was then stored at -80^{o}C until used in the protein assay.

Briefly, 5 µl of homogenate was placed in a 96 well plate. 25 µl of solution A[1] (20 µl of solution S added to every 1 ml of solution A) together with 200 µl of Protein assay solution B (BioRad, Hemel Hempstead, UK) was added. This was carried out in triplicate, with an appropriate series of protein standards (1 - 2,000 µg.ml^{-1} BSA) analyzed at the same time. Standard curves were produced and protein in tissue homogenates calculated from linear regression, see fig.2.7.

The samples were mixed on a rotating plate and left for 15 mins. The plate was then placed in a spectrophotometer (Opsys MR, Dynex Technologies, Worthing, UK) and the plate read at 640 nm.

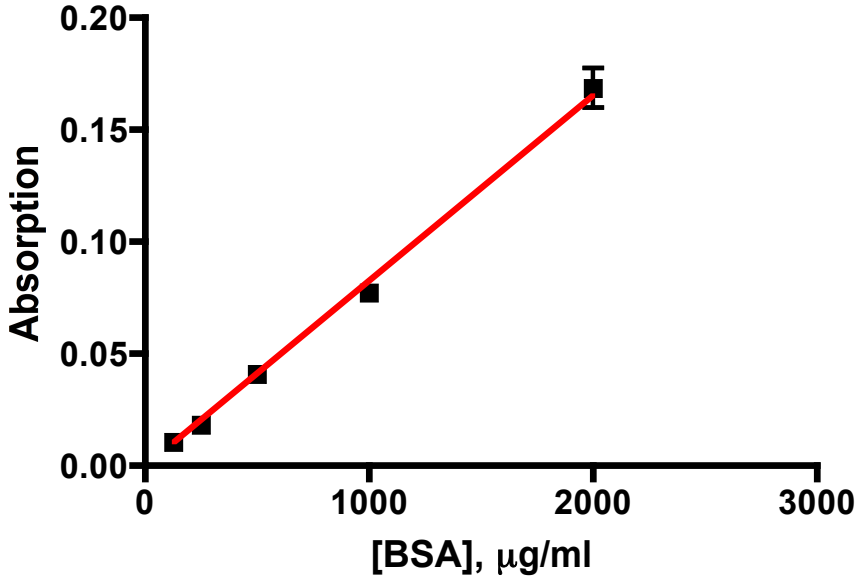

Fig 2.7: Protein standard curve. Sample standard curve from the BioRad protein assay, with absorption at 640 nm against concentration of BSA, $\mu g.ml^{-1}$.

2.11 Tissue sample preparation for HPLC

Tissue was collected from animals deeply anesthetised with isofluorane and immediately frozen and stored in liquid nitrogen. The tissue was stored in a cryovial until ready for freeze-drying. The lid of the cryovials were perforated and rapidly transferred to a freeze dryer pre-chilled at -90°C and left there for 48 hr. The lids of the cryovials were replaced and the tissue was then stored at -80°C.

For the preparation of the homogenate, approximately 20mg of freeze-dried tissue was weighed and transferred into an ice-cooled ground-glass homogeniser (volume 1.5 ml). The weight was multiplied by 25, which gave the volume in millilitres of 0.4M perchloric acid that was added to the tissue. The tissue was then homogenised using a mechanical SS10 stirrer (Stuart Scientific, UK) at a speed of 500 RPM. Subsequently, the homogenate was transferred to an eppendorf tube and centrifuged at 4°C for 3 minutes.

After transferring the supernatant into another cooled eppendorf tube, the pH of the extract was adjusted to 6.0 using 2M potassium hydroxide and pH strips (Sigma-Aldrich, Poole, Dorset, UK). The solution was once more centrifuged at 4°C for 3 minutes, and the supernatant was then stored at -80°.

2.12.1 High performance liquid chromatography

The frozen homogenate of aorta was thawed for 30 minutes before injection of 20 µl of sample into the chromatography system. Care was taken to remove all air bubbles from the HPLC system before running samples in triplicate. Samples were controlled by an SCL-10A (Shimadzu, Tokyo, Japan) controller unit, which

was interfaced with a PC. The sample injector (SIL-10AD, Shimadzu, Tokyo, Japan) also regulated the temperature of the samples, maintained at 19^{o}C. These samples were then passed through a UV-detector (SPD-M10A, Shimadzu, Tokyo, Japan) and collector (FRC-10A, Shimadzu, Tokyo, Japan) (See fig. 2.8).

2.12.2 HPLC Buffers

The whole system was continuously flushed with phosphate buffers (A and B), at a rate of 1 ml.min^{-1}, to optimise preservation of the adenine nucleotides. Buffer A consisted of 150 mM potassium dihydrogen orthophosphate solution and 150 mM potassium chloride solution, adjusted to pH 6.0 with potassium hydroxide. Buffer B was a 15% (v/v) solution of acetonitrile in buffer A. The amount of buffer B was changed linearly between the following time points: 0 minutes 0%, 3.5 minutes 9%, 5 minutes 100%, 7 minutes 100%, 7.1 minutes 0%. The re-equilibration time was 4.9 minutes resulting in a cycle time of 12 minutes between injections.

Chromatographic separation was performed using a C18 reversed-phase column (5 RPC 4.6/150 analytical column, Amersham, Buckinghamshire, UK). Sample peaks were analysed using a chromatography data system, with the adenine nucleotide peaks monitored at 254 nm. The retention time and height of the peaks were analysed, with the adenine nucleotide concentrations derived from standard curves. Selections of samples were spiked with a suitable concentration of standard to demonstrate that the peaks identified the correct nucleotides.

2.12.3 Adenine nucleotide standard solutions

Stock standard solution were prepared in 0.4M perchloric acid and adjusted to a pH of 6.0 using 2M potassium hydroxide and stored at -20°C. Fresh solutions were made before each assay, adding 0.4M perchloric acid adjusted to a pH of 6.0 using 2M potassium hydroxide. Standard solutions covered the range from 0.5 to 20 nM for ATP, ADP and AMP.

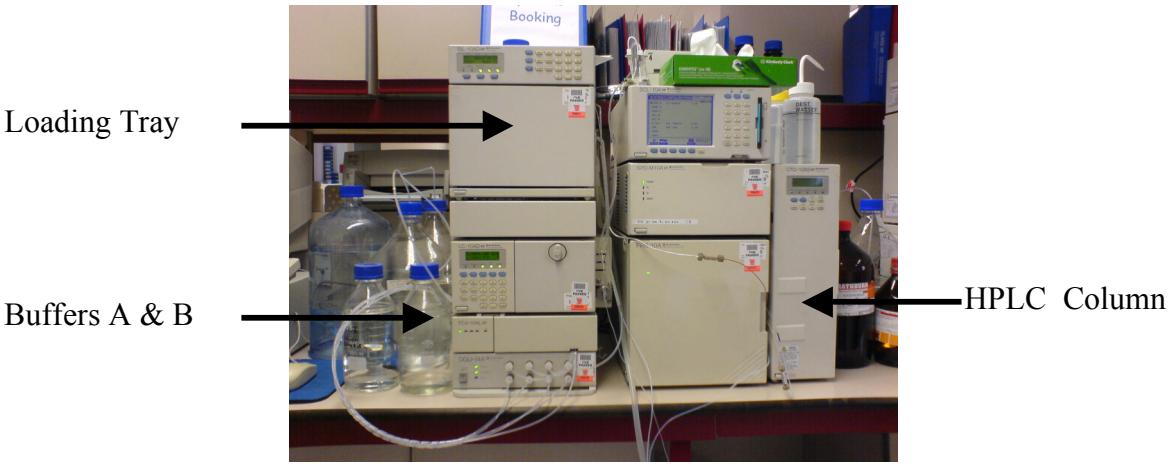

Fig 2.8: The actual HPLC apparatus and setup used in the laboratory

2.13 Drugs and solutions

All drugs were prepared and diluted in water, unless stated otherwise. Cytochalasin D, glibenclamide, jasplakinolide, levcromakalim and PNU 37883A were all diluted in dimethyl sulphoxide (DMSO). The final concentration of DMSO in experimental solutions did not exceed 0.2% (v/v). This was shown not

to affect experimental results. Deta NO (Sigma-Aldrich, Poole, Dorset, UK) was dissolved in PBS.

All chemicals were purchased from Sigma-Aldrich (Poole, Dorset, UK) unless otherwise stated. All antibodies were purchased from Molecular Probes (Amsterdam, Netherlands) and usually diluted in blocking buffer except Alexa Fluor 568 Phalloidin, Anti-α actin antibody, DNAse 1 antibody, were all dissolved in PBS.

Physiological salt solution (PSS) containing in mM: NaCl 112, KCl 5, $MgCl_2$ 1, $NaHCO_3$ 25, NaH_2PO_4 0.5, KH_2PO_4 0.5, glucose 10, $CaCl_2$ 1.8.

2.14 Statistical analysis

All data are represented as mean ± SEM of n observations. Organ bath data was analysed and plotted with a non-linear curve fit and calculation of the EC_{50} using Graphpad Prism 4 (California, USA). These concentration-response curves were adjusting for matching and analysed for variance using two way ANOVA. Confocal microscopy data, generated by LaserPix, was analysed using Student's T test. Significance was set at $P < 0.05$.

Chapter Three

Does cytoskeletal disruption occur in an *in vitro* model of sepsis?

As mentioned in the introduction, the role of K_{ATP} channels in sepsis is well established (Landry & Oliver, 1992; Sorretino et al., 1999). However, the mechanism of their activation in sepsis is not well understood. The cytoskeleton is involved in the regulation of ion channels in various tissues (Strege et al., 2003; Schwiebert et al., 1994; Terzic & Kurachi, 1996), including vascular smooth muscle cells (Loffler-Walz and Quast 1998). Nitric oxide, the production of which is increased in sepsis, causes disruption of cytoskeletal proteins (Chakravortty & Kumar, 2000; Sandau et al., 2001). I therefore sought to investigate if cytoskeletal disruption was one of the mechanisms of K_{ATP} channel dysfunction in sepsis.

3.1 Investigation of the cytoskeleton in an *in vitro* model of sepsis

The role of the cytoskeleton in controlling K_{ATP} channel function was assessed by examining the actin cytoskeleton of rat abdominal aorta and mesenteric artery. I sought proof that the actin cytoskeleton is disrupted in vascular smooth muscle cells in sepsis. This was done using an *in vitro* model of sepsis, in tissues where vascular hyporeactivity was confirmed using the organ bath technique (as described in Chapter 2). Cytoskeletal organisation was examined in two ways; first with immunohistochemistry examining F and G actin in frozen sections and imaged *via* confocal microscopy, and second, by Western blot analysis of F and G actin levels.

3.1.1 Vascular Hyporeactivity in an *in vitro* model of sepsis

Figure 3.1 displays contractile responses to phenylephrine (PE) obtained in fresh mesenteric artery and fresh aorta over a concentration range (10^{-9} -10^{-5}), as per O'Brien & Wilson (2001). Mesenteric artery responsiveness to the same agonist

in the *in vitro* model of sepsis is shown in fig. 3.2. In fig. 3.2A, the concentration-response curve to PE for tissue incubated for 24 hrs is shown, with controls incubated in DMEM (n = 9) alone and septic tissue incubated in DMEM containing 0.1 $\mu g.ml^{-1}$ LPS (n = 10). The control tissues responded to PE with a similar EC_{50} value (3.91 $x10^{-9}$ M) to that of arteries (6.79 $x10^{-9}$ M) not incubated in DMEM (described as "fresh"). However, the rings of tissue incubated in LPS were profoundly unresponsive to PE, barely giving any contractile response even to concentrations as high as 10^{-5}M. This supported the validity of the *in vitro* model of sepsis in mesenteric artery at 24 hrs.

By contrast control tissues incubated for 48 hr in DMEM demonstrated that PE was less efficacious and 10 times less potent, with a significantly lower maximal (Emax) contraction (0.4g vs 1.1g in fresh controls) and a higher EC_{50} value of 1.20 $x10^{-8}$M (fig 3.2B). This was either due to a greater degree of tissue damage to the mesenteric artery following 48 hr incubation or due to iNOS induction, which may be secondary to infection. Despite this, the contraction to PE was greater in tissues incubated in LPS for 48 compared to 24 hr (0.3g of tension compared to < 0.1g tension at 10μM PE, respectively fig. 3.3), which is consistent with previous findings from this laboratory whereby little hyporeactivity to PE was observed in tissues incubated for 48 hr in DMEM with 1 $\mu g.ml^{-1}$ LPS (O'Brien, 2001).

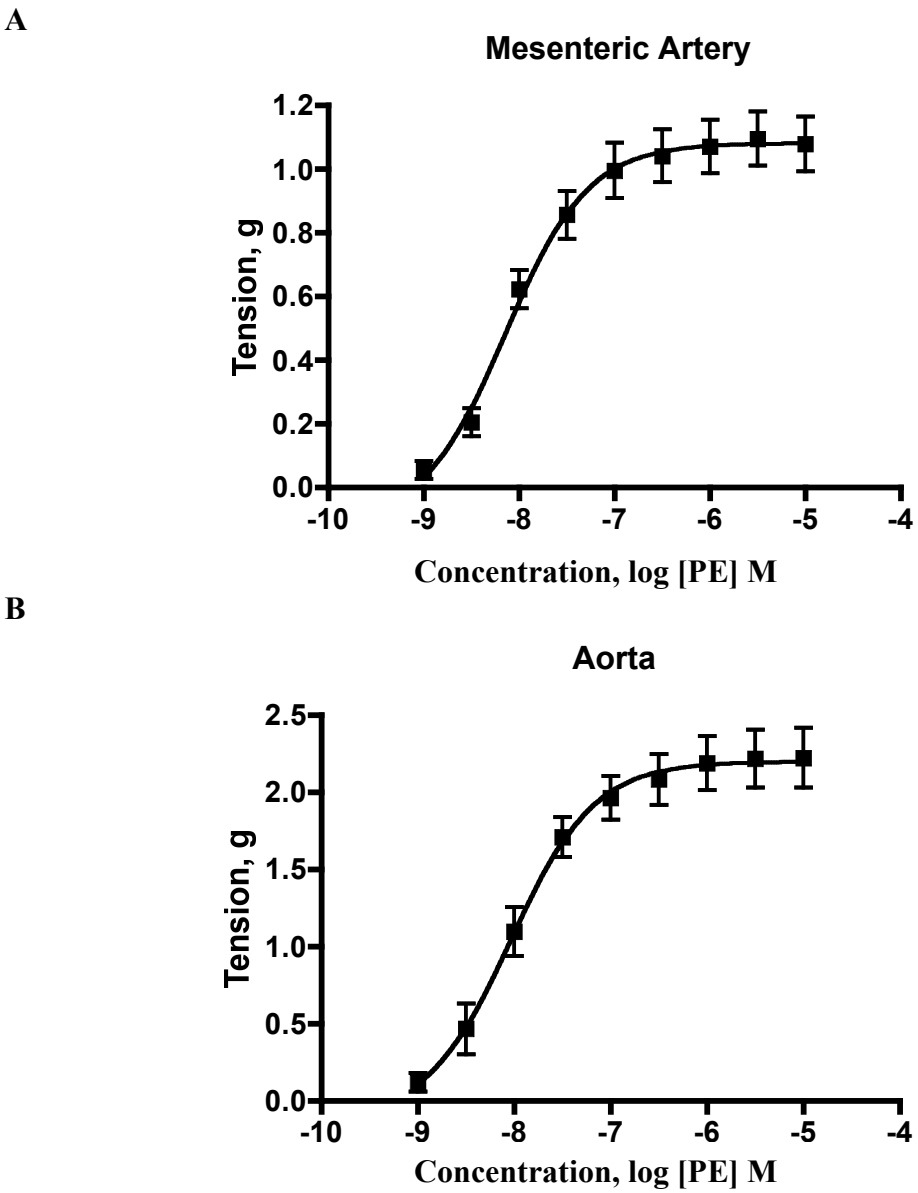

Fig 3.1. **Concentration-response curves to phenylephrine obtained in fresh tissue.** Phenylephrine (PE 10^{-9} – 10^{-5}M) was applied in a cumulative fashion to the organ bath. Concentration-response curves are shown for mesenteric artery (A) and aorta (B), giving EC_{50} values of 6.79 x10^{-9} M (n=15) and 9.17 x10^{-9} M (n = 10) respectively. All data are expressed as mean tension ± SEM.

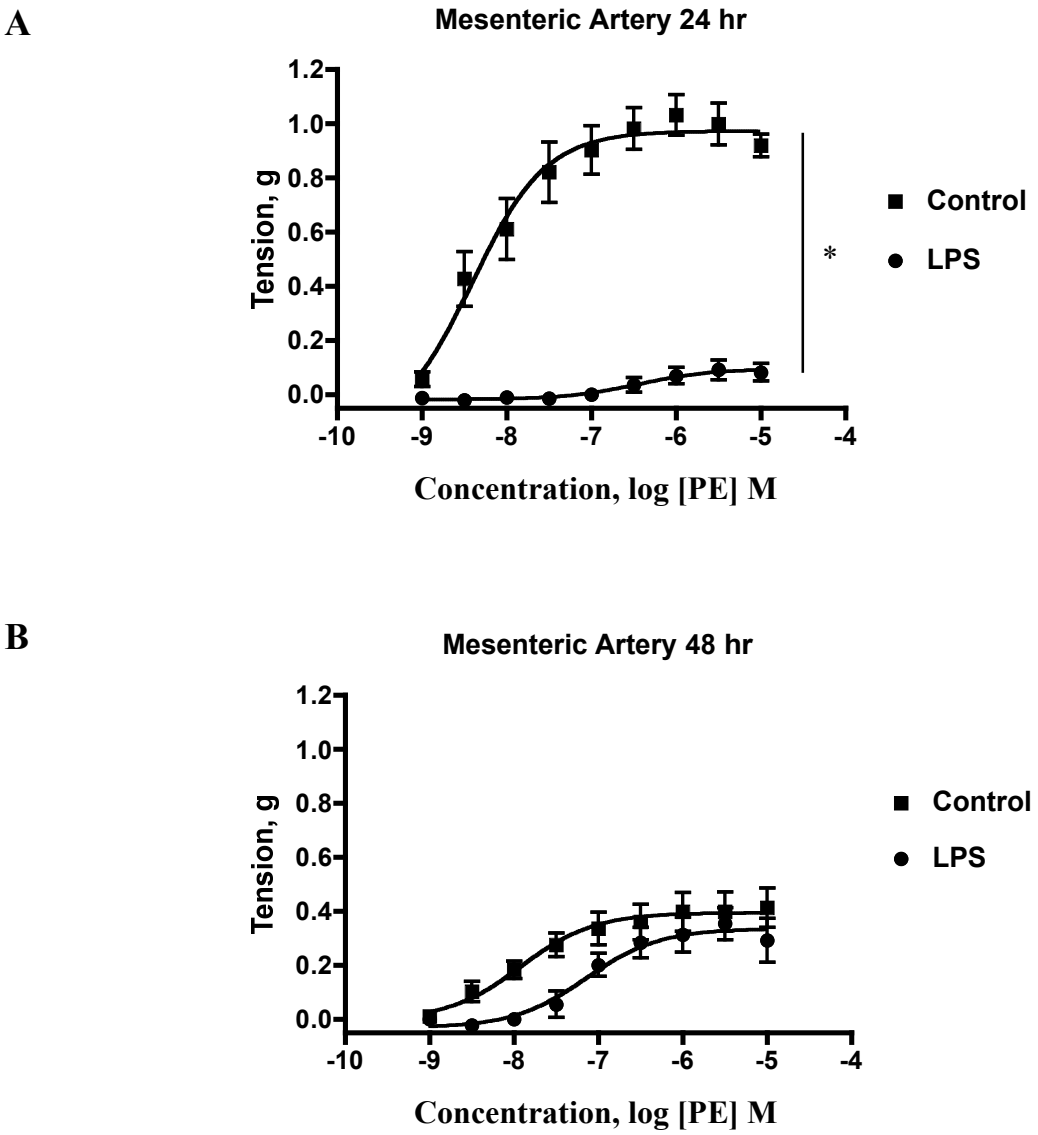

Fig 3.2. **Phenylephrine concentration-response curves in mesenteric artery following 24 or 48 hr incubation in absence or presence of LPS (0.1 μg.ml^{-1}).** Phenylephrine (PE 10^{-9}–10^{-5} M) was added in a cumulative fashion to mesenteric arteries incubated for 24 hr (A) and 48 hr (B) in DMEM ± 0.1 μg.ml^{-1} LPS. The curves in (A) are significantly different ($P < 0.0001$, *) but not in (B) ($P > 0.05$). Data are expressed as mean tension ± SEM. n = 10 (24 hr Control), n = 9 (24 hr LPS), n = 6 (48 hr Control), n = 4 (48 hr LPS).

The results of aortic vascular reactivity in the long term *in vitro* model of sepsis are shown in fig. 3.3. In fig. 3.3A, the concentration-response to PE for tissue incubated for 24 hr is shown, with controls incubated in DMEM for 24 hr (n = 8) and septic tissue incubated in DMEM with 0.1μg.ml^{-1} LPS (n = 8). The septic tissue was almost completely unresponsive to PE. This supported the pharmacological validity of the *in vitro* model of sepsis in rings of aorta at 24 hr. The data were obtained from eight rings of aorta, taken from different animals, with pairing of the control and LPS rings. Aorta incubated for 48 hr (fig. 3.3B) had an EC_{50} of 4.15 x10^{-8} M in controls, with a similar maximum contraction seen in 24 hr controls. Again, the rings incubated in LPS were completely hyporeactive, with a maximal response < 0.1g. The data were obtained from four rings of aorta, representing four different animals, with pairing of the control and LPS rings. Fig 3.4 demonstrates Levcromokalim concentration-response curves in an *in vitro* model of sepsis in rat aorta in presence or absence of LPS. Aorta was incubated for 24 hr (A) and 48 hr (B) in DMEM ± 0.1 μg.ml^{-1} LPS after which levcromokalim (PE 10^{-9}–10^{-5} M) was added in a cumulative fashion to aortic rings. At both incubation time points, relaxation responses to Lev in the presence of LPS were significantly increased compared to control ($P < 0.001$). This therefore demonstrated that the *in vitro* model of sepsis demonstrated abnormal K_{ATP} channel pharmacology, with increased K_{ATP} channel opening.

A

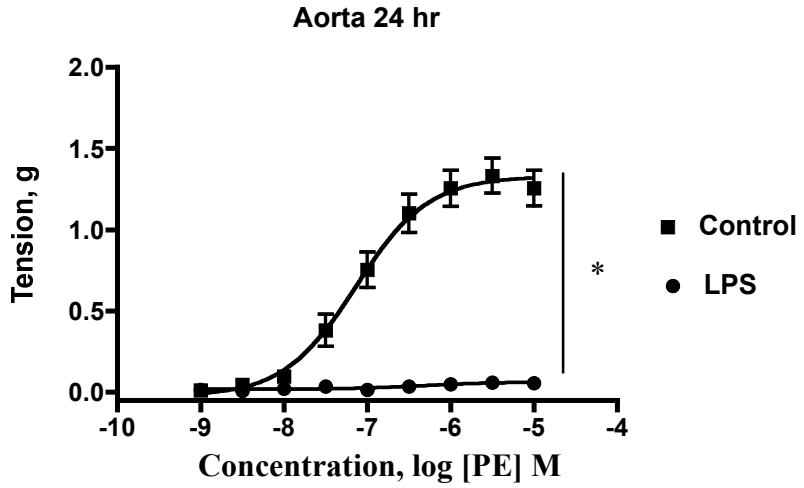

B

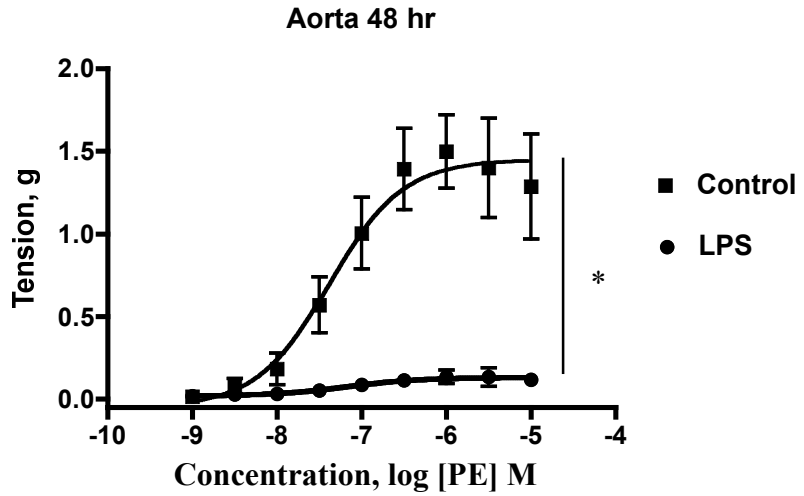

Fig 3.3: **Phenylephrine concentration-response curves in an *in vitro* model of sepsis in rat aorta in presence or absence of LPS.** Aorta was incubated for 24 hr (A) and 48 hr (B) in DMEM ± 0.1 μg.ml^{-1} LPS after which phenylephrine (PE 10^{-9}–10^{-5} M) was added in a cumulative fashion to aortic rings. At both incubation time points, contractile responses to PE in the presence of LPS were significantly depressed compared to control ($P < 0.001$, *). Data are expressed as mean tension ± SEM, n = 8.

A

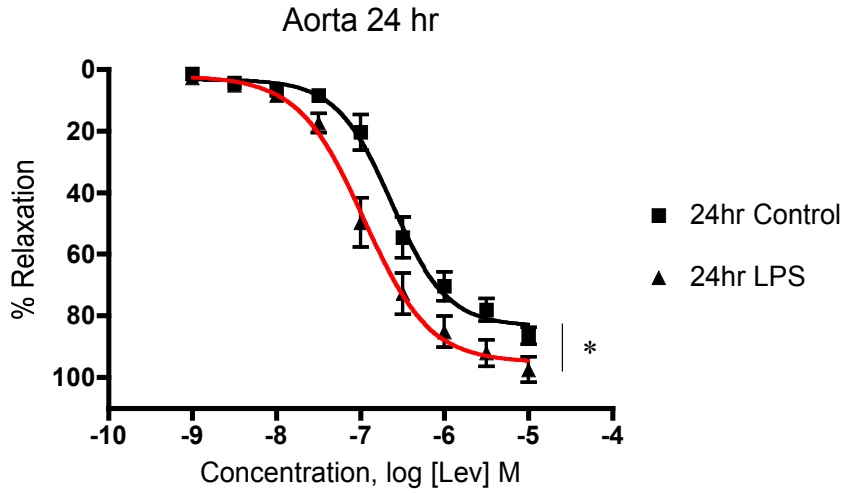

B

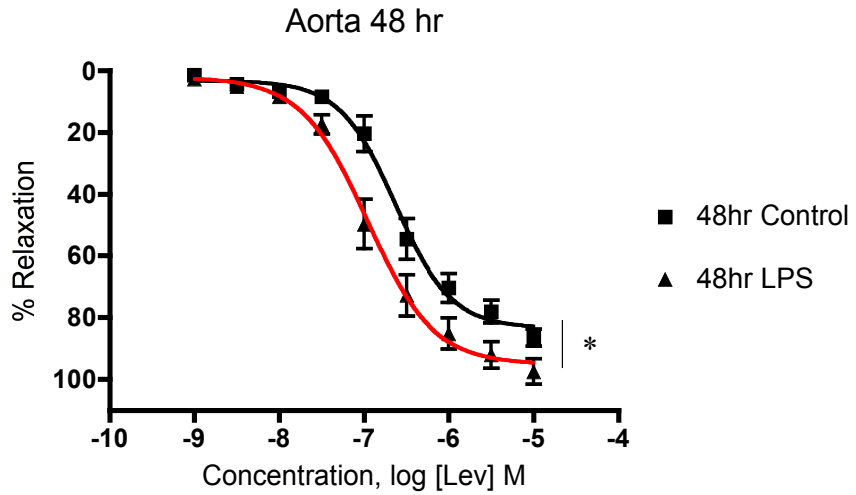

Fig 3.4: **Levcromokalim concentration-response curves in an *in vitro* model of sepsis in rat aorta in presence or absence of LPS.** Aorta was incubated for 24 hr (A) and 48 hr (B) in DMEM ± 0.1 $\mu g.ml^{-1}$ LPS after which levcromokalim (PE 10^{-9}–10^{-5} M) was added in a cumulative fashion to aortic rings. At both incubation time points, relaxation responses to Lev in the presence of LPS were significantly increased compared to control ($P < 0.001$, *). Data are expressed as mean tension ± SEM, n = 8.

3.1.2 Summary of functional assessment of *in vitro* model

Therefore, the results thus far demonstrate that the *in vitro* model of sepsis used was a valid model, demonstrating vascular hyporeactivity comparable to published data (Wilson, 2002; O'Brien, 2001; O'Brien 2005). It was also important to demonstrate that each piece of tissue used in the subsequent confocal imaging studies was functional and either a valid control or a valid representation of vascular smooth muscle from the *in vitro* model of sepsis.

3.2 Confocal microscopy

The previous results section demonstrated that the *in vitro* model of sepsis was valid, with confirmed vascular hyporeactivity consistent with data reported in the literature (Wilson, 2002; O'Brien, 2001; O'Brien 2005). Whilst each ring of aorta, from an individual rat, was assessed in the organ bath, another section of aorta from the same rat was snap frozen, subsequently sectioned and then stained according to the protocols detailed in the method section of the thesis (see Chapter 2). This ensured each image obtained by confocal microscopy was from the same aorta of known contractile function.

3.2.1 Confocal Method Development

A substantial portion of the confocal microscopy experiments represent method development, both the development of the image acquisition protocols, as well as the image analysis techniques. In preliminary experiments, tissue sections were cut to 20 μm thickness. However, the penetration and uniformity of the staining was variable so thinner (10 μm) tissue sections were used for all subsequent

experiments. This produced more uniform staining and thus all images displayed are 10 μm thick. The first set of images were taken from control vessels so as to optimise laser and confocal settings for these samples. Transverse rings of aorta were studied. Initial focussing of the slides was carried out on the elastic lamina to help determine the limits of the imaging boundaries and to limit fluorophore deterioration. As my hypothesis was that sepsis disrupts the actin cytoskeleton, the experimental protocol had to be sensitive enough to observe a decrease in F actin staining, and potentially, an increase in G actin staining. Initial experiments were carried out on control tissues where the fluorophores were excited such that the emitted signal did not saturate pixel intensity, and that the pixel saturation approximated to a normal distribution. This was achieved by examining images with Lasersharp 2000 software (Biorad, Hemel Hempstead, UK) and plotting a histogram of the pixel intensity. Once images were obtained that were normally distributed, the same laser and confocal microscope settings were strictly adhered to for all subsequent images. This enabled the direct comparison of F actin quantification between images and experiments carried out on different days.

In fig. 3.5 evolution of the method for confocal analysis is summarised. Once the control images were optimised, single images from each experimental tissue were obtained. The effect of LPS treatment on F and G actin staining was examined following a 24 hr and 48 hr incubation (n = 4 each, respectively). Based on the unacceptable size of the error bars in the initial experiments (data not shown) it was decided to take two images per section of tissue, henceforth known as the "two image" method. These were then analysed by the methods described in fig. 3.6. The results for this analysis are displayed in fig. 3.11. On further reflection, I

decided that two images per tissue section did not appear representative of the whole vessel. Therefore, all of the sections were re-imaged, this time taking images from three different regions per slide, with the use of the Kalman function (mean of three image acquisitions) and a Z stack across 5μm (in 1μm) steps. Henceforth, this acquisition method will be termed the KZ method. For this, previous tissue samples were re-sectioned and stained, and the results of the KZ method shown in fig. 3.14. This showed that quantitatively different results were obtained between the two analysis methods (compare fig. 3.11 vs fig. 3.14), with the former showing a decrease in F actin at the 24 hr time point, while the latter showing no change. Given this difference, a further three animals were used to obtain aorta incubated for 24 and 48 hr ± LPS (0.1 $\mu g.ml^{-1}$). These were again imaged by the KZ method and analysed via the AOI method and the results shown in fig. 3.15.

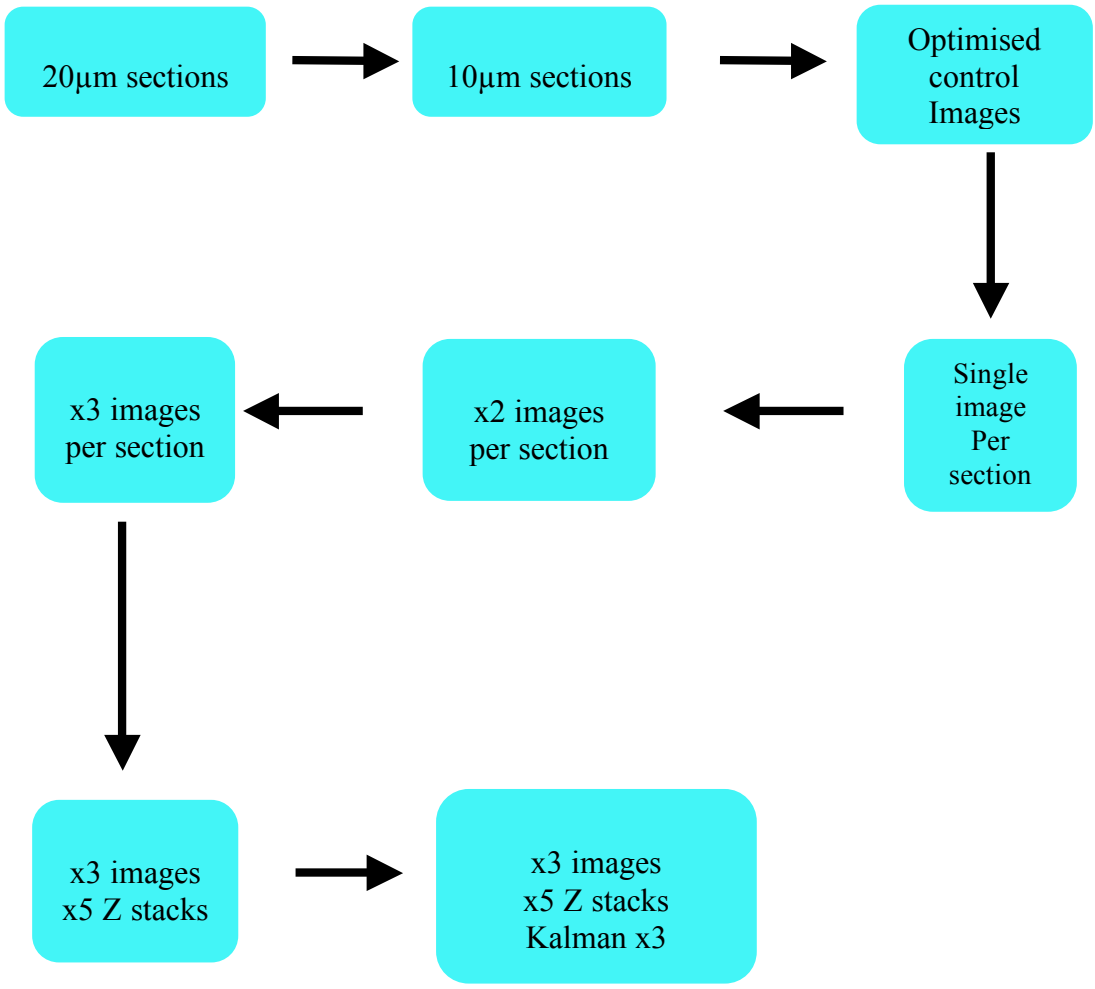

Fig. 3.5: Schema for the evolution and development of the image acquisition protocols. All images were 1024 x 1024 pixels in size. Kalman is a function within Lasersharp 2000, which refers to the acquisition of the mean of a number of images to improve the signal to noise ratio of each image. The ultimate method is termed the KZ method for ease of understanding and reference.

3.2.2 Confocal Image Analysis

The problem of how to analyse the images was approached as follows. The images were obtained via a sequential method of acquisition on the confocal microscope. This meant that an image analysis program (LaserPix, Biorad, Hemel Hempstead, UK) which recognised Biorad software coding, could take a colour image and separate the spectra into red, blue and green. These new images were then displayed as grey scale (0-255). The intensity of each pixel within a given area of interest (AOI) was then calculated using Laserpix (Biorad, Hemel Hempstead, UK). AOI intensity was initially calculated within multiple small squares within the image, with an average pixel saturation being taken.

As described in detail later in this chapter, the earlier analysis method of analysing two images per section is termed the two image method for ease of reference and understanding (fig. 3.6). The final technique of selecting an AOI within each image of the KZ acquisition method (n = 15 per slide) is termed the AOI method, again for reference and ease of understanding (fig. 3.6).

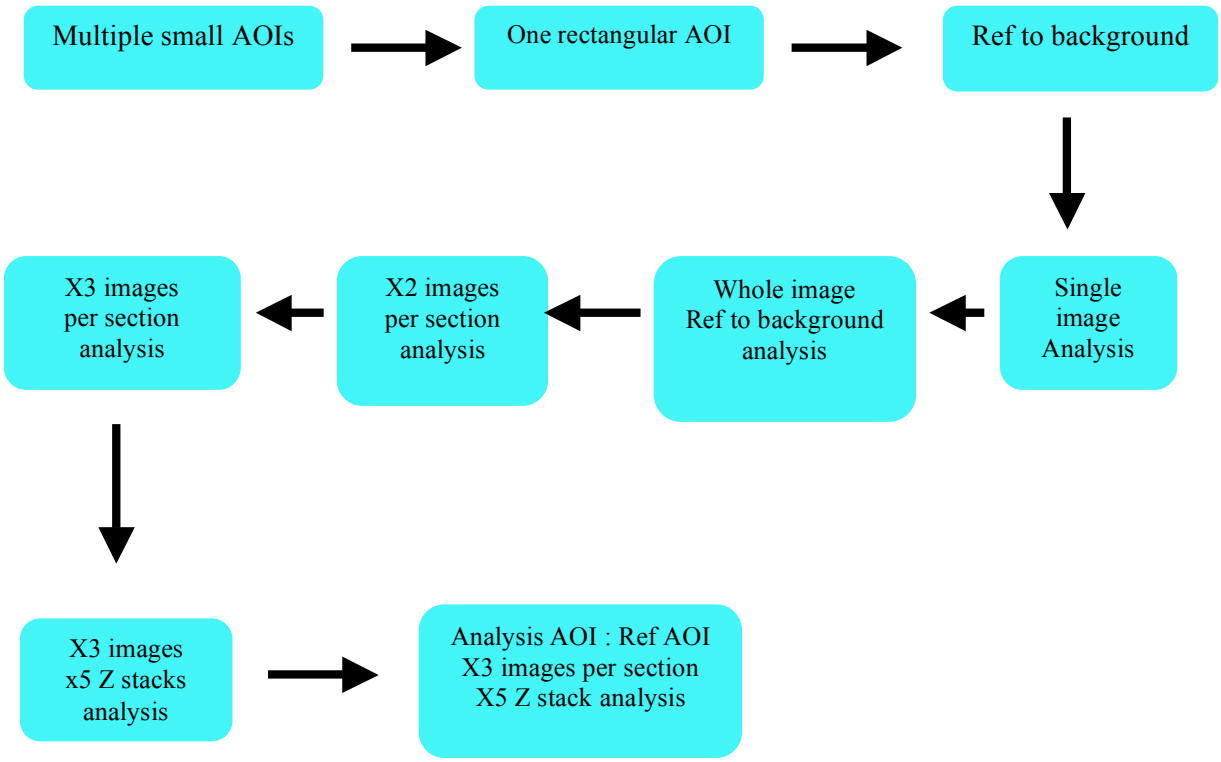

Fig. 3.6: Schema for the evolution and development of the image analysis protocols. AOI stands for area of interest within an image. The ultimate analysis technique is termed the AOI method.

3.2.3 Elastin autofluorescence

As described in chapter 2 an initial problem encountered was how to focus on the 10 μm tissue sections, and from which area of the tissue to obtain images in a non-biased fashion. This was solved by focusing on the elastin contained within vessels, which autofluoresces in the green spectrum (488 nm). Thus, elastin autofluorescence was stimulated using the argon 488nm laser (see fig. 3.7). Moreover, elastin autofluorescence did not appear to vary between either mesenteric artery or aorta (fig. 3.7 A & B) or between long incubation periods, with and without LPS (fig. 3.7 C & D). Furthermore, the green He/Ne laser used to stimulate the Alexa 568 phalloidin did not cause elastin autofluorescence at power ranges below 50% (Fig. 3.8). Therefore, by using a 20% power setting, (fig. 3.8A), I am confident that the F actin signal was not contaminated by elastin autofluorescence. However, images of F actin obtained using 50% green He / Ne power (fig. 3.8C), or greater (fig. 3.8D), would have some elastin signal "contaminating" the F actin signal.

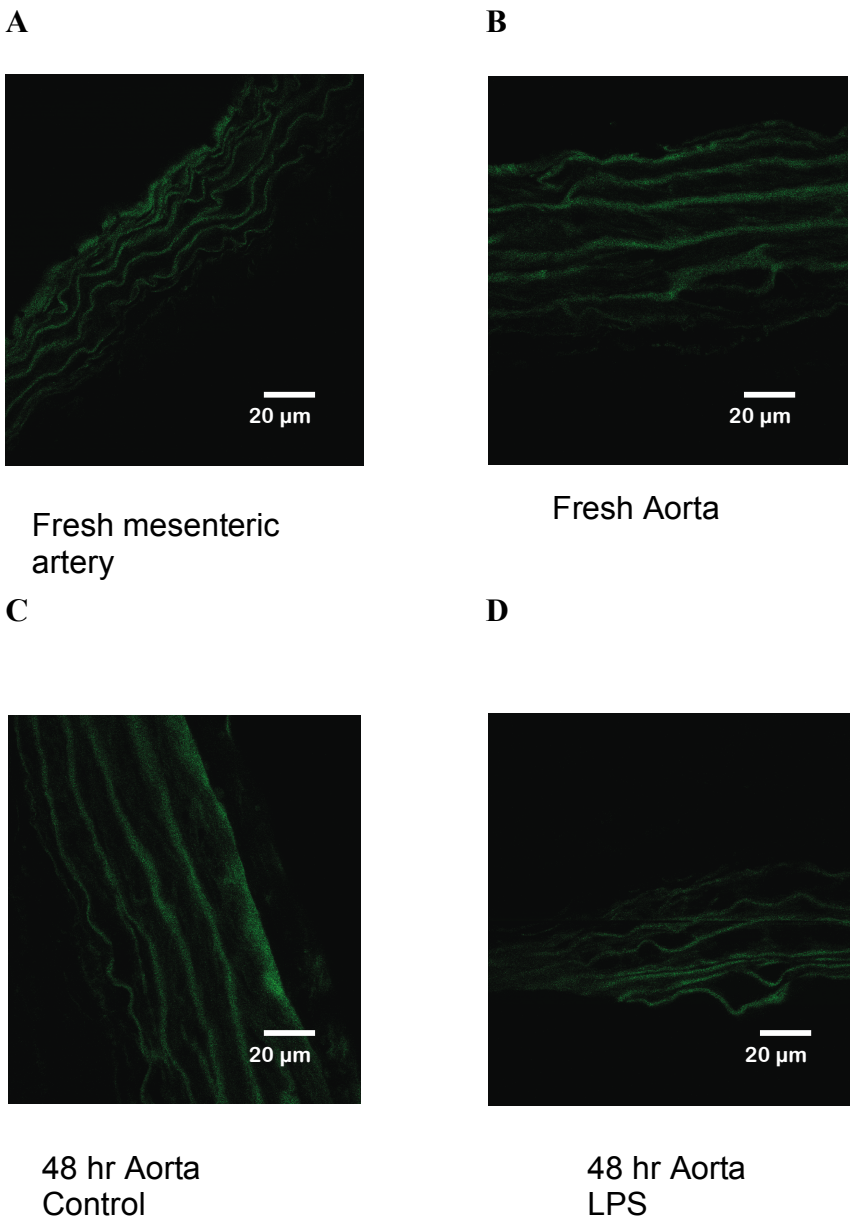

Fig. 3.7: Elastin autofluorescence stimulated by an Argon 488 laser. (A) fresh mesenteric artery, (B) fresh aorta, (C) aorta incubated in DMEM for 48 hr and (D) aorta incubated in DMEM containing LPS (0.1 µg.ml^{-1}) for 48 hr. Bio-Rad Radiance 2100 confocal microscope at x60 magnification.

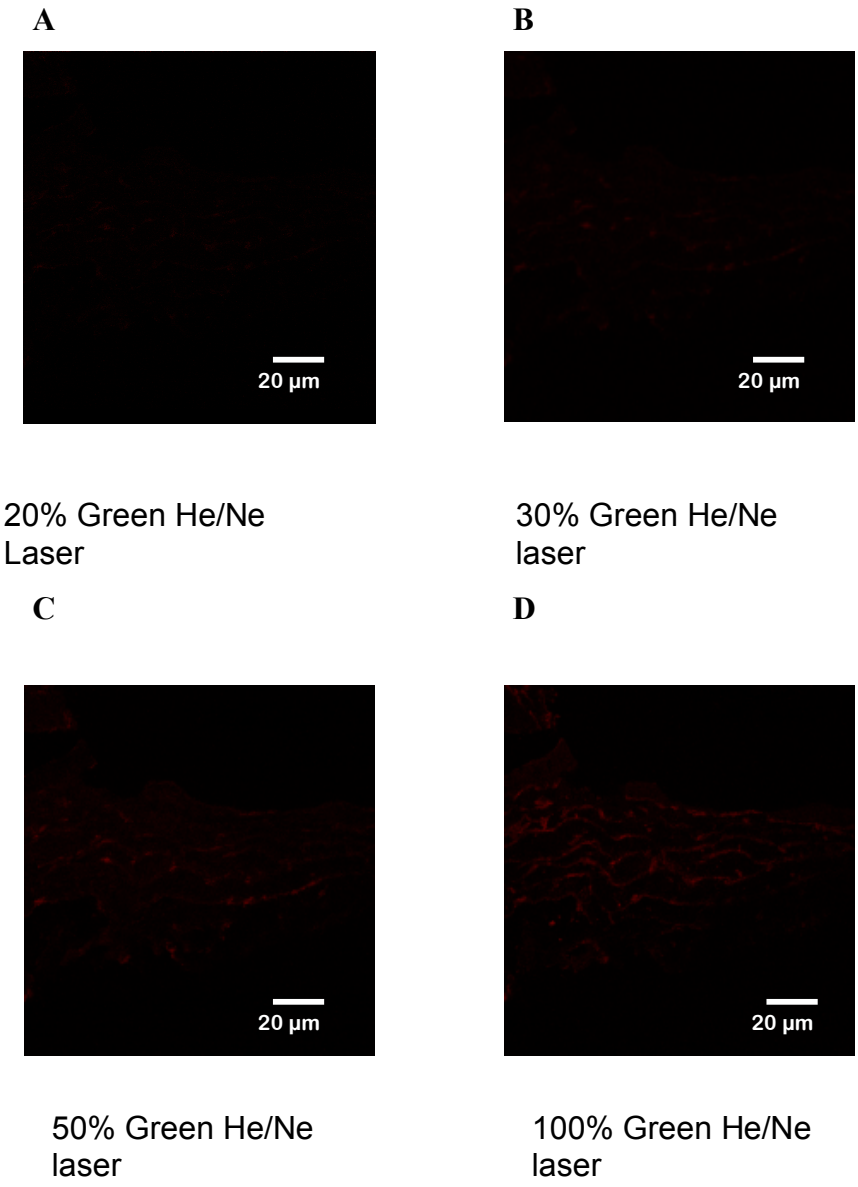

Fig. 3.8: Assessment of the autofluorescence of elastin in rings of mesenteric artery. Sections (10µm) were stimulated with a green Helium/Neon laser (543 nm) at (A) 20% power, (B) 30% power, (C) 50% power and (D) 100% power, demonstrating no signal when < 50% power was used, eliminating false-positive actin staining. A Long pass filter (560 nm), short pass filter (570/590) were used. Bio-Rad Radiance 2100 confocal microscope at x60 magnification.

3.2.4 F & G Actin Staining

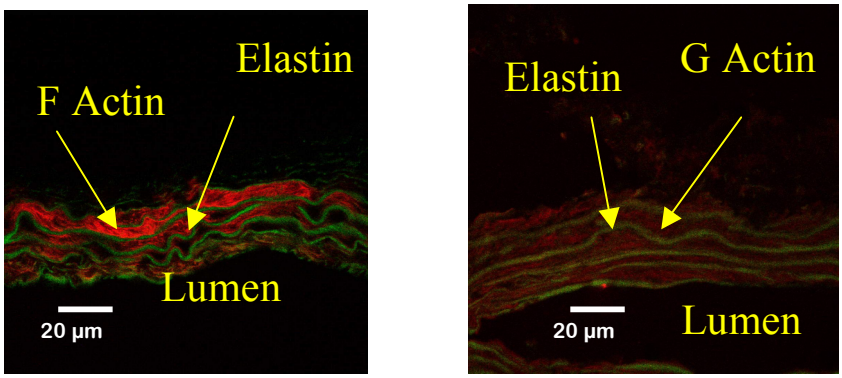

Fig. 3.9 Specimen images of fresh mesenteric artery (10 µm sections) stained for F actin (on the left) and G actin (on the right). F actin was visualised using Alexa Fluor-568 Phalloidin (shown in red), while G actin was visualised using DNAse I Texas Red (again shown in red). In both cases, probes were stimulated with a green Helium/Neon laser (543 nm) and long pass filtered at 560 nm and short pass filtered at 570/590. Bio-Rad Radiance 2100 confocal microscope at x60 magnification.

A F actin

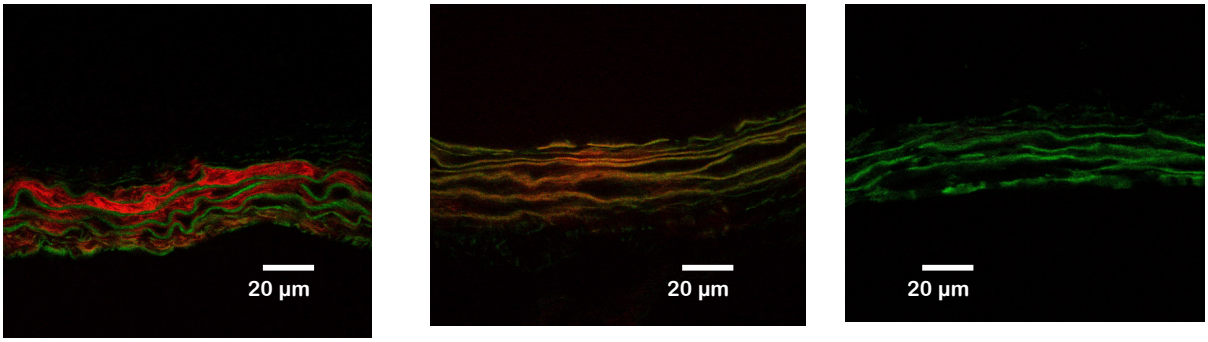

FRESH | 24 hr DMEM | 24 hr DMEM + LPS

B G actin

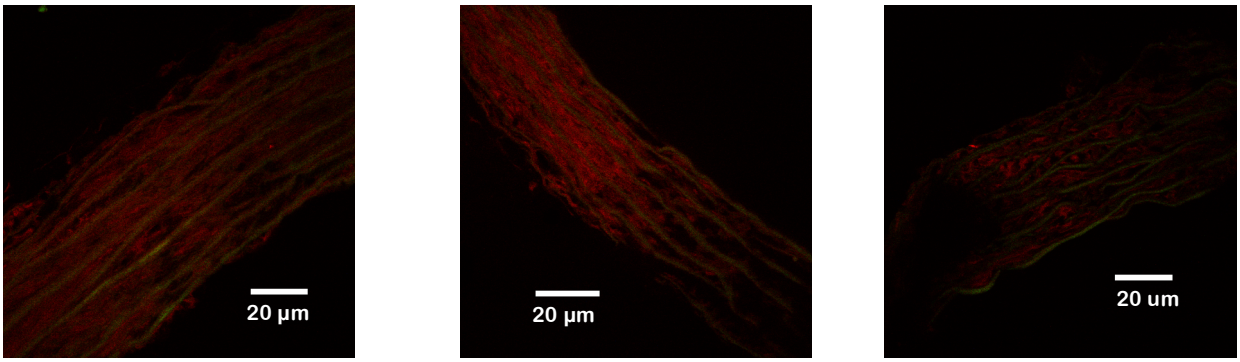

24 hr DMEM | 24 hr DMEM + LPS | 48 hr DMEM + LPS

Fig. 3.10. Specimen confocal images of rat aorta from the long term *in vitro* model of sepsis. Example images of the experiments looking at F (A) and G (B) actin levels in aorta at 0 hr, 24 hr and 48 hr after incubation in DMEM ± LPS (0.1 $\mu g.ml^{-1}$). F actin was visualised using Alexa Fluor-568 Phalloidin, while G actin was visualised using DNAse I Texas Red. Stimulated with a green Helium/Neon laser (543 nm). A Long pass filter (560 nm) and a short pass filter (570/590) were used. Bio-Rad Radiance 2100 confocal microscope at x60 magnification. In each image actin appears red, whilst elastin appears green.

The results for the analysis of aorta incubated in LPS at varying time points (images fig.3.10) are displayed as means in fig. 3.11 (F actin) and fig. 3.12 (G actin). The level of F actin staining seen at 24 hr in the control tissue was not significantly different from tissue freshly removed from the animals (n = 4). However, there was a 52% reduction in F actin immunofluoresence (relative to background) in aorta at 24 hr incubation with LPS (53.7 ± 9.5 for control vs 25.5 ± 3 for LPS, n = 4; $P < 0.05$) (Fig. 3.11). In contrast, the level of G actin staining was not significantly different after 24 hr incubation with LPS in aortic rings (n = 2) (Fig.3.12). At 48 hr, there is a trend towards a reduction in F actin in aorta. However, this was not statistically different (63.5 ± 28.4 for control vs 36.7 ± 6.2 for LPS, $P > 0.05$) (Fig. 3.11). There is no significant difference in G actin levels in aorta at 48 hr (Fig. 3.12). With respect to mesenteric artery, there was also a 65% reduction in F actin immunofluoresence (mean ± SEM) following a 24 hr incubation with LPS (71.5 ± 17.7 for controls vs 24.6 ± 2.5 for LPS, n = 4, $P < 0.05$) (Fig.3.11). At 48 hr, F actin levels in mesenteric artery are difficult to interpret, as there was only one ring of control tissue (Fig. 3.11). There was no change in levels of G actin at the 24 hr time point (Fig. 3.12). At the 48 hr time point, there was a reduction in G actin levels in mesenteric artery control tissue when compared to LPS. However, this was not statistically significant (38.5 ± 2.1 for control vs 55.9 ± 8.1 for LPS, $P > 0.05$) (Fig. 3.12).

A

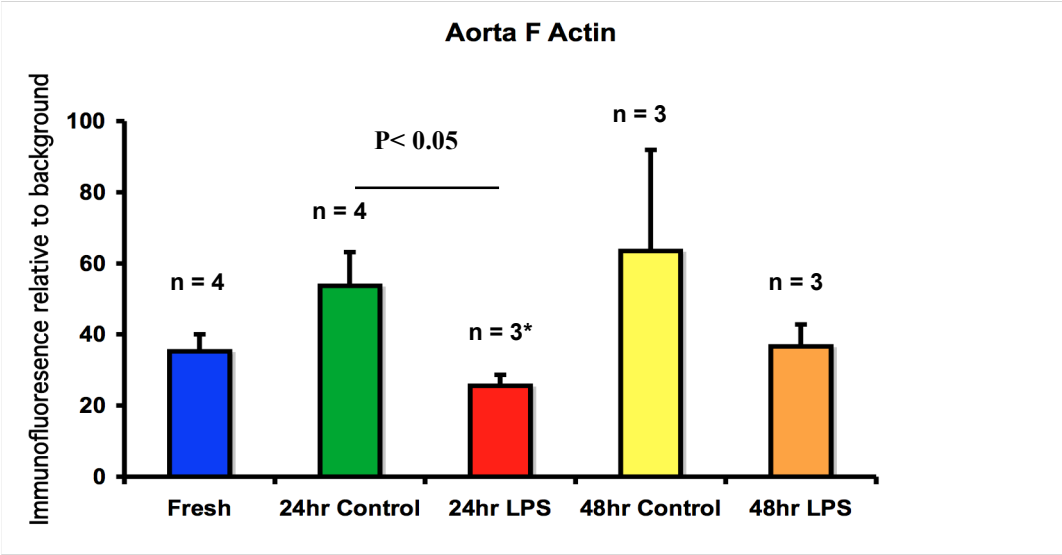

B

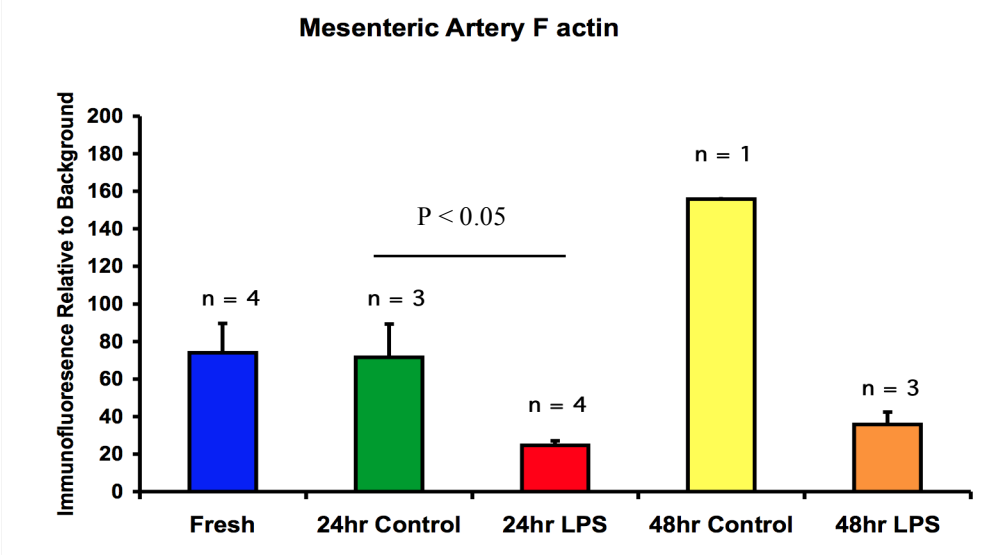

Fig. 3.11: Quantification of F actin in aorta (A) and mesenteric artery (B) (see figure 3.10). Images were taken via the two image method. Data are shown as mean ± SEM. N values different for each condition, as indicated. (* = $P < 0.05$).

A

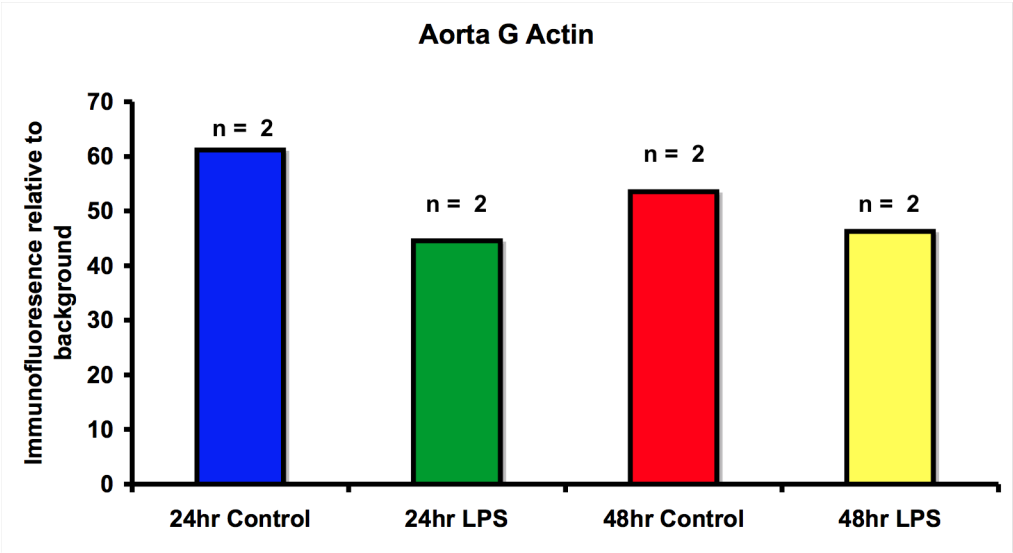

B

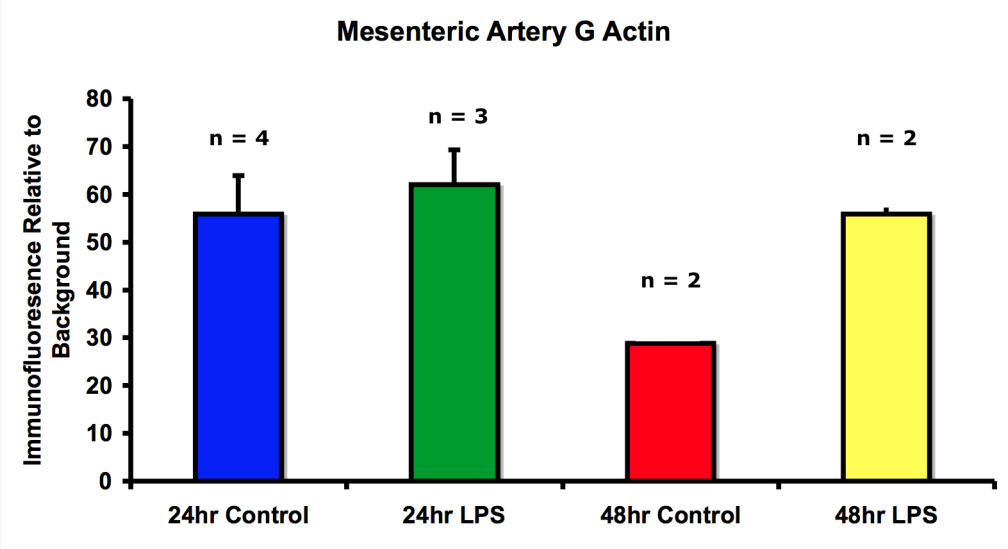

Fig. 3.12. Quantification of G actin in sections from aorta (A) and mesenteric artery (B). (figure 3.6B). Tissue was incubated in DMEM ± LPS (0.1 $\mu g.ml^{-1}$). Images were taken via the two image method. Data are shown as mean ± SEM. Where n = 2, no error bars are displayed. Data not statistically different.

Further analysis was carried out because a fall in F actin was expected, which would be mirrored by a rise in G actin, which did not happen. Additionally, on review of the previous image acquisition methods (two image method), it was decided that two images per section was insufficient and unlikely to be a representative sample to quantify the α actin in each tissue section. Therefore, further experiments on the previous slides were performed using the KZ and AOI methods. These experiments quantifying F actin in aorta after 24 and 48 hr incubation in LPS are shown in Fig. 3.13. At 24 hr incubation with LPS (0.1 $\mu g.ml^{-1}$) there was no change observed, but 48 hr LPS saw a 40% reduction, consistent with the trend seen in Fig. 3.11. To reiterate, the images analysed in fig. 3.13 were obtained with the revised acquisition method, namely using the Kalman function (mean signal from three acquisitions), with three images per slide and a Z stack taken across five microns for each image (KZ method). Furthermore, they were analysed with the revised analysis method of a ratio of the signal within an area of interest (AOI) over the tissue, to the reference AOI taken from the background (termed the AOI method).

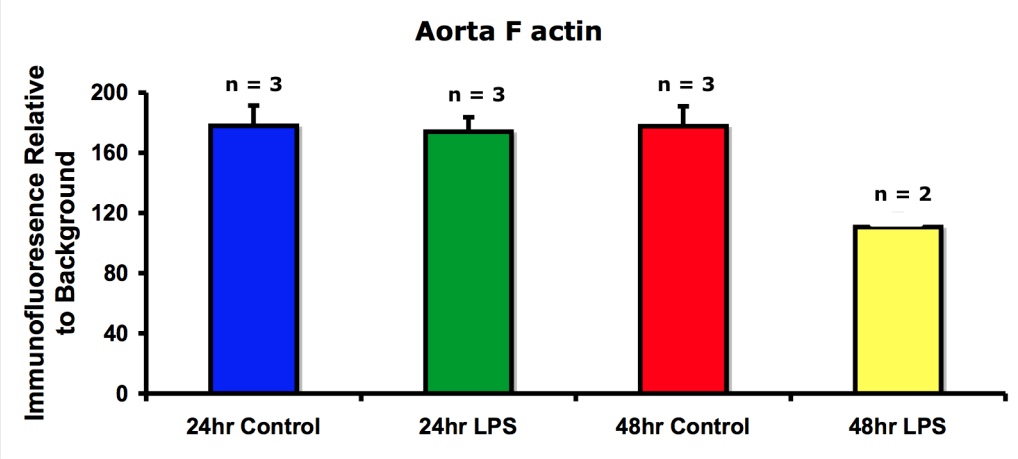

Fig. 3.13. F actin immunofluoresence in aortic sections after incubation in LPS (0.1 µg.ml^{-1}). Images, consisting of a Kalman function (x3), were taken from three areas per slide, with a Z stack (1µm steps) taken over 5µm for each area, (i.e. five images per Z stack, three Z stacks per slide / section of tissue). Therefore, each experiment represents x15 images. N = 3 (x45 images) 24 hr control, 24 hr LPS and 48 hr control. N = 2 (30 images) for 48 hr LPS (no error bars displayed because n = 2). If the Kalman x3 is accounted for, these data represent signals from 135 (for n = 3) and 90 (for n = 2) images, respectively. There was no difference between the 24 hr control and 24 hr LPS tissues. The 48 hr LPS sample trended towards reduction, but was not significantly reduced compared to the 48 hr control. Data are displayed as mean ± SEM.

To examine the possibility that the revised method (KZ acquisition with AOI analysis) was the source of the difference in results, the samples from figure 3.11 were re-sectioned and stained again. This time, images were obtained with the revised, KZ method, and analysed via the revised (AOI) method. The results of this repeated analysis are shown in fig. 3.14. This demonstrated no reduction in the levels of F actin at 24 hr of sepsis (unlike in fig. 3.11), but a fall in levels at 48 hrs both in control and LPS-treated tissues. This result implies that the method of image acquisition could indeed affect the results.

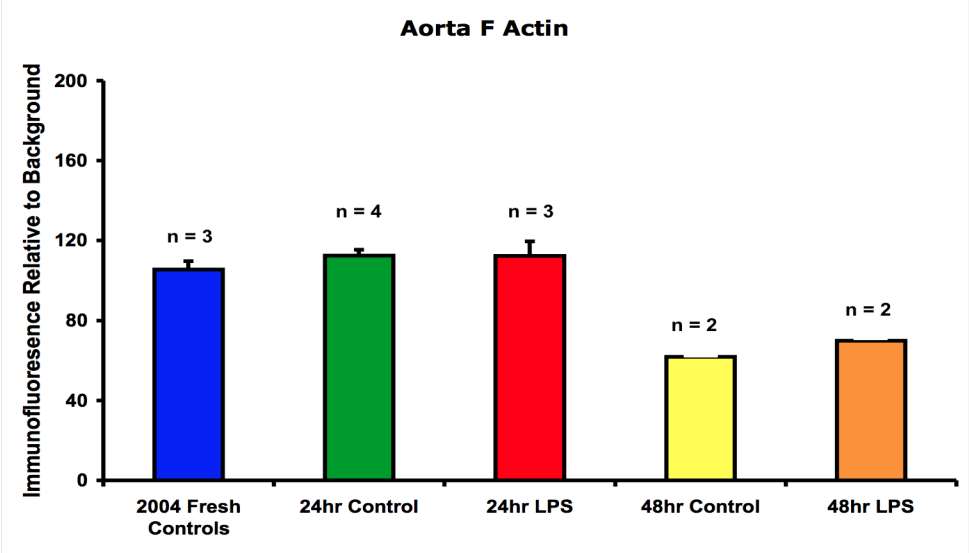

Fig. 3.14 Mean F actin immunofluorescence of rings of aorta exposed to LPS for 24 hr and 48 hr incubation periods. These data were obtained from re-sectioning and staining the same tissue used to generate data in fig. 3.11, but imaged (KZ) and analysed by the same method (AOI) as fig. 3.13. Thus a Z stack of five images, across 5 µm of tissue, and repeated in three areas per tissue section were analysed. N = 3 (x45 images) for fresh controls and 24hr LPS, n = 4 (x60 images) for 24hr controls and n = 2 (x30 images) for controls and LPS treated tissue at 48 hr. Kalman images (n = 3) were taken for all images. Data are displayed as mean ± SEM.

To exclude deterioration of slides and fluorophores stored over a period of time and contributing to the source of the variation, it was decided to repeat the previous experiments with new samples. These samples were processed alongside fresh controls and all samples underwent concurrent organ bath experiments as previously described. These samples were only acquired by the KZ method and analysed via the AOI method. The results of these experiments are displayed in fig 3.15. These demonstrated a trend towards an increase in F actin levels in tissue that had been incubated in DMEM for 24 hr compared to fresh controls, though there was no difference in level of staining in DMEM compared with a 24 hr incubation in LPS (0.1μM). At a 48 hr incubation with LPS, there was a trend towards a decrease in F actin levels

The results of the repeat staining and analysis of the samples contained in fig 3.14 were combined with the results of the staining and analysis of the subsequent samples contained in fig. 3.15. This was valid because the same image acquisition method (KZ) and image analysis method (AOI) was utilised. Additionally, a new batch of Alexa 568 fluorophore was used for both. No statistically significant difference was observed between any of the samples (fig. 3.16).

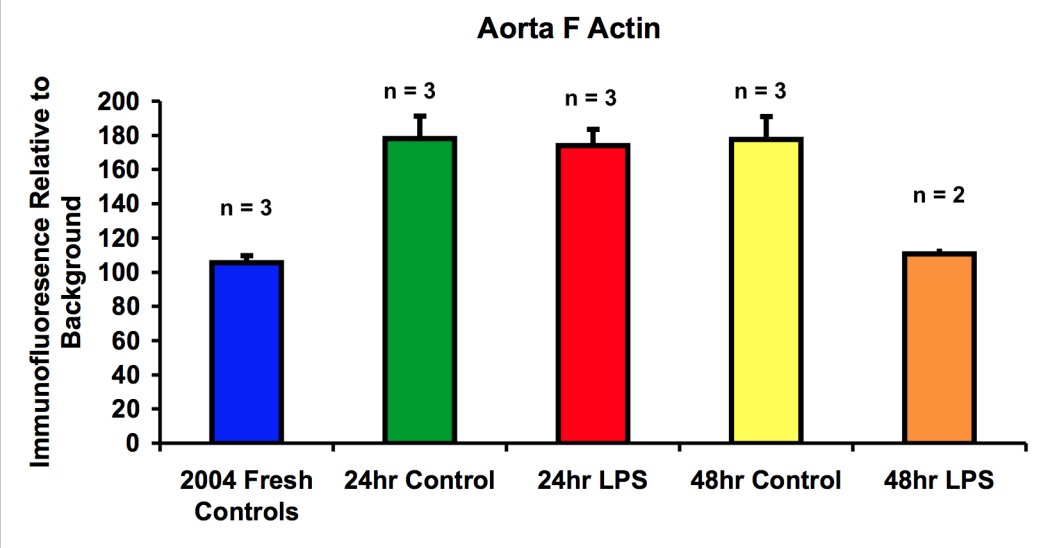

Fig. 3.15 Mean F actin immunofluorescence in rat aorta sections repeated one year subsequent to original analysis , obtained via KZ technique and analysed via AOI technique. Data are displayed as mean ± SEM.

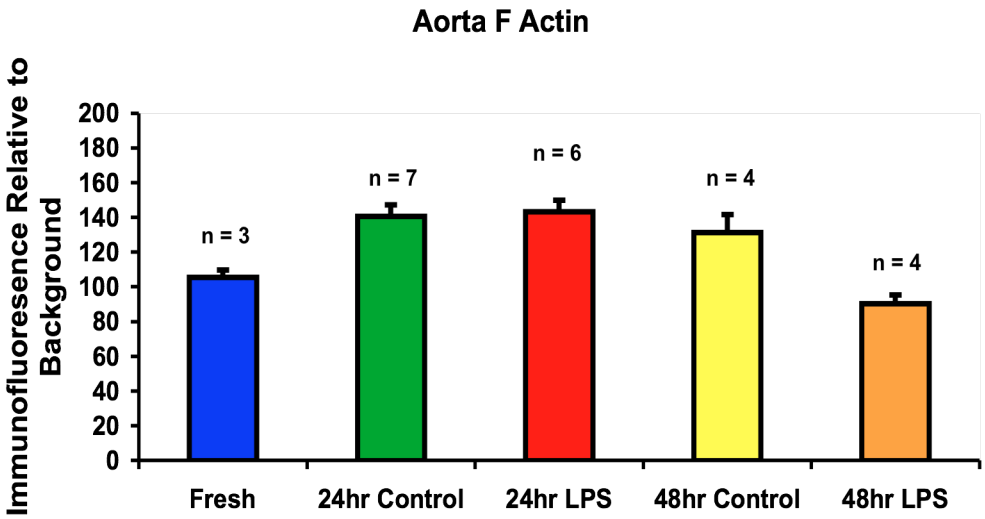

Fig. 3.16 Mean F actin immunofluorescence in rat aorta from 2003 and 2004, obtained via KZ technique and analysed via AOI technique. Data are displayed as mean ± SEM.

3.2.5 Confocal imaging and image analysis quality control

Due to the considerable development in the way samples were imaged and analysed over a period of time, a set of positive controls were designed to answer two fundamental questions:

1) Are immunohistochemistry and confocal microscopy sensitive enough methods to demonstrate differences in F actin after incubation with the actin cytoskeleton disruptor cytochalasin D?

2) Is there a significant reduction in F actin staining in rings of aorta after incubation with 10 $\mu g.ml^{-1}$ LPS (100 times greater concentration than previously used) for 24 hr?

Staining for F-actin under the conditions mentioned above are shown in fig. 3.17 (1:40 Phalloidin staining), with quantification analysis shown in fig. 3.18. These demonstrated that the confocal technique was sensitive enough to observe a significant reduction in F actin after incubation with cytochalasin D (10 μM) (concentration developed from pilot data, not shown) for 2 hr. However, it also demonstrated that, after 24 hr of incubation in DMEM +/-LPS (10 $\mu g.ml^{-1}$) there was a considerable reduction in F actin levels both in controls and in LPS (Fig. 3.18). This result was at odds with results demonstrated in fig. 3.16 and is discussed later. These actual images suggested less staining of the tissues with phalloidin than previously seen, which raised the possibility that the decreased F actin in the 24 hr controls was an artefact. The immunohistochemistry protocol was adjusted to increase the permeabilisation step from 5 mins to 15 mins and to increase the concentration of Alexa 568 phalloidin from a 1:40 to a 1:20 dilution.

However, the images obtained produces over-saturated images in the control when stimulated with the previous laser settings.

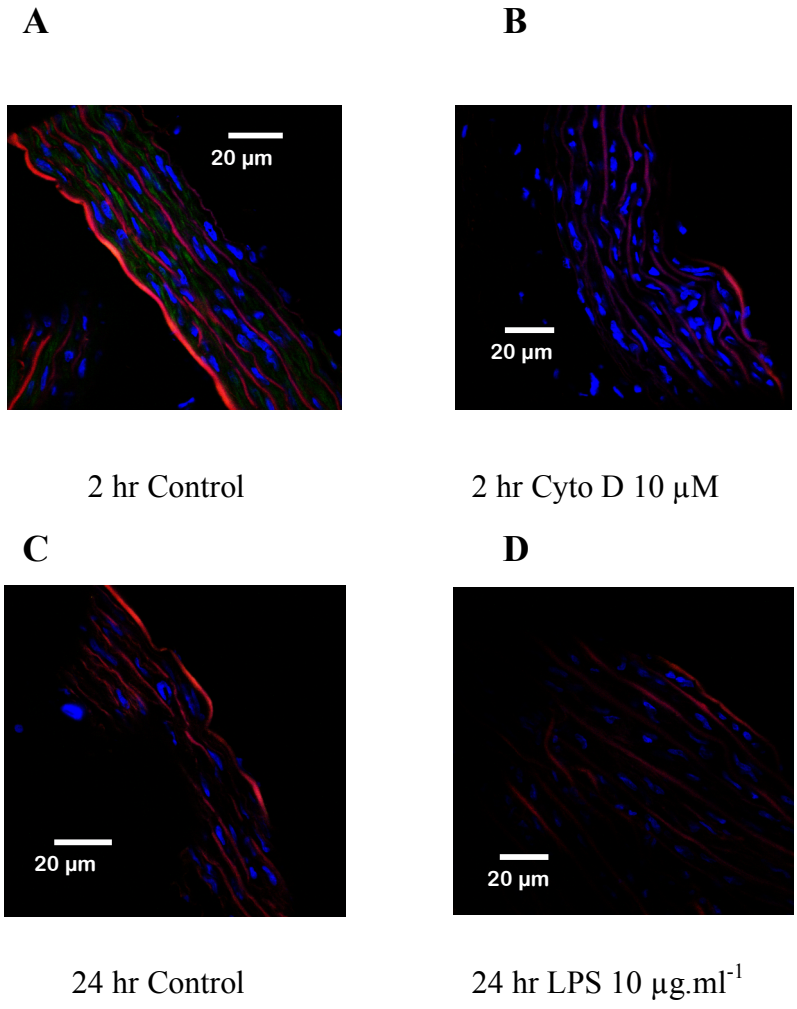

Fig. 3.17. Staining of F-actin with Phalloidin following cytochalasin and LPS treatment. Confocal images of aortic sections stained for F actin (in green) and a nuclear stain (TO-PRO in blue), with elastin appearing red. Aorta incubated (A) in DMEM for 2 hr, (B) in DMEM containing cytochalasin D (10 µM) for 2 hr, (C) in DMEM for 24 hr and (D) in DMEM containing LPS (10 µg.ml^{-1}) for 24 hr. F actin: Alexa Fluor-568 Phalloidin was used at a dilution of 1:40 and the probe stimulated with a green Helium/Neon laser (543 nm). A long pass filter (560 nm)

and a short pass filter (570/590) were used. Bio-Rad Radiance 2100 confocal microscope at x60 magnification.

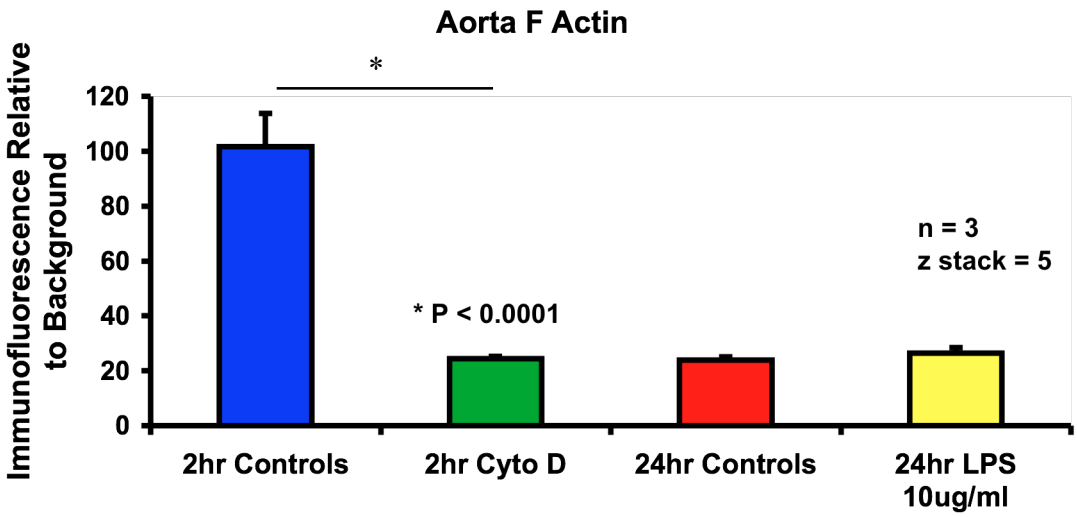

Fig. 3.18. Quantification of F actin staining in aorta. Mean data from examples shown in Fig. 3.17. Images analysed by taking AOI ratio to a background AOI as reference. n = 3 (Z stack of five images each, x3 per tissue, with a Kalman of 3 = 135 images per group). There is an 80% reduction in F actin in the 2 hr Cyto D group when compared to 2 hr controls ($P < 0.0001$). Data are shown as mean ± SEM.

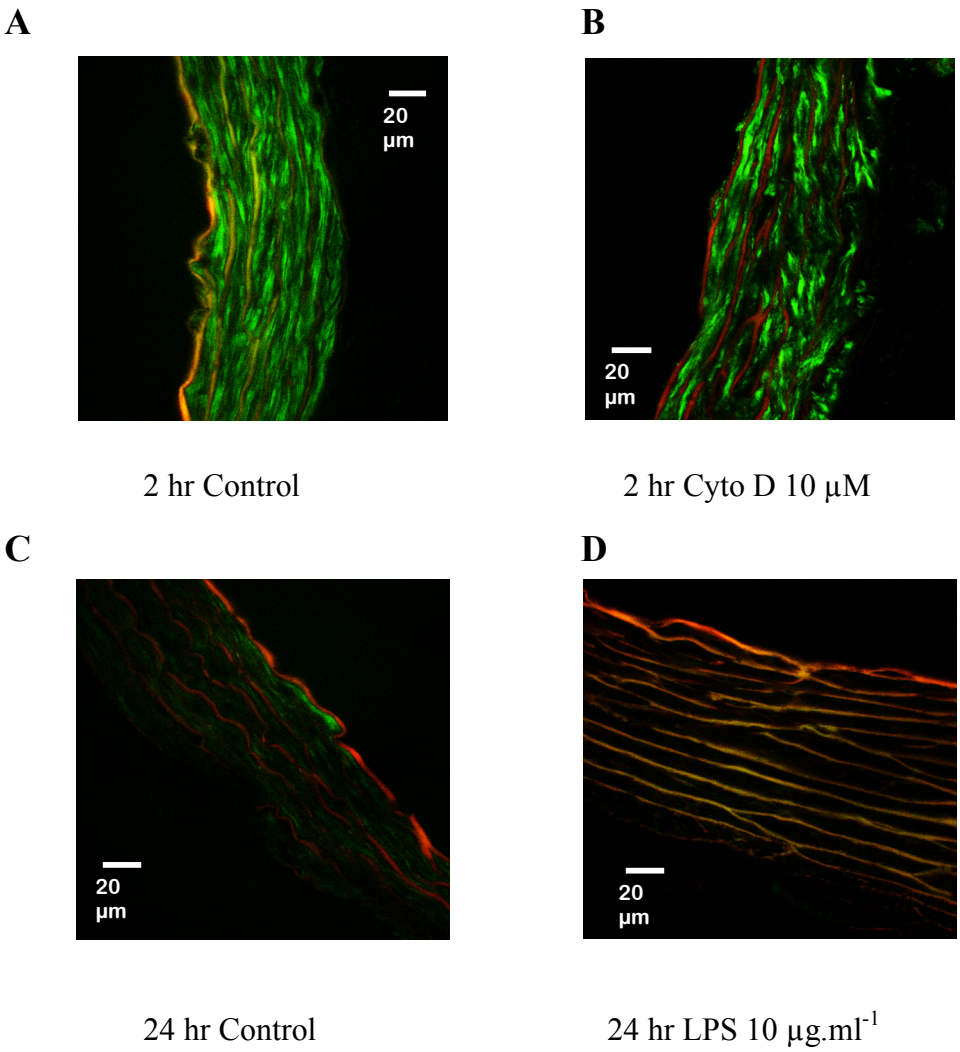

Fig. 3.19. Images of F actin in positive controls using 1:20 phalloidin dilution. A. Aorta incubated in DMEM for 2 hr. B. Aorta incubated in DMEM + Cytochalasin D (10 µM) for 2 hr. C. Aorta incubated in DMEM for 24 hr. D. Aorta incubated in DMEM + 10 µg.ml^{-1} LPS for 24 hr, n = 1. F actin: Alexa Fluor-568 Phalloidin (Molecular Probes, Amsterdam, Europe). Stimulated with a green Helium/Neon laser (543 nm). A long pass filter (560 nm) and a short pass filter (570/590) were used. Bio-Rad Radiance 2100 confocal microscope at x60 magnification. In these images actin appears green and elastin red.

3.2.6 Summary of confocal quantification experiments

The results demonstrated that there was significant development and evolution of both the image acquisition and image analysis methods. The final KZ method for image acquisition is a representative sampling of each section. The AOI analysis method was a reproducible method for analysis of the images. The results demonstrated that the trend towards a reduction in levels of F actin seen in aorta sample with the earlier techniques was not reproducible. The trend towards reduction of F actin levels at 48 hr LPS persisted, but were not significantly different in the final analysis method used.

3.3 Assessment of α actin protein content by Western Blot

Western blot analysis was carried out to examine the effects of LPS on the total α actin content in rings of aorta. On visual examination the Western blots (Fig.3.20) demonstrated no difference between the levels of total actin (F and G) seen at 24 hr and 48 hr of LPS incubation when compared to either their time-matched controls, or to fresh controls. The fresh control samples in the 24 hr and 48 hr blots were from the same three animals. The 24 hr LPS samples (A) were taken from the same animals as the three samples labelled 24 hr controls, whereby half of the vessel was incubated in DMEM and the other half incubated in DMEM containing 0.1 $\mu g.ml^{-1}$ LPS. The 48 hr experiments also represent tissue from three animals, with the same protocol as used in the 24 hr experiment.

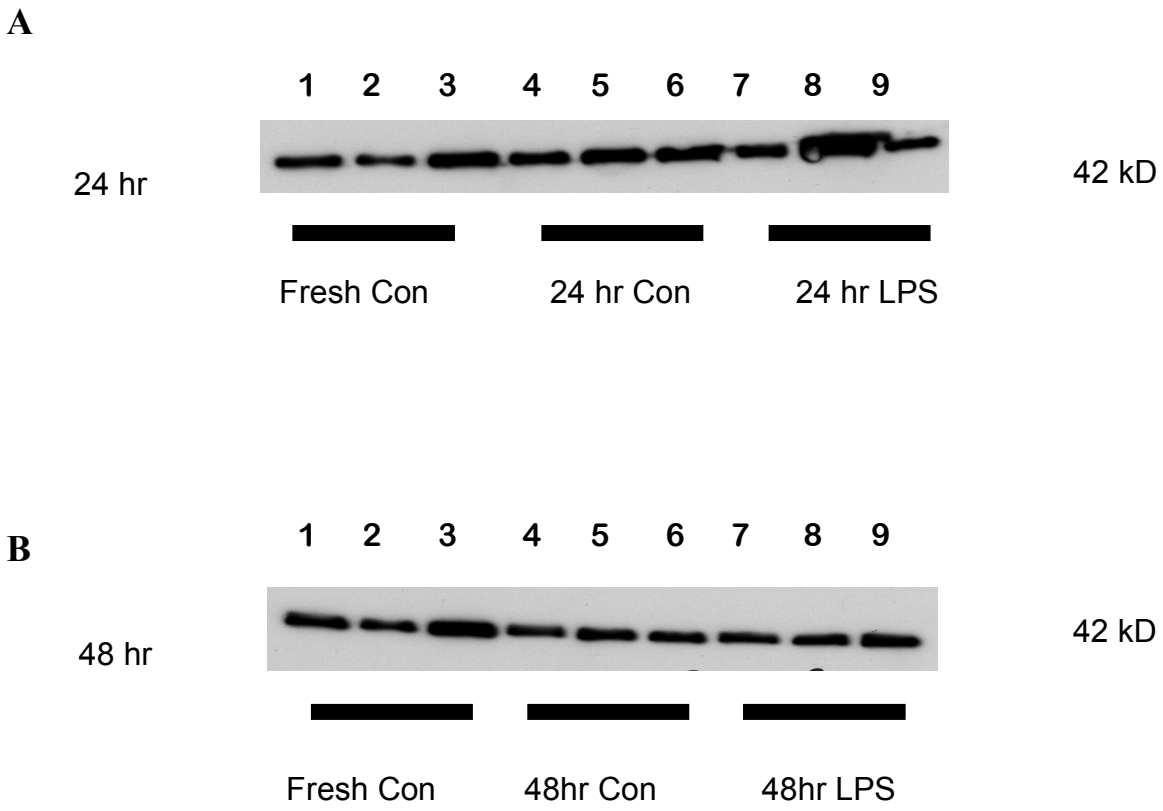

Fig. 3.20. Western blots of total α actin in rings of aorta at 0, 24 hr & 48 hr time points ± LPS. Western blots of total (F and G) alpha actin taken from rings of aorta in fresh tissues (fresh con) and those incubated in DMEM for 24 hr (A) and 48 hr (B). Lanes 1-3 represent homogenates from fresh controls (n = 3), where the same sample was used in both blots. Lanes 4-6 represent 24 hr (A) and 48 hr (B) incubations in DMEM, while lanes 7-9 represent samples incubated in DMEM with LPS (0.1 $\mu g.ml^{-1}$) for 24 hr (A) and 48 hr (B), respectively (n = 3 for all conditions).

3.3.2 Separation of α actin into filamentous (F) and globular (G) components

The western blots in fig. 3.20 demonstrated that there was no change in the levels of total α actin in the *in vitro* model of sepsis at 24 hr and 48 hr time-points, despite the demonstration that these tissues were hyporeactive to PE in the organ bath studies (see fig. 3.2). Therefore, I proceeded to examine the hypothesis that the levels of F actin were reduced in sepsis, while that of G-actin may increase. As mentioned in Chapter 1, α actin consists of filamentous (F) and globular (G) actin. F actin is essentially polymerised G. Therefore, to examine levels of F actin, I initially had to separate out the G fraction from the F. This was achieved by developing a centrifugation protocol, which is summarised in the schema in fig. 3.21, with the actual Western blots demonstrated in fig. 3.22

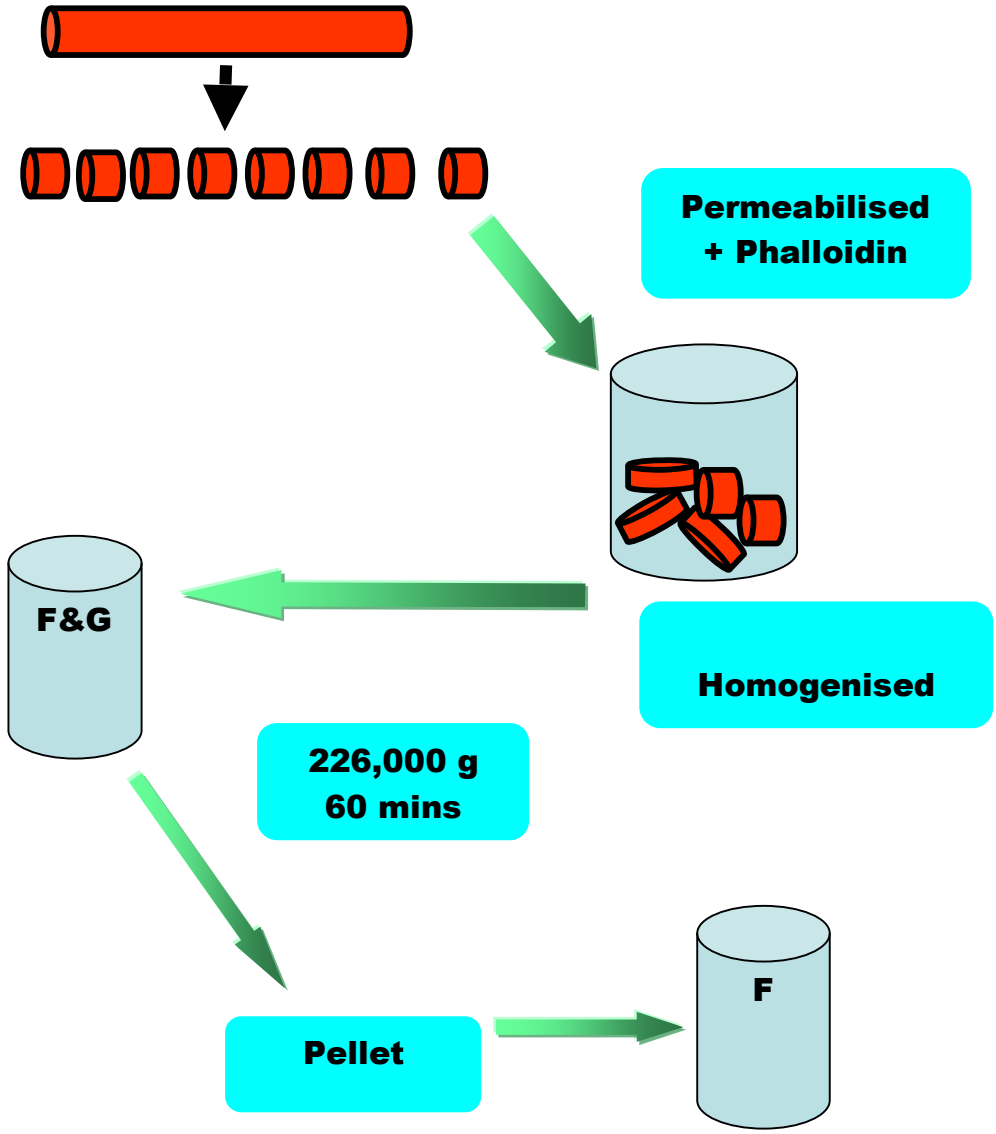

Fig. 3.21. F and G actin separation technique. Schema showing the modified centrifugation step to remove excess G actin from the F actin sample, a step introduced in the method described in fig.2.3. This step resulted in the generation of an F actin pellet free from contamination with G actin.

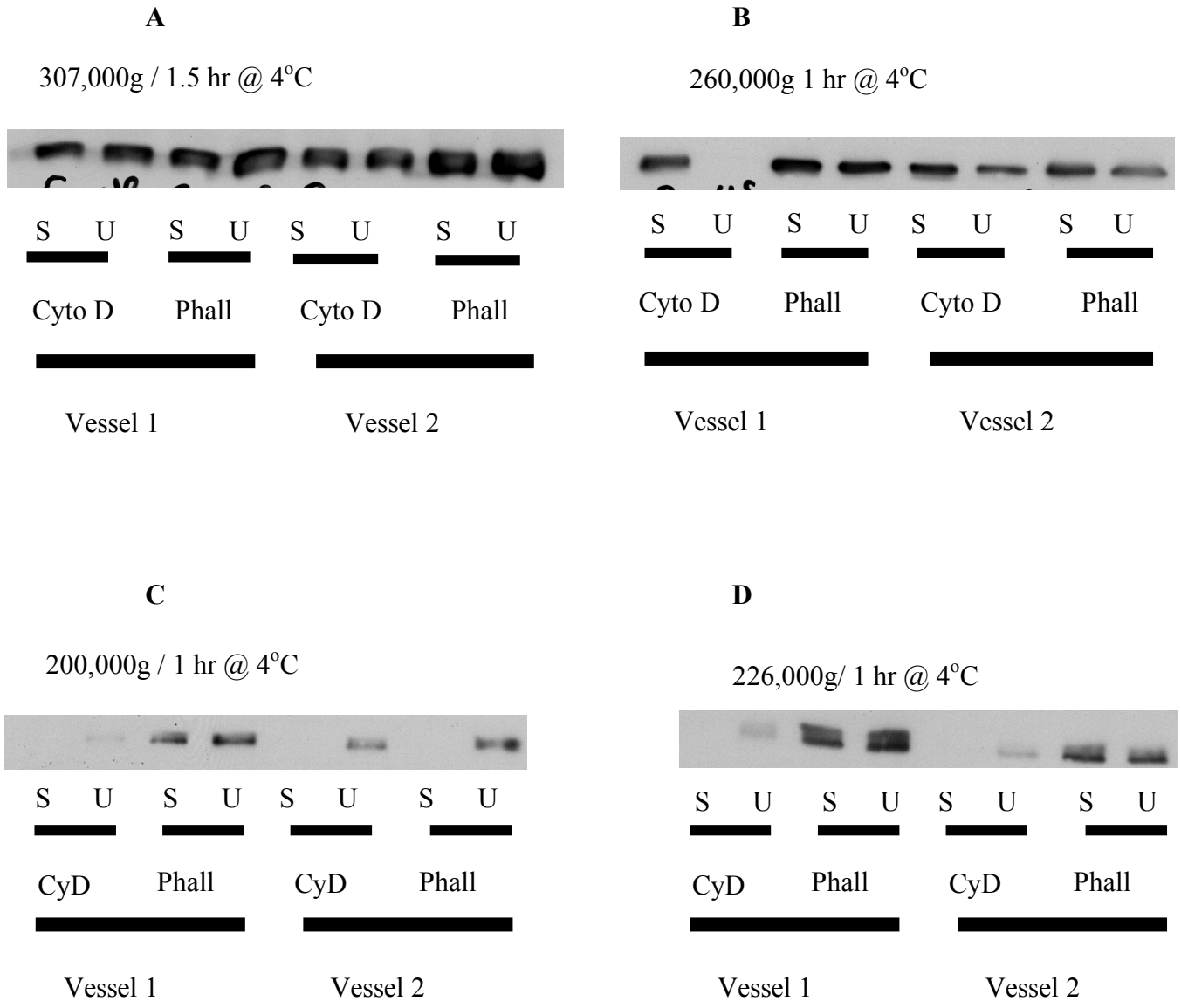

Fig. 3.22. Western blots showing F actin separation. Positive controls for F and G actin are shown, where each blot is taken from two vessels, with half of the sample incubated for 4 hr in phalloidin (F actin control) and half incubated for 4 hr in cytochalasin D (G actin control). Each sample was further divided into unspun (U) or those that have undergone an additional centrifugation step (S) at a speed, time and temperature as indicated on the blot. Incubation time was 4 hr for all samples.

The separation of F and G actin was essentially achieved by modifying the centrifugation step. The sample was initially spun at 307,000g for 1.5 hr at 4°C (fig.3.22A). This displayed contamination of the F actin sample with G actin since the tissue incubated in cytochalasin D still had signal after the centrifugation step (labelled "S"), when compared to the sample of tissue which has not undergone this step, (labelled "U"). The reduction of the centrifugal force to 260,000g for 1 hr displayed a similar picture (fig.3.22B). Reduction to 200,000g for 1 hr caused significant loss of the F actin signal (fig.3.22C) suggesting that this force was not enough to sediment F actin. However, centrifugation of the F actin sample at 226,000g for 1 hr at 4°C displayed clear separation of the F and G actin (fig. 3.22D).

3.3.3 Assessment of F actin in 24 hr & 48 hr *in vitro* models of sepsis

This centrifugation protocol was then applied to aortic samples incubated for 24 hr and 48 hr in LPS (0.1 $\mu g.ml^{-1}$). The Western blots showed no difference in F actin levels in tissue incubated in LPS for either 24 (fig.3.23A) or 48 (fig.3.23B) hr when compared to their respective time controls or when compared to fresh controls. The fresh controls in A and B were from the same tissue samples, n = 3, while the 24 hr and 48 hr samples were from three separate animals, with pairing (same animal) of the appropriate controls with the LPS samples.

The blots in fig. 3.23 were incubated in anti-alpha actin mouse antibody at a 1:10,000 dilution. These blots appeared saturated and were therefore stripped of antibody (as per ECL ™ Western blot protocol) and then re-exposed to anti-alpha actin mouse antibody at a higher (1:50,000) dilution (fig. 3.24). These blots

appeared to suggest that there was less F actin in all of the 48 hr samples (compare A with B). However, on more careful inspection of lanes 7-9 in both blots, the very same fresh control tissue samples appeared to give different signal strengths. This was therefore more likely to be due to differential stripping of the blots.

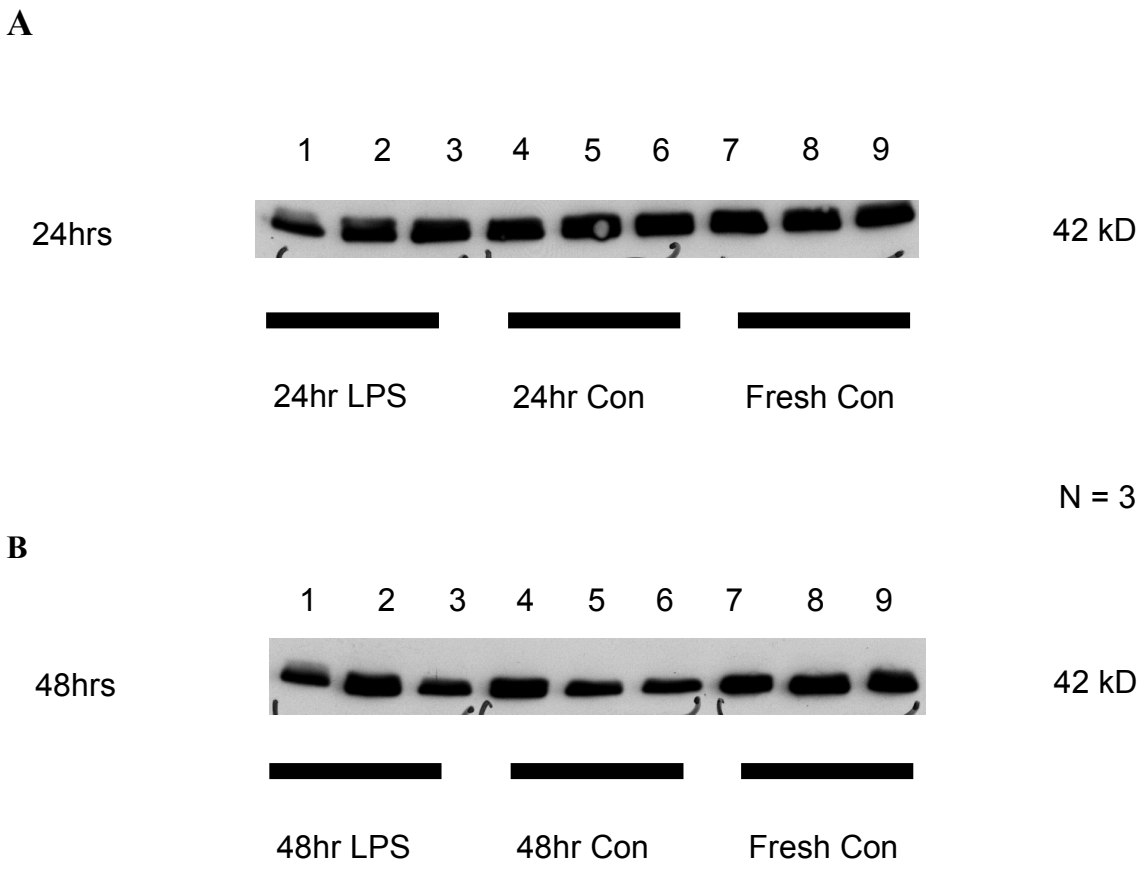

Fig. 3.23. Western blots of aorta tissue, staining for F actin using 1: 10,000 anti-alpha actin antibody. Shows Western blots of F actin from rings of aorta incubated for 24 hr (A) and 48 hr (B). Anti-alpha actin mouse antibody was used to identify F actin (1:10,000 dilution). Lanes 1-3 represent incubation in DMEM with LPS (0.1 $\mu g.ml^{-1}$) for 24 hr (A) and 48 hr; both blots (A and B) were loaded with the same fresh control samples, as a between-blot control. Lanes 4-6 of both blots represent 24 hr (A) and 48 hr (B) incubations in DMEM, lanes 7-9 of both blots represent homogenates from fresh controls (n = 3 for all conditions).

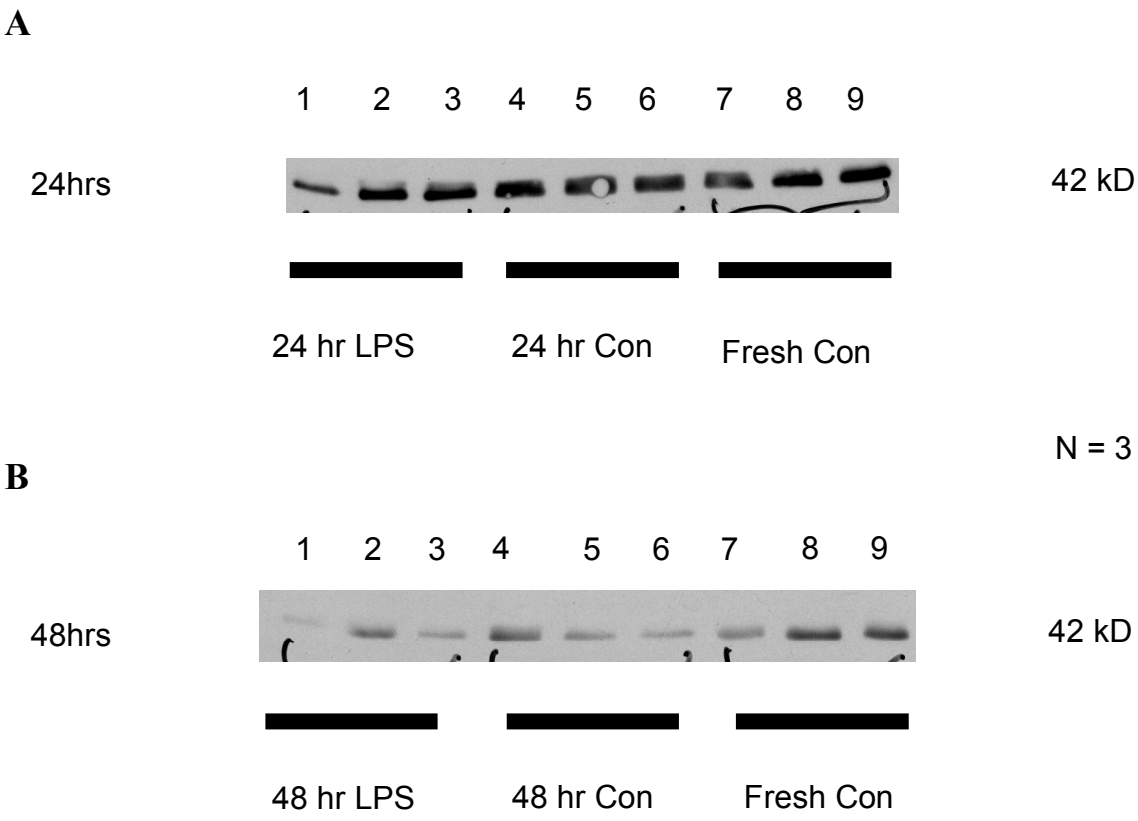

Fig. 3.24. F actin using 1: 50,000 dilution of anti-alpha actin antibody. Western blots of F actin from rings of aorta incubated for 24 hours (A) and 48 hours (B). These blots were the same as those in fig. 3.23, but were stripped of antibody and re-incubated with anti-alpha actin mouse antibody, but this time at a 1:50,000 dilution. Lanes 1-3 represent incubation in DMEM with LPS (0.1 $\mu g.ml^{-1}$) for 24 hours (A) and 48 hours, respectively; both blots (A and B) were loaded with the same fresh control samples, as a between-blot control. Lanes 4-6 of both blots represent 24 hour (A) and 48 hour (B) incubations in DMEM, with Lanes 7-9 of both blots represents homogenates from fresh controls (n = 3 for all conditions).

3.3.4 Summary of Western blot experiments

The Western blot experiments demonstrated there was no change in the levels of total α actin (F and G) in rat aorta in an *in vitro* model of sepsis (fig. 3.20). The experiments also demonstrated the development of a reproducible technique for the separation of F and G actin in this tissue. This separation was best achieved using centrifugation of homogenates of rat aorta at 226,000 g for 1 hr at 4^{o}C (fig. 3.22). Furthermore, there was no reduction in the levels of F actin in rat aorta seen at 24 hr and 48 hr time points in an *in vitro* model of sepsis (fig. 3.23). However, the concentration of anti-α actin antibody used (1:10,000) may have been too high and that a lower concentration may be required (fig. 3.24). The Western blots also demonstrated that the stripping of previously stained blots was a variable technique (fig. 3.24).

3.4 Discussion of results

In patch-clamp studies, once the K_{ATP} channel is opened, application of ATP to the intracellular surface of the channel is insufficient to close the channel, unless further G actin is added (Terzic, 1996). This pattern of dysfunction, which includes increased agonist opening and decreased ability of the antagonists to close the channel, is remarkably similar to the pattern seen in *in vitro* models of sepsis (Wilson, 2002). With this in mind, I investigated the hypothesis that cytoskeletal disruption underlay the altered K_{ATP} channel pharmacology in sepsis.

The results demonstrated that vascular tissue obtained from Sprague-Dawley rats was still functional post-dissection, and on incubation with DMEM and LPS behaved in a reproducible fashion (Fig.3.1-3.3) (Wilson, 2002).

I developed a method for the study and quantification of alpha actin, using immunohistochemistry and confocal microscopy (Fig.3.5 & 3.6). However, the reproducibility of the quantification method was variable and largely did not correlate with functional data. When considering the final method of image analysis, there was little change in F-actin levels at a time (24 hrs) where rings were found to be hyporeactive to PE in the presence of LPS (Fig.3.16). There were however differences in the quantification results that depended on the method of acquisition and analysis (compare fig. 3.11A vs fig. 3.14 vs fig. 3.16). However, as these methods evolved, the KZ method was probably a more representative sampling of the tissue, with more images per section. This demonstrated no significant decrease in F actin at 24 hr and an insignificant trend towards a decrease on F actin at 48 hr (Fig. 3.16).

There were no significant differences seen in the levels of G actin in any of the tissues (fig.3.12). However, due to the problems with the early methods and the need for significant development of method, not enough time was available to analyse the G actin levels using the confocal microscope. Once the problems of reproducibility were recognised, the majority of time and effort went into optimising the technique the KZ method of acquisition and the AOI method of analysis (Fig. 3.6). I therefore concentrated on the F actin signals in aortic tissue.

The biochemical assessment of the actin cytoskeleton also required significant and time-consuming method development. Western blots of total actin did not demonstrate any change in sepsis (Fig. 3.20). However, this could have been as a consequence of the filamentous F actin being converted into globular G actin.

Having developed a technique for separation of F and G actin (Fig. 3.21 and Fig. 3.22), I demonstrated that there was no change in the levels of F actin at the 24 hr LPS or 48 hr LPS time points (Fig. 3.23). The Western blots demonstrated in fig. 3.23 were overly saturated, so I therefore attempted to re-examine the blots with a weaker concentration of antibody (1:50,000 vs 1:10,000). However, the process of stripping the antibody from the gels in order to re-stain them caused artefactual differences in staining (Fig. 3.24). This is seen in the differences in the staining of the fresh control samples, which are from identical tissue preparations. The fresh controls are less stained on the 48 hr blot (Fig. 3.24B) when compared to the 24 hr blot (Fig. 3.24A).

If time had permitted, I should have also gone on to run gels of the supernatant in the F and G actin separation protocol (Fig. 3.21). This would have allowed me to assess any changes in the levels of G actin. However, the primary hypothesis was that there was a change in F actin in sepsis. The blots should also have been stained for a house-keeping protein as an internal control. However, there was a limited supply of tissue homogenate to work with, because of the repeated running of gels in optimizing the method of extraction and method of staining. Each sample of tissue run on a Western Blot was from an overall piece of tissue that had also been examined in the organ bath for vascular hyporeactivity, as well as in the confocal microscope. Notwithstanding this, the method for separation of F and G actin was reproducible and valid. Again, because of the considerable time spent during method development and despite starting out to examine both aorta and mesenteric artery, I was only able to examine rat aorta. Ideally, all of these experiments should also be repeated in rat mesenteric artery.

My original hypothesis stated that sepsis would disrupt the cytoskeleton. However, I was unable to demonstrate any correlation between the confocal, biochemistry and organ bath results. One potential hurdle in quantifying changes in the cytoskeleton is that actin is such an abundant protein. Hence, a change in F actin of less than fifty percent of total may be difficult to observe against a high background signal. This was demonstrated by the fact that the homogenates loaded onto the SDS-page gels had first to be diluted by a factor of ten, with a dilution of the anti-alpha actin antibody as low as 1 in 50,000 for some experiments.

If there was a contribution to vascular hyporeactivity, this may be related to alteration of the force-transduction mechanism of vascular smooth muscle, rather than alteration of the control mechanisms of the K_{ATP} channel. Alteration in the actin-myosin coupling required for muscle contraction may be impaired in sepsis, indirectly supported by the evidence that total actin leaks from cells into plasma during sepsis (Mounzer & Moncure, 1999; Dahl & Schiodt, 2003). However, I saw no changes in total actin (Fig. 3.20).

Interestingly, there appear to be differences between the responses of aorta and mesenteric artery from the same animal, dissected at the same time and incubated in identical conditions. The mesenteric artery appeared to show more recovery from hyporeactivity in the 48 hr model of sepsis, whereas rings of aorta were equally hyporeactive at 24 and 48 hr. (fig. 3.4B and fig.3.5B respectively). Notwithstanding this, the analysis of the confocal images suggests that there may have been more F actin in mesenteric artery when compared to aorta (see fresh

controls in fig. 3.11A & 3.11B). There did not appear to be any differences in the quantified levels of G actin (see fresh controls fig.3.12A 7 3.12B). These characteristics may be similar to the differences in the ratio of F and G actin seen between striated and smooth muscle (9:1 versus 1:1) (Cipolla, Gokina & Osol, 2002). This may reflect differences in the intravascular pressure that the vessels are exposed to.

3.5 Conclusion

The semi-quantitative techniques I utilised were probably inadequate tools with which to answer the question "does cytoskeletal disruption alter K_{ATP} channel function in sepsis?" Study of more subtle, sub-cellular, cytoskeletal proteins (such as syntaxin Ia) in cellular or electrophysiological studies (such as patch clamping or rubidium efflux) may offer a more targeted and fine-tuned approach, especially in trying to determine if the cytoskeleton alters ion channel function in those tissues. Alternatively, examination of actin in isolated VSMCs, via the confocal microscope, may have highlighted alterations in the cellular organisation of actin, as a stress response, rather than trying to quantify changes on actin (Saidi et al., 1997).

It is unlikely that the actin cytoskeleton of vascular smooth muscle cells is completely unaffected by sepsis, given that it is such an abundant protein and the evidence that NO alters actin in small intestine (Banan, Fields, 2000), kidney (Sandau, 2001) and liver (Aslan, 2003). Altered actin in sepsis is also evidenced by altered actin-binding proteins (e.g. gelsolin) in sepsis (Lee & Waxman, 2007).

Targeting the cytoskeleton is probably not a therapeutic option in view of the widespread role of the cytoskeleton. However, actin may itself be injurious in sepsis (Erukhimov et al, 2000), and mopping up plasma actin may prevent this injury in sepsis (Messaris, 2007).

Chapter Four

Does Nitric Oxide directly enhance K_{ATP} channel function in sepsis?

Introduction

Activation of the ATP-sensitive potassium (K_{ATP}) channel, via the iNOS pathway, contributes to the vascular hyporeactivity seen to catecholamines in sepsis (Hall et al., 1996; Sorrentino et al., 1999). Relaxation to K_{ATP} channel openers (e.g. levcromakalim) is potentiated in *in vivo* and *in vitro* models of sepsis (Sorrentino et al., 1999; Chen, 2000; Wilson, 2002). The precise mechanism of this potentiation is unknown, but in short-term (4hr) LPS models this probably involves NO since potentiation of levcromakalim-induced relaxation could be prevented by pre-treatment with an iNOS inhibitor (Wilson, 2002). However, in *in vitro* models greater than 6 hours, inhibition of NO production only partially reversed hyporeactivity to PE or potentiation of levcromakalim-induced relaxation (O'Brien et al., 2001; Wilson & Clapp, 2002). This may be because mechanisms other than the NO pathway are involved, e.g. the arachadonic acid pathway (O'Brien et al., 2001). Alternatively, it may have been because irreversible damage had occurred to the K_{ATP} channel (Wilson & Clapp, 2002). Indeed, the K_{ATP} channel function appears to be altered in *in vitro* models of sepsis, such that there is an uncoupling of the ability of drugs acting via the SUR to close the channel (Wilson & Clapp, 2002; O'Brien et al., 2005), but drugs acting directly on the ion-channel pore retain their ability to close the channel (Wilson & Clapp, 2002; O'Brien et al., 2005). Therefore experiments were designed to examine whether or not I could enhance K_{ATP} channel function by exposing tissues to exogenously generated NO, to explore the hypothesis that this was a direct NO effect and not secondary to any other down-stream consequences of LPS, e.g. cytokines or arachidonic acid.

4.1 iNOS induction and NO production in an *in vitro* model of sepsis

N-(3-(Aminomethyl)benzyl)acetamidine (1400W) is a highly specific inhibitor of iNOS, which works by preventing the dimerisation of iNOS both *in vivo* and *in vitro* models (Garvey, et. al 1997). This inhibitor was thus used to assess whether it could reverse vascular hyporeactivity induced by LPS in rat aorta. For these experiments aortic rings were incubated in DMEM with 1400W (10 μM) (Garvey et al., 1997) in the presence and absence of LPS (0.1 μg ml^{-1}) for either 24 hrs or 48 hrs as indicated. 1400W is a slow, but tight binding and highly iNOS selective inhibitor (Garvey et al., 1997) and the inhibition of iNOS lasts for over 2 hrs after exposure (Garvey et al., 1997). Fig. 4.1 shows that 1400W was able to substantially reverse vascular hyporeactivity induced by 48 hr LPS causing a significant shift in the EC_{50} for PE ($7.1.10^{-8}$ M vs $6.7.10^{-8}$ M, $P = 0.001$). Surprisingly, it had little effect at the 24 hr time point ($P > 0.05$).

In control tissues no significance difference was seen with co-incubation of 1400W, suggesting insignificant iNOS induction in control tissues following incubation in DMEM (fig. 4.1).

Fig. 4.2 demonstrates that mesenteric artery incubated at the 48 hr time point contracted sub-maximally. Control tissue incubated with 1400W (10 μM) was similarly affected, excluding iNOS induction as a cause of the hyporeactivity in controls. Data are not displayed for 24 hr LPS and 1400W in mesenteric artery. This was because of a lack of an endothelial response in the majority of these tissues.

A

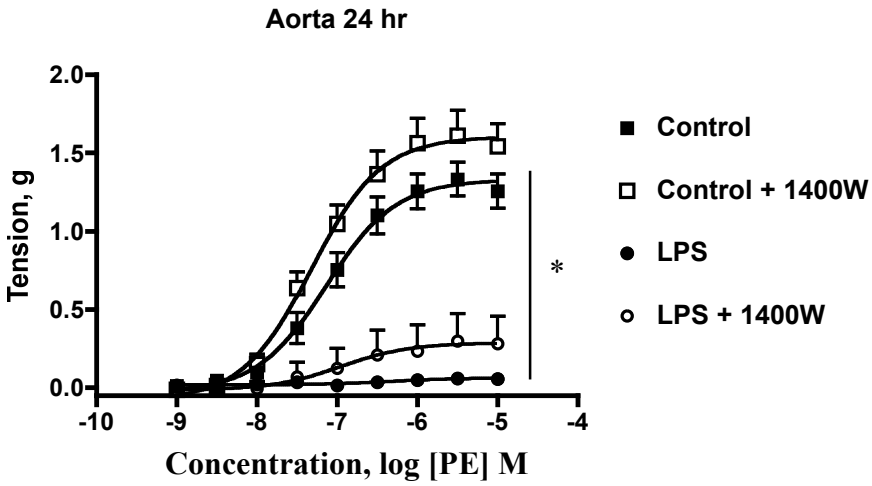

B

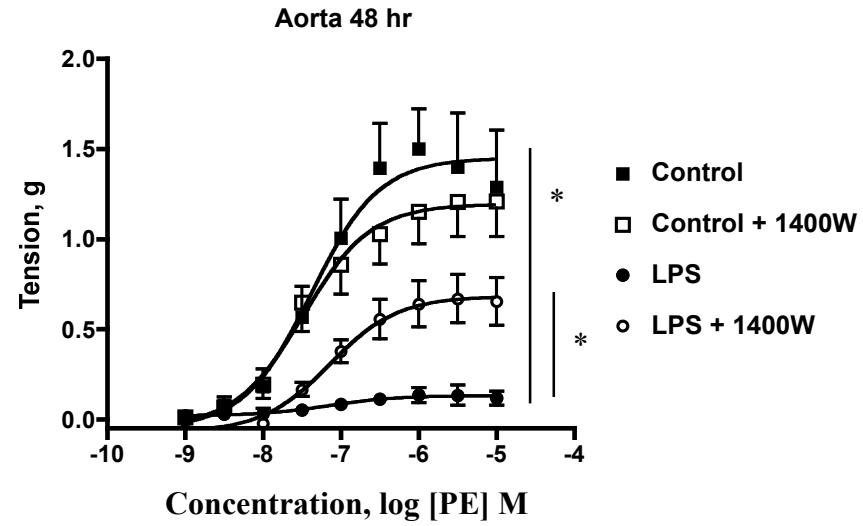

Fig 4.1 Effects of the iNOS inhibitor 1400W on aortic vascular reactivity in an *in vitro* model of sepsis. PE (10^{-9}–10^{-5} M) concentration-response curves at 24 hr (A) and 48 hr (B) time points, where tissues were incubated in DMEM ± 0.1 $\mu g.ml^{-1}$ LPS in the presence and absence of 1400W (10 μM). Data are displayed as mean ± SEM (n = 4 for all groups). 1400W causes a significant reversal of sepsis-induced hyporeactivity at the 48 hr (EC_{50} = $7.1.10^{-8}$ M vs $6.7.10^{-8}$ M, P = 0.001, *), but not the 24 hr time point (P > 0.05).

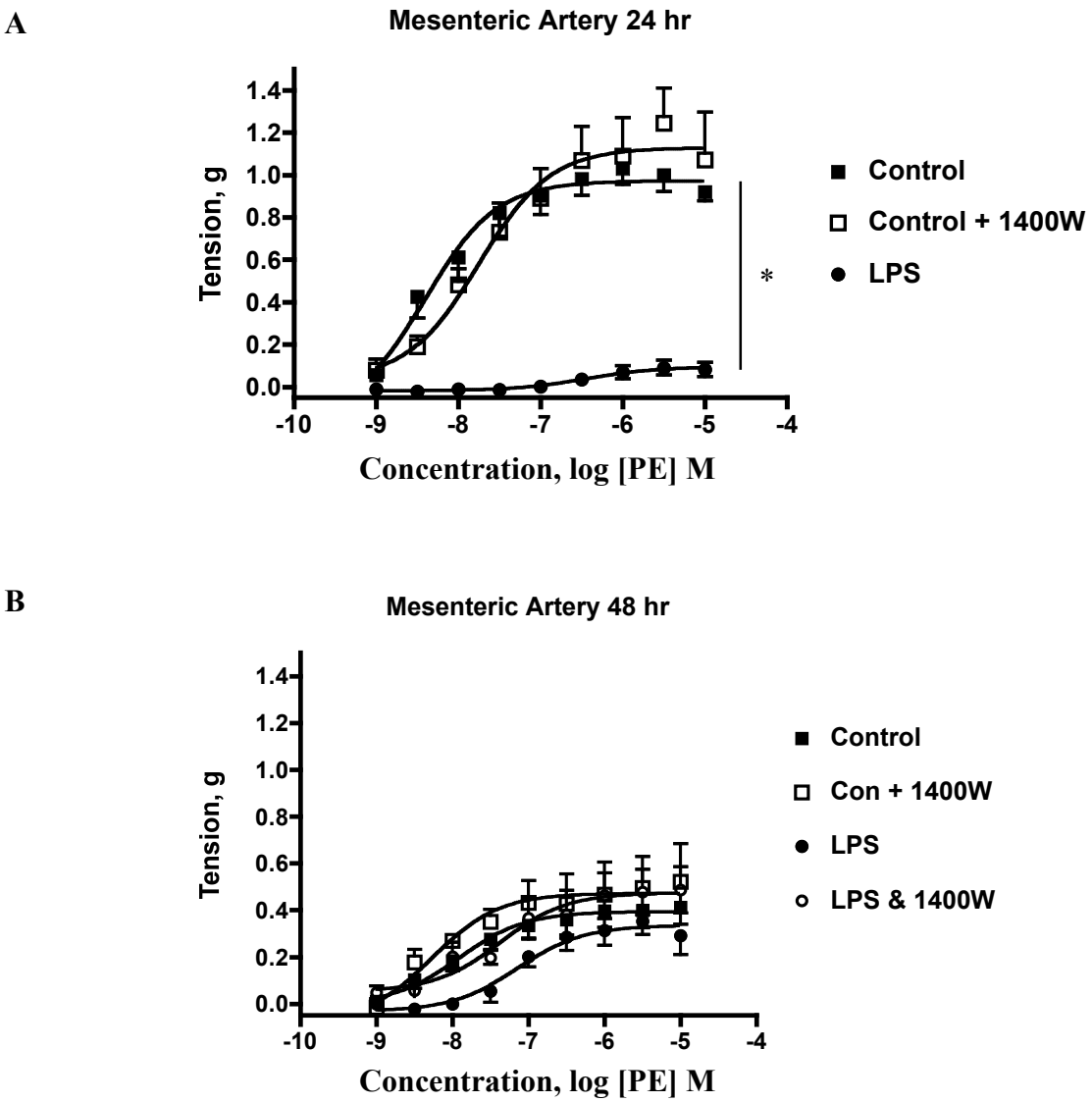

Fig 4.2 Effects of the iNOS inhibitor 1400W on the *in vitro* model of sepsis in mesenteric artery. PE (10^{-9}–10^{-5} M) concentration-response curves at 24 hr (A) and 48 hr (B) time points. Tissue was incubated in DMEM ± 0.1μg.ml^{-1} LPS ± 1400W (10 μM). Data are displayed as mean ± SEM. 1400W did not cause a significant inhibition of the LPS-induced hyporeactivity at the 24 hr or 48 hr time points (P > 0.05). (24 hr control, n = 9; 24 hr control + 1400W, n = 3; 24 hr LPS, n = 10; 48 hr control, n = 6; 48 hr control + 1400W, n = 2; 48 hr LPS, n = 4; 48 hr LPS + 1400W,n=2).

4.2 Determination of the Deta NO concentration required to mimic NO release in an *in vitro* model of sepsis

To examine the hypothesis that opening of the K_{ATP} channel in sepsis was a direct NO effect on the channel, a pure NO donor (Deta NO) was selected (Griffiths, 2001) (see chapter 2, section 2.4.5, p 7). Previous results from this laboratory have shown in a similar organ culture model to the one used here that LPS produces micromolar (2 μM mg^{-1} protein) levels of nitrite (breakdown product of NO) in the supernatant of tissues incubated for 20 hrs (O'Brien, 2005). Therefore, I calculated what concentration of Deta NO was required to release a similar range of NO. To ensure sufficient concentrations of NO to detect an effect, a concentration of 10 μM NO was selected. It is known that one mole of Deta NO releases 2 moles of NO and that the decay half life ($t_{1/2}$) for Deta NO is 1200 mins at 37^{o}C at pH 7.4 (Sigma Aldrich data sheet). Using the graphical analysis programme GraphPad Prism, a theoretical decay curve was plotted and it was possible to calculate what concentration of Deta NO would be required to release 10 μM NO over a given time period (fig. 4.3). Thus 10 μM of Deta NO would theoretically decay by half after 20 hr, at 37^{o}C, pH 7.4, thereby releasing 10 μM of NO. Confirmation of the amount of NO released by the *in vitro* model of sepsis (LPS 1μg/ml) and by 10 μM Deta NO was sought by measuring the amount of nitrite produced by both experiments. Nitrite levels were measured using the Griess assay, which is based on a diazotisation reaction, with a subsequent colorimetric measurement (Chapter 2). The data in fig 4.4 demonstrates that the *in vitro* model produced 3.1 μM nitrite per μg protein compared to 2.0 μM nitrite per μg protein in controls ($n = 7$, $P < 0.05$). Additionally, I demonstrated that 10 μM Deta NO produced 11.1 μM nitrite per μg protein (fig 4.4). This was greater than

the level of nitrite produced by the *in vitro* model of sepsis and greater than the control tissue (n = 5, P < 0.005) (fig. 4.4). This confirmed that the incubation of rings of aorta in 10 μM Deta NO for 20 hr, at 37°C and pH 7.4 released an adequate amount of NO. This then enabled me to investigate whether or not NO had a direct effect on the K_{ATP} channel.

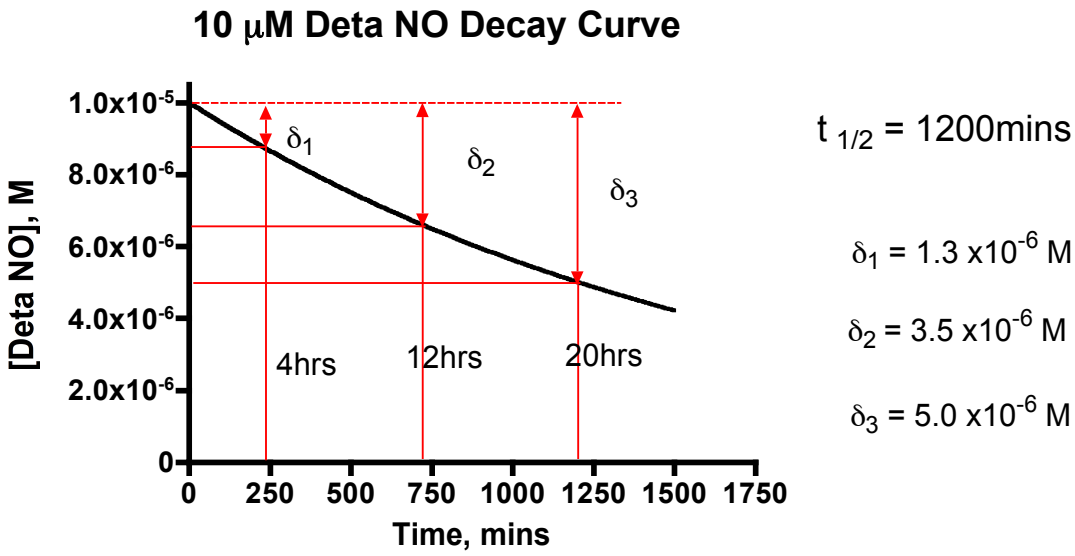

Fig 4.3. Deta NO theoretical decay curves based on a half-life of 20hr at 37°C, pH 7.4. This theoretical decay curve demonstrates that to achieve the release of 10 μM NO (to mimic NO release in the *in vitro* model of sepsis) requires incubation of tissues with 10 μM Deta NO for 20 hr.

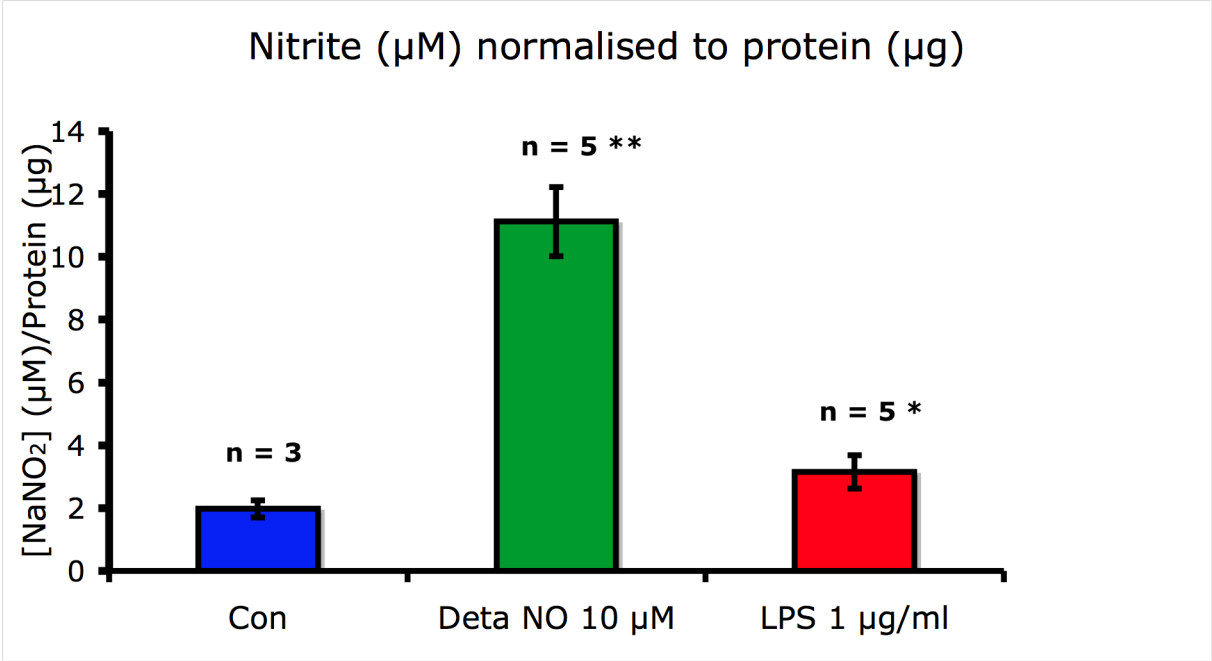

Fig. 4.4. Nitrite levels produced by Deta NO or LPS after 20hr incubation. Rings of aorta are incubated in DMEM in the absence or presence of either LPS (1 µg/ml) or 10 µM Deta NO for 20 hr, 3.15 µM nitrite per µg of protein were generated. This was statistically significantly higher than the nitrite generated in aorta incubated in DMEM alone (1.98 µM per µg protein) (* = $P < 0.05$). Incubation of tissue in 10 µM of Deta NO for 20 hr generated sufficient nitrite (11.12 µM per µg protein) to mimic this *in vitro* model of sepsis. This was also significantly greater than controls (** = $P < 0.005$). Data are displayed as mean ± SEM, where the n value for each condition is as indicated.

4.3 K_{ATP} channel function in an *in vitro* model of sepsis

The contribution of K_{ATP} channels to the vascular hyporeactivity seen in sepsis can be studied by examining the effect of K_{ATP} channel openers on pre-contracted rings of blood vessel (Chen, 2000). In sepsis, the relaxation curve to the K_{ATP} channel opener pinacidil was reported to be shifted to the left in septic animals (Chen, 2000), possibly indicating that a sepsis-induced intracellular factor may be synergising with pinacidil to open more K_{ATP} channels and cause greater relaxation (Chen, 2000). In an *in vivo* model of sepsis (described in Chapter 2, section 2.3), I found a potentiation of levcromakalim-induced relaxation in thoracic aorta taken from these septic rats at 24 hr after the insult (fig. 4.5). There was a small but significant left-shift in the concentration response curve (EC_{50} $1.9.10^{-7}$ M compared to EC_{50} $3.4.10^{-7}$ M in sham animals; n = 4; n=8, P = 0.0004)

Subsequently, a series of experiments were performed whereby rat aorta was pre-incubated in Deta NO (10 μM) for 20 hr, and the relaxant response to different concentrations of levcromakalim assessed. If the potentiation of K_{ATP} channels in sepsis were due to a direct NO effect, then I would predict a left-shift of the levcromakalim concentration response curves in the tissue incubated in 10 μM Deta NO. In these studies, rat aortae were pre-contracted with phenylephrine (3 μM) and levcromakalim-induced (10^{-9} – 10^{-5}M) relaxation examined in the presence of Deta NO (10 μM) at 4 hr and 20 hr time points. Pre-incubation with Deta NO did not affect relaxation to levcromakalim at the two time points (Fig. 4.6 & Fig. 4.7).

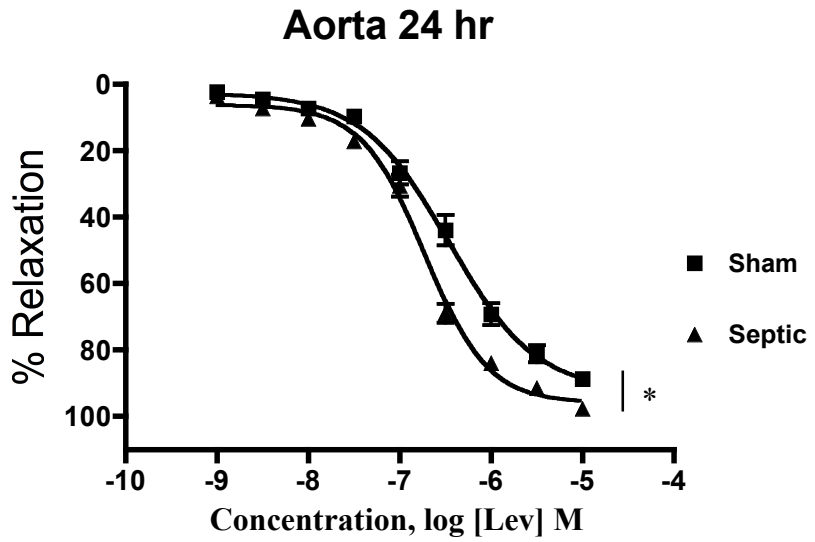

Fig. 4.5 Levcromakalim (10^{-9} – 10^{-5}M) relaxation curves in rat thoracic aorta taken from an *in vivo* model of sepsis. Tissue was pre-contracted with PE (3μM). 24 hr sham animals: EC_{50} = $3.4.10^{-7}$M, n=4. 24 hr septic animals: EC_{50} = $1.9.10^{-7}$M, n = 8. ($P < 0.005$, *). Mean % relaxation ± SEM.

A.

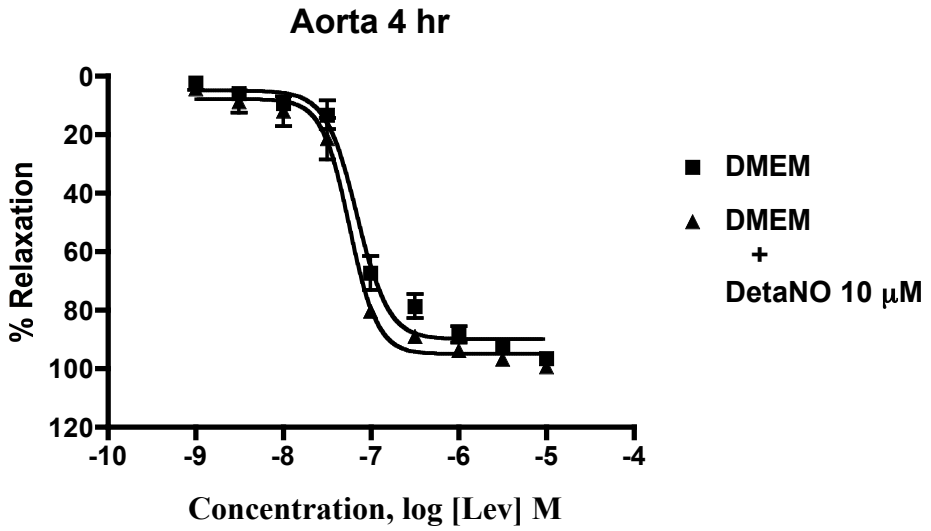

B.

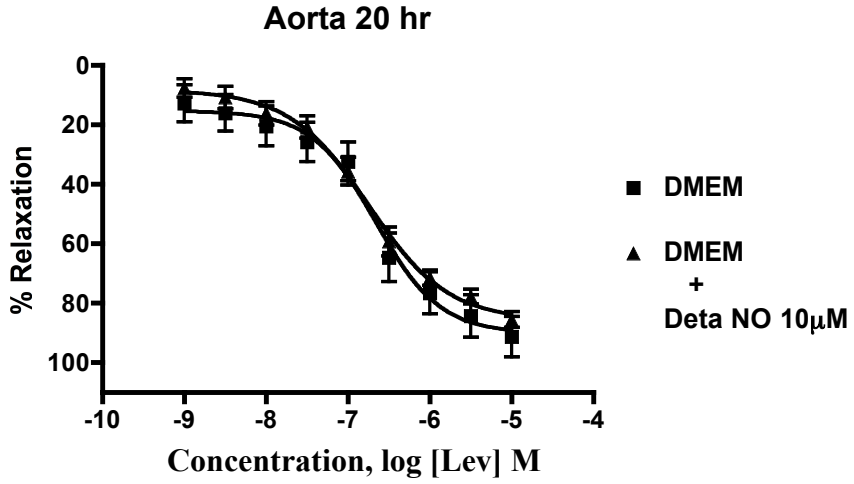

Fig 4.6 A. Levcromakalim relaxation response curve generated in the presence or absence of Deta NO 10 μM, where rings have been incubated for 4hr (A) or 20 hr **(B).** Tissues were pre-contracted with PE (3μM) and data shown as mean % relaxation ± SEM.

	4hr Control	4hr DetaNO (10 µM)	20hr Control	20hr DetaNO (10 µM)
EC_{50}	7.0×10^{-8} M	5.7×10^{-8} M	2.1×10^{-7} M	1.6×10^{-7} M
N	4	4	4	4
P value		0.1		0.57

Fig 4.7: EC_{50} values obtained from concentration-response curves for levcromakalim in rat thoracic aorta. Two-way ANOVA (repeated measures) were used to analyse differences between the concentration-response curves.

4.4 Discussion of NO activation of the K_{ATP} channel

Increased iNOS expression is a central feature of sepsis. There are increased levels of nitrate and nitrite and increased activity of iNOS in both *ex vivo* and *in vitro* (Hernanz *et al.*, 2004) and *in vivo* (Rees *et al.*, 1998) models of sepsis. Increased levels of NO breakdown products have been reported in septic patients (Evans *et al.*, 1993; Ochoa *et al.*, 1991), with evidence of nitration in skeletal muscle. Nitric oxide plays a significant role in activation of the K_{ATP} channel in sepsis (Hall et al., 1996; Sorrentino et al., 1999; Thiemermann, 1997). The exact mechanism of activation remains unknown, but is likely to involve the NO-cGMP pathway (Wilson, 2002; O'Brien et al., 2001; Han et al., 2002).

One of the earliest indications that NO may be activating K_{ATP} channels in sepsis came from the work of Miyoshi and colleagues (Miyoshi, Nakaya et al. 1994). They demonstrated in patch-clamp studies from cultured coronary cells, that L-Arginine, which preferentially activates iNOS, caused persistent activation of K_{ATP} channels in endotoxin-treated but not control cells. Activation was blocked

by methylene blue, an antioxidant with both guanylate cyclase and NO synthase inhibitor activity, suggesting involvement of both NO and cyclic GMP. Interestingly, the effects could not be mimicked by NO donors even though they produced greater amounts of NO in the bathing medium. Likewise, the involvement of K_{ATP} channels in NO donor-induced relaxation may require prior endotoxin treatment (Wilson and Clapp 2002) or the presence of superoxide (Ohashi, Faraci et al. 2005). This raises the intriguing possibility that the iNOS pathway yields additional or more stable factors that work in concert with NO to cause persistent channel activation in sepsis. Indeed calcineurin activity is substantially reduced by nitric oxide and/or superoxide (Sommer, Coleman et al. 2002), the net effect would be to hyperphosphorylate the K_{ATP} channel and cause substantial opening even at normal ATP levels (Wilson, Jabr et al. 2000). Moreover, peroxynitrite, a much more reactive species than NO, is a powerful oxidant capable of nitrating tyrosine residues, causing lipid peroxidation and reacting with thiols and iron-containing compounds. Superoxide produces glibenclamide-sensitive relaxation in carotid and cerebral vessels, involving both cyclic GMP-dependent and cGMP-independent mechanisms (Wei, Kontos et al. 1998; Ohashi, Faraci et al. 2005) and is a widespread dilator of many vascular beds.

I investigated whether or not there was a direct effect of NO on the K_{ATP} channel, initially by trying to replicate the increased relaxation to the KCO levcromakalim. Deta NO is a pure NO donor, producing two moles of NO for every mole of Deta NO that decays. However, despite generating levels of NO similar to that released in a LPS *in vitro* model of sepsis (10 μM), I was unable to mimic potentiation of

the K_{ATP} channel seen in sepsis (Chen et al., 2000; Wilson & Clapp, 2002). The data demonstrated that nitric oxide was involved in the vascular hyporeactivity seen in the *in vitro* model of sepsis (fig. 4.1). Therefore, the NO pathway is involved in activation of the K_{ATP} channel, but this is not a direct effect of NO on the proteins of the channel, and is likely to involve down-stream effectors, possibly cGMP and PKG (Han et al., 2002). It is possible that despite the calculations utilising the decay characteristics of Deta NO, sufficient levels of NO did not penetrate the cell to alter K_{ATP} channel function. However, the measurement of nitrite levels in the DMEM used demonstrated levels in the correct range (O'Brien et al., 2001) and 1400W is very tissue permeable (Garvey et al., 1997). Notwithstanding this, in sepsis NO may be produced in a variable pattern maybe with peaks in production, whereas, the NO released via Deta NO is based on decay kinetics, in a more gradual fashion (fig. 4.3). The use of tissue instead of cells may have inadvertently mopped up and absorbed excess NO, possibly via the production of nitrated and nitrosylated thiols (Dalle-Donne, 2000). The *in vitro* model of sepsis did not include FBS (O'Brien et l., 2001), one of the best-known buffers of NO, but a slow-release form of nitrosothiols (Dalle-Donne, 2000).

The lack of significant reversal at 24 hr may be secondary to the washing out of 1400W in the organ bath during the priming of the tissue, without the reapplication of 1400W just prior to the cumulative concentration-response curve. However, 1400W was present for the entire duration of the incubation prior to placing the rings in the organ bath. Therefore, in LPS-treated tissue, iNOS induction may occur, but its dimerisation is prevented by the 1400W (Garvey et

al, 1997). 1400W is a tightly binding inhibitor of iNOS (Garvey et al., 1997). It is 5000-fold more selective for iNOS than eNOS and is highly selective for rat tissue (Garvey et al., 1997). Additionally, its effects last for at least 2 hours (Garvey et al., 1997) and may even last longer than this. However, in view of the partial response seen in aorta at 48 hr (fig. 4.1 B), there may have been a washout effect. Interestingly, other authors have only added 1400W to the organ bath, prior to application of vasoconstrictors (O'Brien et al., 2001; Wilson, 2002). Whilst this may not be an issue for short (4 hr) incubation periods (Wilson, 2002), it is likely to be important in models of sepsis that are significantly longer, as demonstrated by O'Brien and colleagues (O'Brien et al., 2001). NO production occurs around 2 hours after incubation with LPS (Hall et al., 1996) and therefore in 24 hr and 48 hr models, incubation without 1400W means that the tissue is exposed to significant levels of NO until 1400W is added to the organ bath. This is likely to affect the outcome of the experiment if NO has injurious effects on the tissue, such as nitration (Giannopoulou et al., 2002) or nitrosylation (Dalle-Donne, 2000). Significantly, 1400W has a slow time of onset (Garvey et al., 1997), but this should not be an issue once co-incubated with tissue and LPS in my 24 hr and 48 hr experiments. To exclude the possibility of a washout effect in the future, 1400W should be co-incubated and subsequently added again in the organ bath prior to investigation with PE and levcromakalim.

Other possibilities for the absence of inhibition of hyporeactivity to LPS (fig. 4.1 A) could include insufficient concentrations of NADPH in the tissue, as NADPH is an essential cofactor for 1400W, without which its efficacy is profoundly reduced (Garvey et al., 1997). Additionally, 1400W may have had toxic effects on

small quantities of tissue, contributing to the very abnormal concentration-response curves seen in mesenteric artery (fig. 4.2 B). Older iNOS inhibitors, such as the bisisothioureas, can be quite toxic (Garvey et al., 1997), but this has so far not been observed with 1400W (Garvey et al., 1997).

The lack of potentiation of levcromokalim in the presence of Deta NO (fig 4.6) may have been due to inadequate concentrations of Deta NO, but as described above, the levels of nitrite measured (fig. 4.4) do not support this. However, it is possible that for NO to abnormally open the K_{ATP} channel, the presence of other factors such as LPS itself, IL-1 and/or TNF alpha are required.

Finally, the initial observation that levcromokalim-induced relaxation was not potentiated meant that the Deta NO model could not be followed up. In future, should the model be refined to be able to reproduce this, then further experiments using cGMP and PKG inhibitors would be necessary, to be able to conclude that this was a direct NO effect on the channel. Examination of the nitration and nitrosylation status of the K_{ATP} channel protein would then offer further confirmation.

In conclusion, there is good evidence that NO production is involved in the abnormal opening of the K_{ATP} channel in sepsis (O'Brien et al., 2001; Wilson, 2002), but the exact mechanism is unknown. I have been unable to demonstrate that this is a direct NO effect. It is possible that NO opens the K_{ATP} channel via multiple mechanisms, including the cGMP/PKG pathway (Han et al., 2002), with

phosphorylation of the channel protein (Han et al., 2002). Increased channel expression is also likely to play a role (Shi et al., 2010).

Chapter Five

Does an altered metabolic state cause K_{ATP} channel dysfunction in an *in vivo* model of sepsis?

5.1 **Vascular hyporeactivity in an *in vivo* model of sepsis**

The *in vivo* model of sepsis was used to study the role of the K_{ATP} channel in sepsis, specifically its role in sepsis-induced vascular hyporeactivity. For each of the animals used, the thoracic aorta was removed and frozen in liquid nitrogen, as per the protocol described in Chapter Two (section 2.11). This tissue was later used to measure levels of the nucleotides ATP, ADP and AMP in the blood vessel wall. The abdominal aorta was removed and placed in Hanks' Balanced Salt Solution (Invitrogen, Paisley, UK), buffered with 2mM bicarbonate and 10 mM HEPES, as per O'Brien et al. (2001). This fresh tissue was then mounted in the organ bath to further investigate the pharmacology of the K_{ATP} channel.

Figure 5.1 demonstrates that the vessels were hyporeactive to PE at both the 24 hr (fig 5.1A) and 48 hr (fig. 5.2A) time points. The control vessel concentration-response curve was significantly different from the septic concentration-response curve at both the 24 hr and 48 hr time points. The relaxation concentration-response curves to levcromakalim were also significantly shifted to the left, demonstrating an increased ability of levcromakalim to open the K_{ATP} channel in sepsis (fig. 5.1B and 5.2B, respectively). This is consistent with previous work showing this phenomenon (Chen et al, 2000; O'Brien et al, 2005).

These experiments demonstrate that a greater open probability of the K_{ATP} channel in septic abdominal aorta in this *in vivo* model of sepsis, and that this contributes to vascular hyporeactivity. There was potentiation of levcromakalim-induced relaxation which was significant at the 24 hr time point, but not at 48 hr.

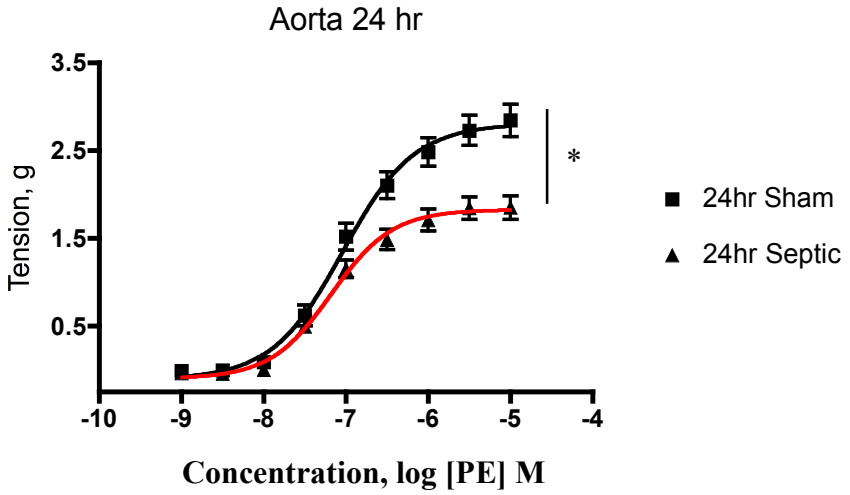

B

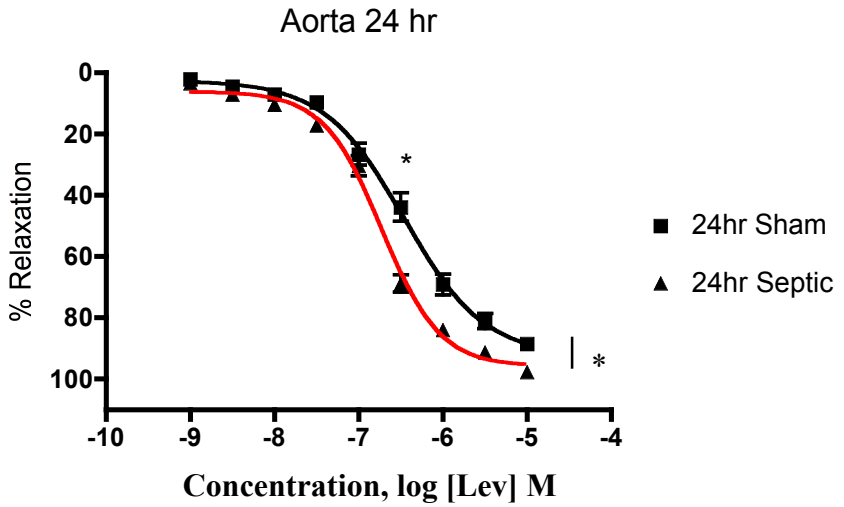

Fig 5.1. *Ex vivo* assessment of aortic vascular reactivity after 24 hr of *in vivo* sepsis (faecal peritonitis) in a rat model. A. Concentration-response curves to phenylephrine in rings of abdominal aorta taken from sham (n=4, EC_{50} $9.1.10^{-8}$ M) and septic animals (n=8, EC_{50} $6.6.10^{-8}$ M) ($P < 0.005$, *)**. B.** Concentration-response curves of levcromakalim in rings of abdominal aorta taken from sham (n=4, EC_{50} $3.4.10^{-7}$ M) and septic animals (n=8, EC_{50} $1.9.10^{-7}$ M) ($P < 0.005$, *). Data are displayed as mean ± SEM. * Points statistically significantly different.

A

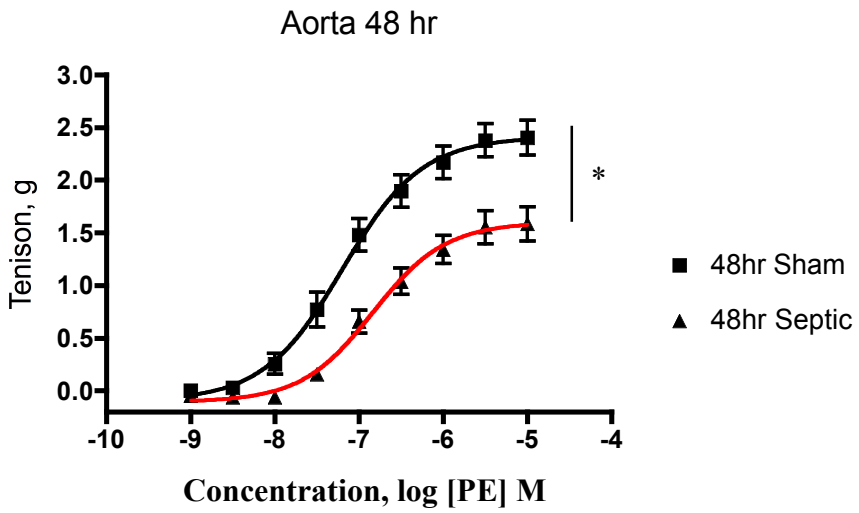

B

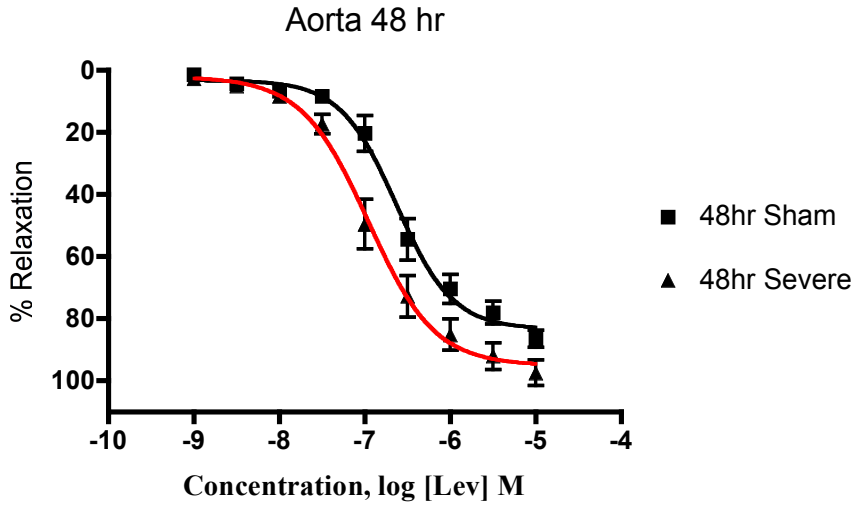

Fig 5.2. *Ex vivo* assessment of aortic vascular reactivity after 48 hr of *in vivo* sepsis (faecal peritonitis) in a rat model. A. Concentration-response curves to phenylephrine in rings of abdominal aorta taken from sham (n=4, EC_{50} $1.7.10^{-7}$ M) and septic animals (n=8, EC_{50} $1.5.10^{-7}$ M) ($P < 0.005$, *)**. B.** Concentration-response curves of levcromakalim in rings of abdominal aorta taken from sham (n=4, EC_{50} $1.7.10^{-7}$ M) and septic animals (n=8, EC_{50} $1.1.10^{-7}$ M) ($P > 0.05$). Data are displayed as mean ± SEM.

I subsequently used this model as a basis for further experiments testing two hypotheses:

1) That the open state of the channel was due to an abnormality in the control of the ion channel pore by the SUR (Wilson & Clapp, 2002).

2) That the open state of the K_{ATP} channel in sepsis was due to either a decrease in the ATP level in the vascular smooth muscle cells, and/or an increase in ADP, with a consequent decrease in ATP: ADP ratio.

5.2 Abnormal control of the ion channel pore by the SUR

The pharmacology of the channel alters in sepsis, whereby the ability of glibenclamide to close the channel is lost yet that of the pore-blocking drugs is retained (Wilson & Clapp, 2002). I initially sought to verify this phenomenon by using the specific pore-blocking agent PNU-37883A and the sulphonylurea receptor inhibitor, glibenclamide to reverse the relaxation caused by the K_{ATP} channel opener levcromakalim in rings of abdominal aorta taken from the *in vivo* model of sepsis. If K_{ATP} channel pharmacology is altered in sepsis by affecting the sulphonylurea receptor, then PNU-37883A should be more effective in improving vascular reactivity, because its action is not dependent on the SUR as it binds to the ion channel pore directly. The results of these experiments are shown in Figs. 5.3 and 5.4. Both PNU-37883A and glibenclamide were used at 10μM concentration (adapted from O'Brien et al., 2005). At 24 hr, PNU-37883A only partially reversed levcromakalim-induced relaxation, with a significant difference between septic and sham tissue (Fig. 5.3; 38% vs 90%, $P < 0.05$). However, at 48 hr, the ability of PNU-37883A to fully reverse relaxation was restored, with no

difference seen between sham and septic responses (Fig. 5.3, 82% vs 90%, P > 0.05).

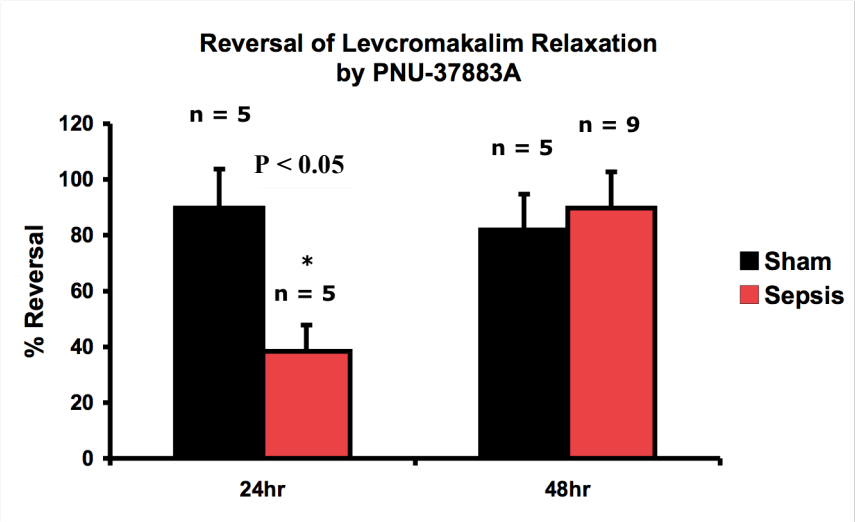

Fig 5.3 Percentage reversal of levcromakalim-induced relaxation by the pore inhibitor PNU-37883A in aortic rings taken from the *in vivo* sepsis model. Data displayed as mean ± SEM. There was a significant reduction in the ability of PNU-37883A (10 μM) to reverse levcromakalim-induced (3 μM) relaxation in aorta taken from septic animals at 24 hr (90% vs 38%, P < 0.05). No difference was seen at 48 hr.

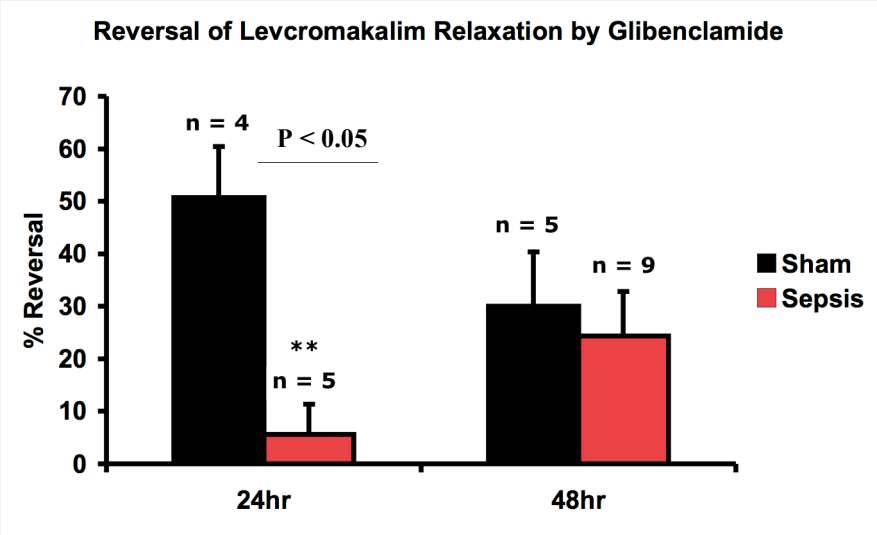

Fig 5.4 Percentage reversal of levcromakalim-induced relaxation by the sulphonylurea inhibitor, glibenclamide in aortic rings taken from the *in vivo* model. Data displayed as mean ± SEM. There was a significant reduction in the ability of glibenclamide (10 μM) to reverse levcromakalim-induced (3 μM) relaxation in aorta taken from septic animals at 24 hr (51% vs 6%, $P < 0.05$) but not at 48 hr (24% vs 30%).

Comparison of PNU-37883A and glibenclamide responses is shown in Fig 5.5. In aorta taken from 24 hr sham animals, PNU-37883A fully reversed levcromakalim-induced relaxation (90%) compared to glibenclamide (50%) though this difference was not significantly different ($P > 0.05$). The degree of reversal by both drugs was significantly different at 24 hr for septic tissue (38% vs 6%, $P < 0.05$) and at 48 hr for both sham (82% vs 30%, $P < 0.02$) and septic (94% vs 24%, $P < 0.001$) tissue.

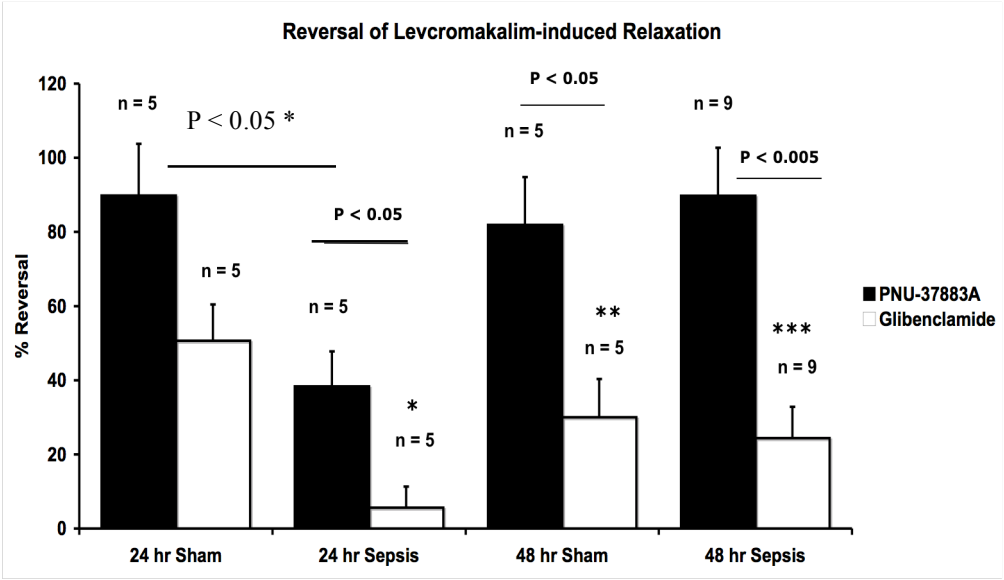

Fig 5.5 Percentage reversal by PNU-37883A (10 µM) or glibenclamide (10µM) of levcromakalim-induced relaxation in rings of abdominal aorta taken from the *in-vivo* model. Analysed using 1-way ANOVA. All significant differences are annotated, all other comparisons were non-significant ($P > 0.05$). Data displayed as mean ± SEM.

These experiments assessed the ability of the K_{ATP} channel pore blocker PNU-37883A to reverse levcromakalim-induced relaxation. While PNU-37883A only partially reversed relaxation in 24hr septic tissue, it fully reversed relaxation at 48 hr. Glibenclamide reversal of relaxation was significantly reduced in 24 hr septic tissue, but there was some degree of recovery in 48 hr septic tissue. I also found that PNU-37883A was more potent at reversing levcromakalim-induced relaxation than glibenclamide in all tissues. This difference was greater in septic tissue, supporting the hypothesis that pore-blocking drugs are more effective at closing the K_{ATP} channel in sepsis compared to drugs acting via the SUR subunit.

5.3 Adenine nucleotide levels in vascular smooth muscle in an *in vivo* model of sepsis

Adenine nucleotides are important regulators of K_{ATP} channel function (Nelson & Quayle) and these levels are altered in sepsis (Brealey, 2004). Therefore, I carried out a series of experiments to measure adenine nucleotides in aorta from the *in vivo* model of sepsis to determine if alterations in ATP, ADP or AMP were associated with the altered K_{ATP} channel function observed in sepsis.

Standard curves were generated for each of the nucleotides (ATP, ADP and AMP). Additionally, tissue samples were spiked with nucleotides to internally validate the method.

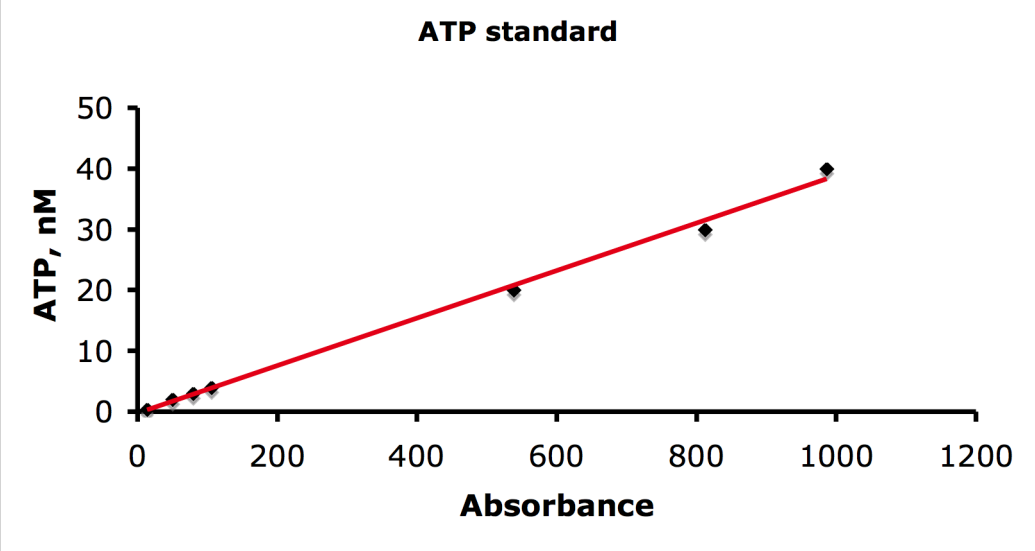

Fig. 5.6: Standard curve for ATP concentration (nM) measured using HPLC.

A

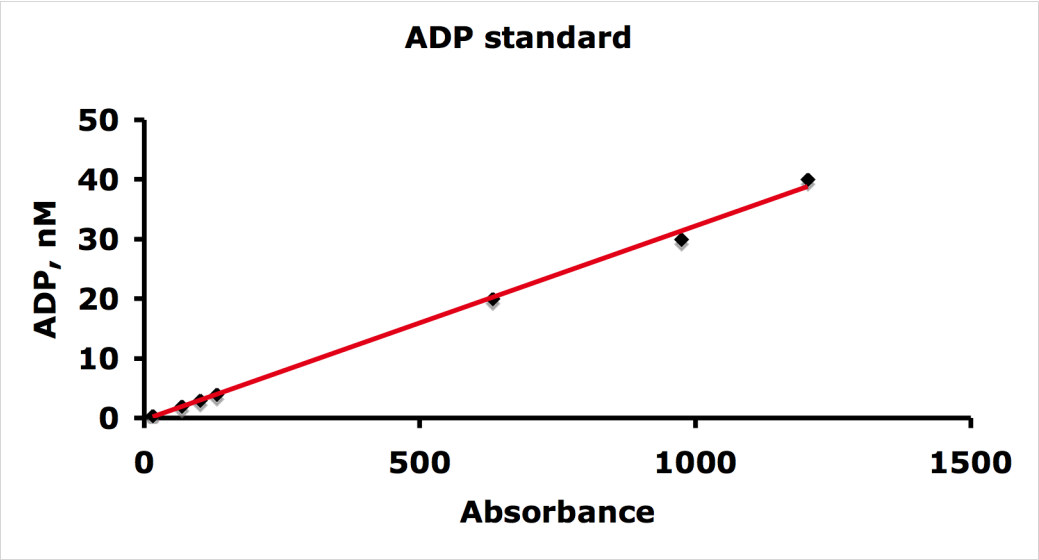

B

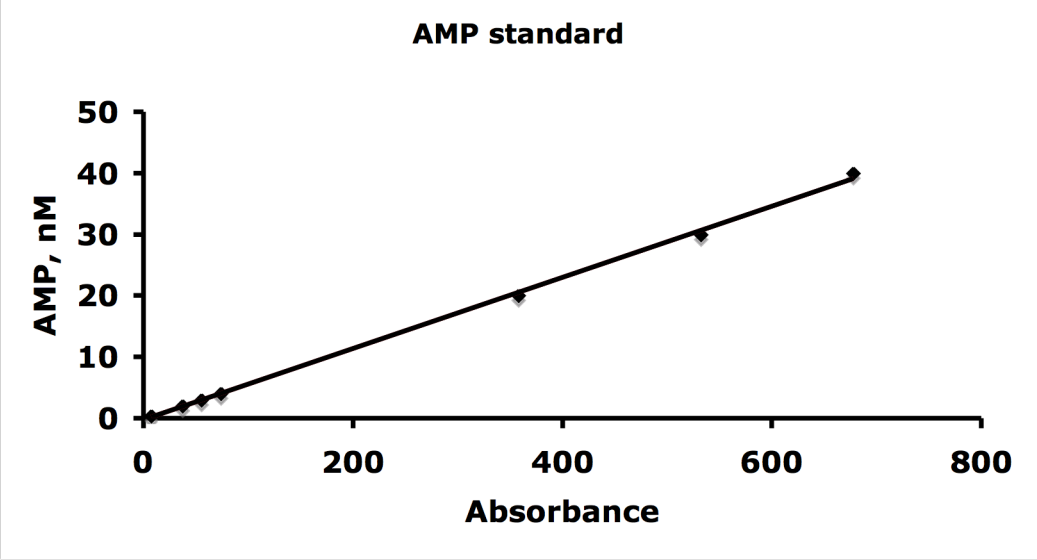

Fig 5.7: Standard curves for **A.** ADP and **B.** AMP concentration (nM) measured using HPLC.

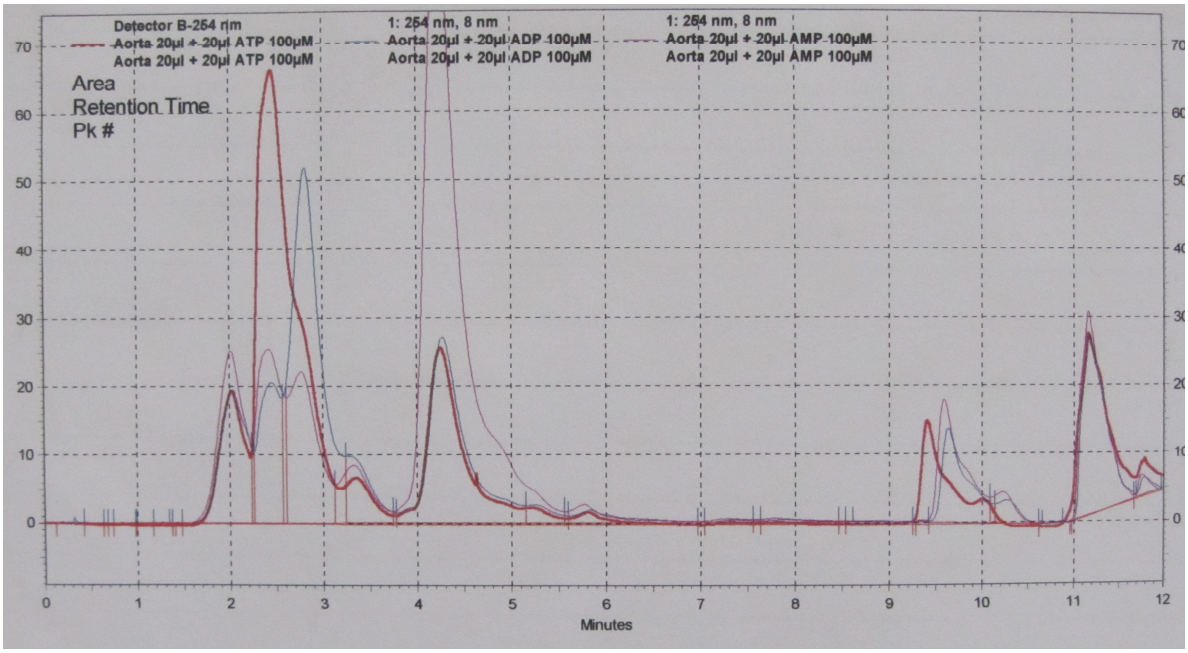

Fig. 5.8. HPLC measurement of adenine nucleotide levels in rat aorta, spiked with an additional 100 µM ATP, ADP and AMP.

The thoracic aortae were removed from deeply anaesthetised rats as described in chapter two (section 2.3). These samples were then flash-frozen in liquid nitrogen, freeze-dried and homogenised, prior to processing for HPLC. The samples were processed via high performance liquid chromatography, (see section 2.12). Using 1-way ANOVA, no significant change in ATP concentration was seen at either 24 hr ($p > 0.05$) or 48 hr ($p > 0.05$) (Fig 5.9).

No significant changes were seen in ATP levels when the animals were divided into mild, moderate and severe sepsis groups however numbers in each group were probably too small to address this question adequately (Fig. 5.10).

Nevertheless, abdominal aorta removed concurrently did demonstrate marked vascular hyporeactivity, so low energy levels of ATP are unlikely for this.

A similar pattern was seen for ADP and AMP levels in sepsis (Figs. 5.11 and 5.13, respectively). A trend towards a decrease in ADP and AMP levels were seen in the 48 hr severe sepsis group (Fig. 5.12), though, using 1-way ANOVA, this did not reach statistical significance ($P > 0.05$).

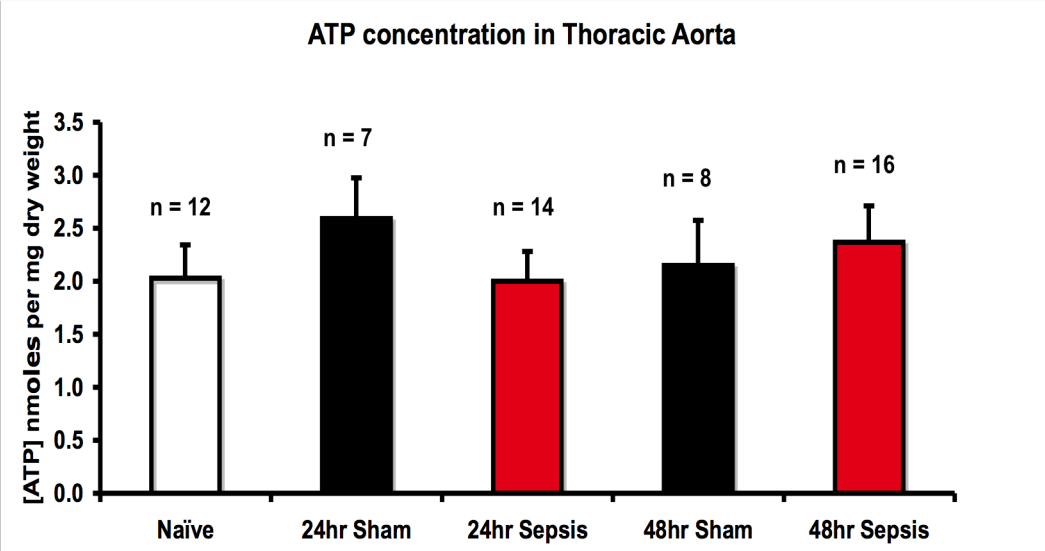

Fig. 5.9: ATP levels from thoracic aorta, normalised to mg dry weight of tissue. No significant difference was seen between naïve animals and sham animals, or between sham and septic animals at any time point ($P > 0.05$). Data are displayed as mean ± SEM.

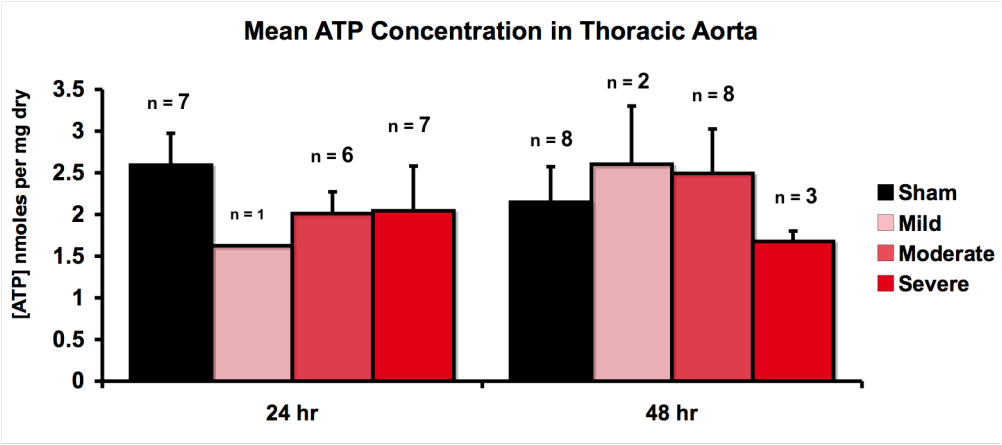

Fig. 5.10: ATP levels from thoracic aorta, normalised to mg dry weight of tissue. Using 1-way ANOVA, no significant difference was seen between any groups ($P > 0.05$). Data displayed as mean ± SEM.

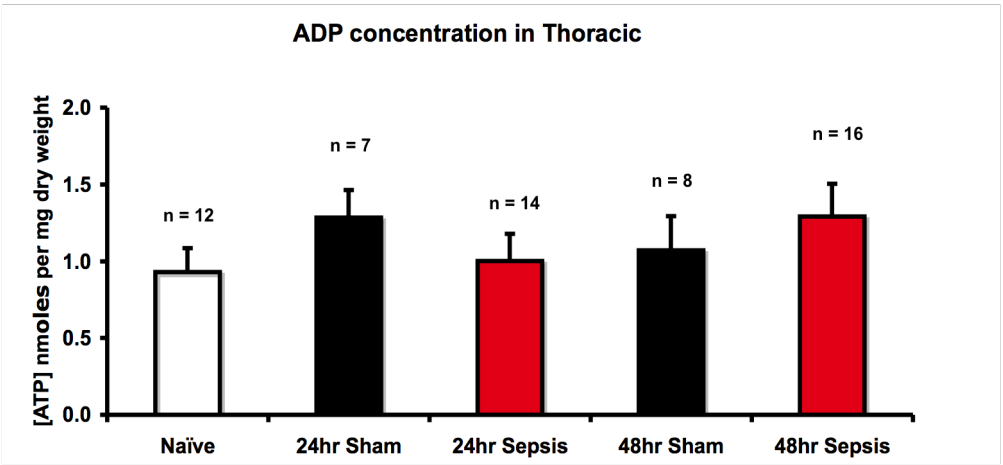

Fig. 5.11: ADP levels from thoracic aorta, normalised to mg dry weight of tissue. Using 1-way ANOVA, no significant difference was seen between any groups ($P > 0.05$). Data displayed as mean ± SEM.

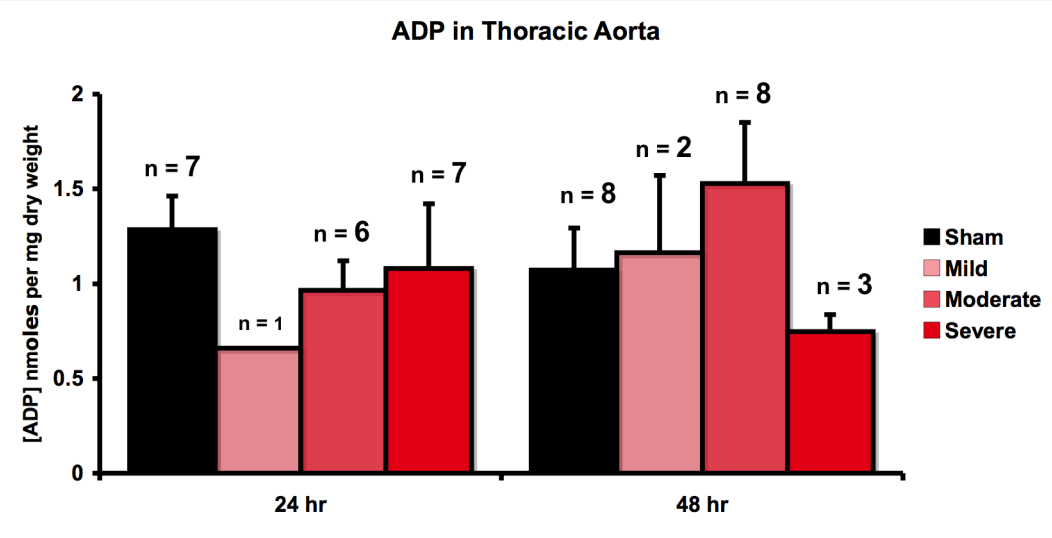

Fig. 5.12: ADP levels from thoracic aorta, normalised to mg dry weight of tissue.

Using 1-way ANOVA, no significant difference was seen between any of the groups ($P > 0.05$). Data are displayed as mean ± SEM.

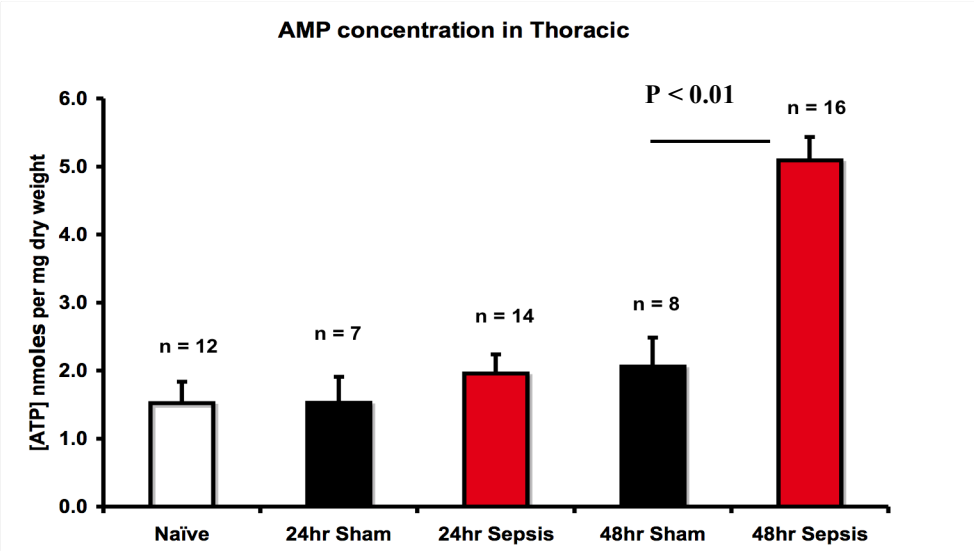

Fig. 5.13: AMP levels from thoracic aorta, normalised to mg dry weight of tissue. Using 1-way ANOVA, AMP levels were raised at 48hr sepsis when compared to 48hr sham ($P < 0.01$). Data are displayed as mean ± SEM.

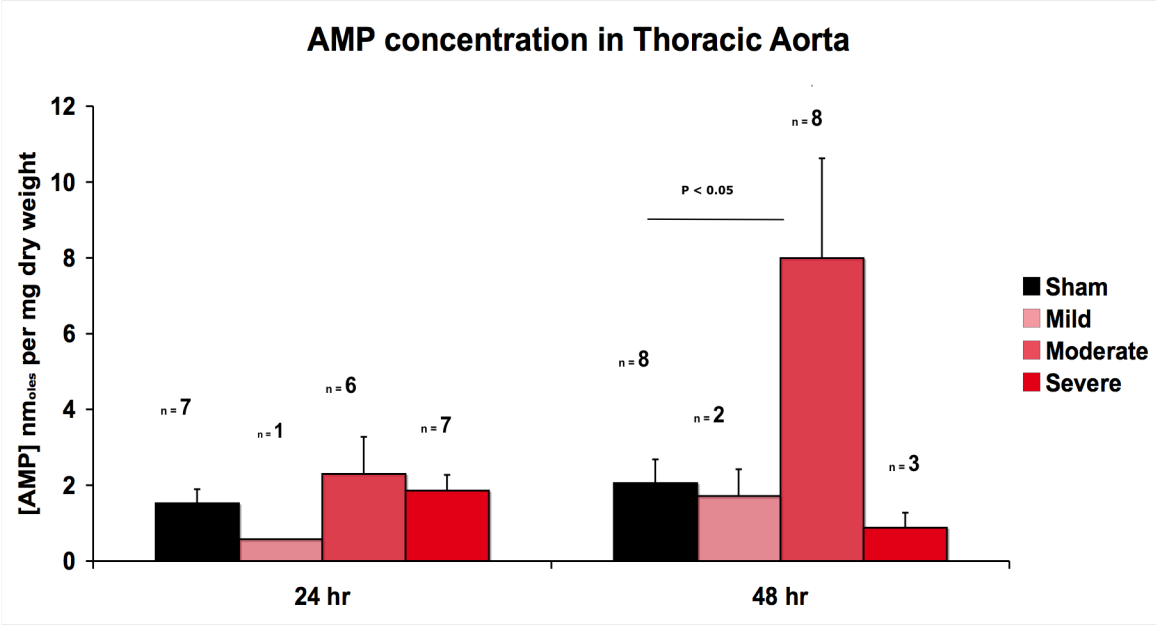

Fig. 5.14: AMP levels from thoracic aorta, normalised to mg dry weight of tissue. No significant difference was observed in AMP levels from aortae taken at 24 hr from sham animals, and septic animals from all severity groups, 1-way ANOVA, $P > 0.05$. At 48 hr the AMP level in the moderate severity group was significantly elevated when compared to 48hr sham only ($P<0.05$). Data are displayed as mean ± SEM.

These experiments demonstrated no significant difference in adenine nucleotide levels in thoracic aorta taken from this rat peritonitis model of sepsis compared to sham animals. Vascular hyporeactivity (fig. 5.1) and altered K_{ATP} channel pharmacology (fig. 5.5) have however been demonstrated in these tissues.

I therefore proceeded to measure adenine nucleotide levels in thoracic aorta from an *in vitro* model of sepsis, as described in Chapter two. Previous experiments demonstrating altered pharmacology of the K_{ATP} channel (Wilson & Clapp, 2002; O'Brien et al, 2005) have not been repeated.

5.4 Adenine nucleotide levels in vascular smooth muscle in an *in vitro* model of sepsis:

ATP, ADP and AMP levels were measured in thoracic aorta incubated in DMEM ± LPS (100 $ng.ml^{-1}$) for 24 and 48 hr periods. The thoracic aortae were obtained as described in Chapter Two. The samples were processed via high performance liquid chromatography, again as described in Chapter Two. Levels of ATP were unaltered with sepsis (Fig. 5.15). ADP levels were un-interpretable with many negative values being obtained (data not shown). AMP levels were significantly reduced in all septic tissues and in control tissue, compared to naive tissue (Fig 5.16).

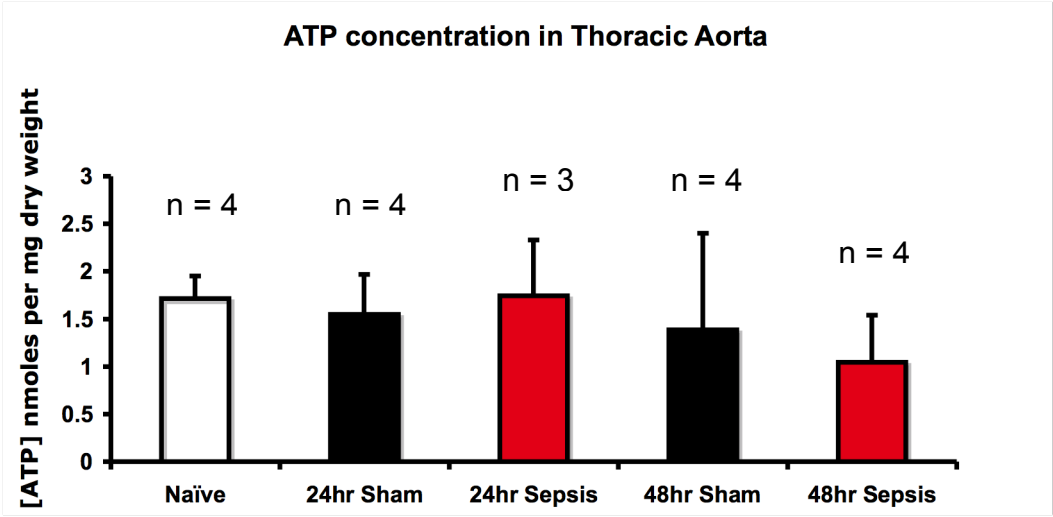

Fig. 5.15: ATP levels from thoracic aorta from an *in vitro* model of sepsis, normalised to mg dry weight of tissue. Using 1-way ANOVA, no significant difference was seen between samples ($P > 0.05$). Data displayed as mean ± SEM.

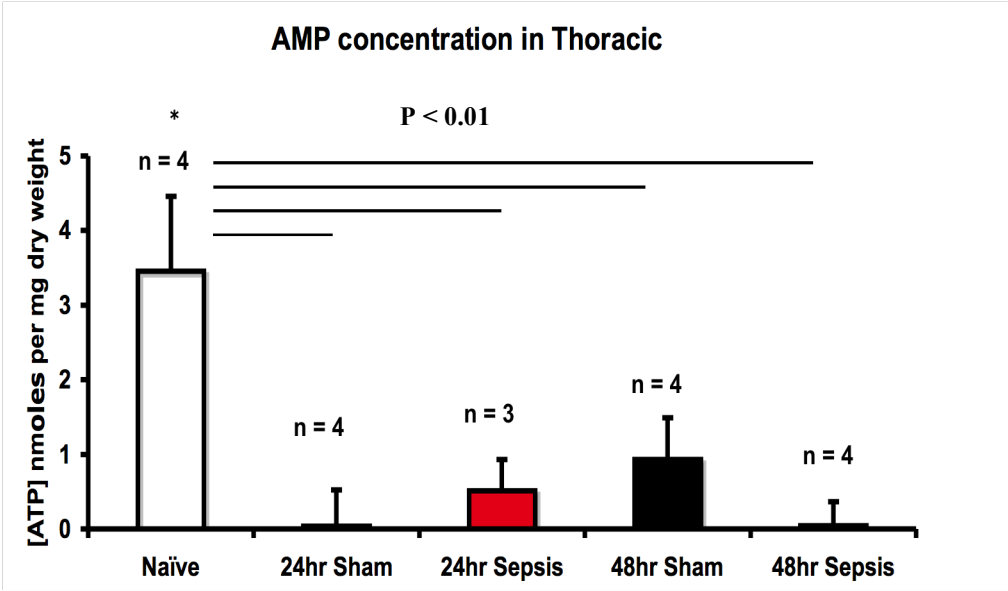

Fig. 5.16: AMP levels from rat thoracic aorta, normalised to mg dry weight of tissue, **in an *in vitro* model of sepsis**. A significant difference was observed between naïve animals and all other groups ($P < 0.01$), with the exception of the 48 hr sham group ($P > 0.05$). No significant difference was seen between any of the 24 hr or 48 hr tissue values ($P > 0.05$). Data displayed as mean ± SEM.

These experiments demonstrated that ATP levels in rings of rat thoracic aorta were unchanged in an *in vitro* model of sepsis, possibly with a trend towards a reduction at the 48 hr sepsis time point. However, levels of ADP in the tissue were almost non-existent. Incubation of tissue in DMEM ± LPS caused a significant reduction in levels of AMP measured in the tissue.

5. 5 Discussion

With the use of HPLC, I demonstrated that there was no alteration in the levels of ATP in either an *in vivo* or *in vitro* model of sepsis. This was despite demonstrating that the tissue used was a valid model via the proven, altered pharmacology of the K_{ATP} channel. It is possible that the levels of ATP were altered, but the method used was too insensitive to measure it. Alternatively, it may be sub-cellular, compartmentalised ATP that varies in sepsis, thus altering the K_{ATP} channel. These results were surprising, considering that ATP is such a potent controlling mechanism of the channel, and that clinical studies have shown altered levels of K_{ATP} in sepsis (Brealey et al., 2002). However, this was demonstrated in skeletal muscle, not in vascular smooth muscle.

Measurements of adenine nucleotides were more reproducible in the *in vivo* model of sepsis. This may have been simply due to the fact that the *in vivo* model meant that a whole thoracic aorta could be homogenised each time, thereby reducing the amount of error due to dilution. The *in vitro* model required the incubation of rings of aorta in DMEM ± LPS. Therefore, it is possible that the rings of vessel were too small to accurately measure adenine nucleotides. Alternatively, adenine nucleotides are better preserved and maintained in the *in vivo* model, hence potentially strengthening the validity of such models over *in vitro* models. All the more so since I clearly demonstrated altered K_{ATP} channel pharmacology in the *in vivo* model.

There was a significant increase in AMP levels in septic tissue and has important implications for the metabolic state of the cell and subsequently K_{ATP} channel

function. It is possible that it represents increased ATP and ADP breakdown, in the attempt of the cell and tissues to maintain sufficient ATP levels for overall cellular function. The very low levels of ADP measured in the *in vitro* model may be real. However, in view of the abnormally low levels measured in the naive samples, I suspect that it was more likely artefactual, and ideally should be repeated. However, the overall pattern of results suggests that the technique is not reproducible in small rings of tissue, with low levels of total protein. Measurement of sub-cellular levels of adenine nucleotides, in the context of patch-clamp studies or rubidium efflux experiments would potentially offer interesting information on the metabolic alteration of the cell and K_{ATP} channel in sepsis, however, the above difficulties may be even more exaggerated.

The K_{ATP} channel links the metabolic state of the cell to membrane potential and vascular tone. In sepsis this channel is abnormally activated. Intracellular ATP inhibits channel activity. Lower ATP levels are seen in skeletal muscle of eventual non-survivors of septic shock when compared to eventual survivors (Brealey et al., 2002). This is associated with mitochondrial dysfunction with the degree of inhibition of complex I correlating with the clinical severity of illness and with NO production (Brealey et al., 2002). Indeed, the effect of NO on K_{ATP} channels in the pancreas is secondary to decreased ATP via inhibition of phosphofructokinase (Tsuura *et al.*, 1994). The concept of mitochondrial dysfunction is supported by the inhibition of mitochondrial function seen in human umbilical vein epithelial cells incubated with serum from septic patients (Boulos *et al.*, 2003). This is not surprising as NO and its metabolites (including

peroxynitrite) have been shown to inhibit complexes I and IV of the mitochondrial respiratory chain (Brown *et al.*, 1994; Clementi *et al.*, 1998).

It is well recognised that gross metabolic abnormalities occur in septic shock, which contribute to the development of multi-organ failure. Some of these effects may be related to alterations in tissue oxygen utilisation. A low oxygen consumption has been observed in patients with severe sepsis, with a better prognosis in those achieving higher values of global oxygen delivery and consumption (Pollack *et al.*, 1985). However, septic patients and (well-resuscitated) animal models often demonstrate an increase in tissue oxygen tension (Boekstegers *et al.*, 1991; Rosser *et al.*, 1996). This suggests adequate delivery, but impaired utilisation of oxygen. As greater than 90% of oxygen consumed by the body is for mitochondrial generation of ATP via oxidative phosphorylation, mitochondrial dysfunction is therefore implied (Singer *et al.*, 1999).

In primate and rat models of sepsis, morphological evaluation of mitochondria by electron microscopy has shown swelling and distortion of the mitochondrial structure, including disruption of the matrix (Kantrow *et al.*, 1997; Simonson *et al.*, 1994). These structural changes were associated with a decrease in cellular oxidative capacity and a progressive loss of mitochondrial cytochrome *c* oxidase function. In other studies, decreases in mitochondrial respiration and cytosolic ATP levels have been reported but generally only in longer term (>16 hr) endotoxic models (Singer *et al.*, 1999).

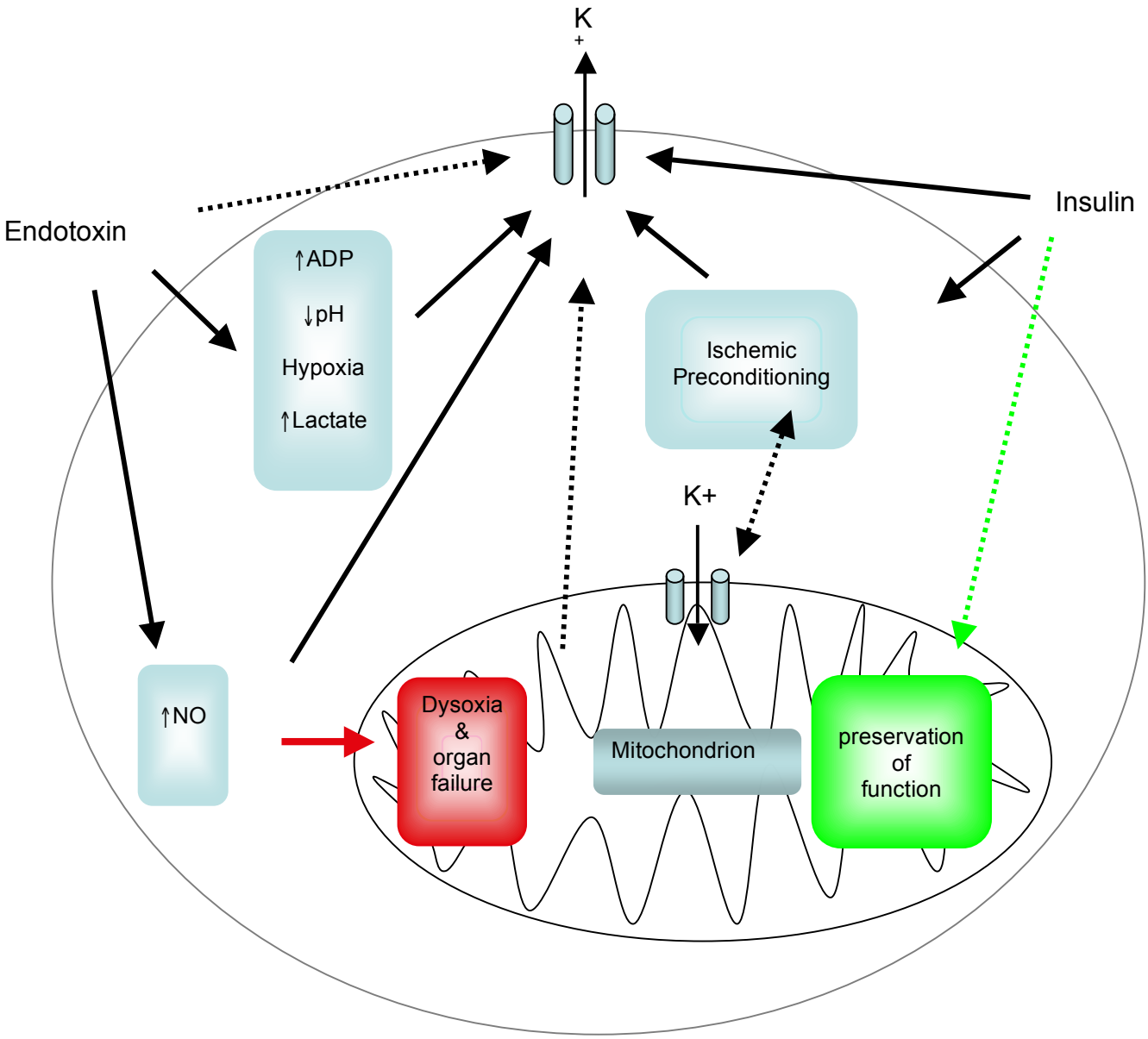

Figure 5.17: Cartoon illustrating a potential mechanism by which endotoxin opens the K_{ATP} channel both in the membrane of cells and in the mitochondrial membrane, thus inducing mitochondrial dysfunction and, potentially, multiorgan failure (Buckley et al., 2006). Conversely, one mechanism by which insulin could exert its beneficial effects in sepsis may be by opening mitochondrial K_{ATP} channels, but when the cell is in a physiologically preserved metabolic state.

Matrix volume is considered to be an important regulator of mitochondrial metabolism (Halestrap, 1994). The main factor determining mitochondrial volume is the balance between K^+ fluxes across the inner membrane and the passage of anions and water. K^+ homeostasis, in turn, is maintained by influx of K^+ through electrochemically driven uniporters and K^+ efflux through the K^+/H^+ exchanger. K_{ATP} channels have also been found in the inner mitochondrial membrane (Inoue *et al.*, 1991) and evidence suggests that these channels regulate mitochondrial K^+ influx (Jaburek *et al.*, 1998; Szewczyk *et al.*, 1996). Observations that glibenclamide and ATP inhibit mitochondrial swelling, whereas potassium channel openers potentiate swelling suggest that K_{ATP} channels play a key role in volume regulation (Holmuhamedov *et al.*, 1998; Szewczyk *et al.*, 1996). Since K_{ATP} channels would open secondary to falling ATP levels and/or increases in nucleotide diphosphates, these channels may well become activated during sepsis. In addition, opening of K^+ channels in mitochondria increases respiration, and slows down the production of ATP by the mitochondria. This and the increased cytosolic cytochrome c are indicators or apoptosis (Holmuhamedov *et al.*, 1998). The potential role that this plays in sepsis is rather more difficult to understand, but may indicate increased apoptosis.

Overproduction of NO appears to contribute to mitochondrial dysfunction; either through direct interaction with components of the electron transfer chain and/or indirectly through K_{ATP} channel activation. It has recently been reported that NO can directly compete with oxygen to inhibit cytochrome *c* oxidase and complex IV activity (Brookes *et al.*, 1999; Brown, 1997). It was postulated that some of these effects might be related to the formation of peroxynitrite, a highly oxidising

metabolite of NO. Furthermore, NO has been shown to cause membrane depolarisation in liver mitochondria, although the mechanism for this remains to be elucidated (Schweizer *et al.*, 1994).

Tight control of glucose levels with insulin infusion has been shown to reduce the mortality of surgical patients from MOF secondary to septic shock (van den *et al.*, 2001), and this may be due to either tighter glycaemic control or the insulin infusion. Insulin plays a key role in cardiomyocyte protection from ischaemia-reperfusion injury (LaDisa *et al.*, 2004); and this acts via several mechanisms, including protein tyrosine kinase, phosphatidylinositol-3- kinase p70s6 kinase, NO pathways (Gao *et al.*, 2002; Jonassen *et al.*, 2001) and via an actin cytoskeleton-dependent mechanism (Shimoni *et al.*, 1999). Conversely, hyperglycaemia has been shown to promote apoptosis via activation of p53 (via O-glycosylation) and p38 MAP-kinases (Fiordaliso *et al.*, 2001). Not only does insulin protect against ischaemia-reperfusion, but it may also be involved in ischaemic preconditioning via K_{ATP} channels activation (Gross *et al.*, 1992) with the mitochondrial K_{ATP} channels playing an important role, via a PKC-dependent pathway (Takashi *et al.*, 1999).

In considering sepsis and ischaemic preconditioning, it may be helpful to firstly consider them as opposite ends of the same spectrum. Ischaemic preconditioning is the promotion of cell survival in a low oxygen state by the prior *opening* of the mitoK_{ATP} channel (Fiordaliso *et al.*, 2001; Gross *et al.*, 1992; Gross *et al.*, 2000; Holmuhamedov *et al.*, 1998; Jonassen *et al.*, 2001; LaDisa *et al.*, 2004; Takashi *et al.*, 1999). Conversely, the beneficial effects of insulin in sepsis may well be

secondary to the *closing* of the mitoK$_{ATP}$ in a high oxygen state (with reduction of apoptosis), albeit due to decreased oxygen utilisation and not to a decrease in oxygen delivery (Boekstegers *et al.*, 1991; Rosser *et al.*, 1996; Singer *et al.*, 1999). It may therefore be interesting to study the phenomenon of ischaemic preconditioning during sepsis. One would postulate that the effect is abolished. However, the beneficial effects of insulin in ischaemic preconditioning are apparently linked to the *opening* of the K$_{ATP}$ channel in cardiac myocytes (LaDisa *et al.*, 2004). This contradicts the hypothesis that insulin *closes* the mitoK$_{ATP}$ in sepsis. Therefore, the alternative is that insulin *opens* the mitoK$_{ATP}$ in sepsis as well as in ischaemic preconditioning, with sepsis also being seen as a "functionally" low oxygen state, with increased glycolysis. This is supported by the normal histological findings of organs taken from patients who died of multiorgan failure secondary to sepsis (Hotchkiss *et al.*, 2003).

Insulin is known to enhance K$_{ATP}$ channel function in both neurons (Spanswick *et al.*, 2000) and rat skeletal muscle (Tricarico *et al.*, 1997), resulting from a decreased sensitivity to ATP (Tricarico *et al.*, 1997). However, unlike the survival of surgical patients with sepsis (van den *et al.*, 2001), the survival of ischaemic myocardium is independent of blood glucose concentration (LaDisa *et al.*, 2004; Jonassen *et al.*, 2001). K$_{ATP}$ channels in the pancreas have been shown to be inhibited by increases in glucose levels that are within the physiological range (Misler *et al.*, 1989).

It is possible that insulin somehow regulates the mitochondrial K$_{ATP}$ channels and thereby maintaining mitochondrial and organ integrity, and preventing the organ

from entering a state of bioenergetic/metabolic shut-down. However, the evidence is conflicting, with some research showing that insulin keeps the K_{ATP} channel open, and that this is associated with increased survival (LaDisa *et al.*, 2004; Tricarico *et al.*, 1997; van den *et al.*, 2001), whilst others show that opening of K_{ATP} channels in mitochondria is associated with apoptosis (Holmuhamedov *et al.*, 1998). The majority of the evidence for preventing cell death is based on studies using cardiomyocytes, whereas promotion of apoptosis comes from other tissues, namely neuronal (Yu *et al.*, 1997) and pancreas. Indeed, the closure of K_{ATP} channels in eosinophils reduces their survival (Bankers-Fulbright *et al.*, 1998); one could postulate that this is a component of a mechanism for down-regulating the inflammatory response in sepsis. One crucial factor in the role of insulin is the timing of its administration, with protection if administered early in ischaemia-reperfusion injury and no effect on infarct size if administered 15 minutes into reperfusion (Jonassen *et al.*, 2001). Further research is needed to examine if the protective effects of insulin reducing multiorgan failure in sepsis are secondary to its effects on the mitochondrial K_{ATP} channels of the organs at risk.

Many of the features of sepsis contribute to its high mortality rate. However, the aetiology of the vascular hyporeactivity that is seen is not yet fully understood. The role of the K_{ATP} channel in vascular hyporeactivity means that the energy state of the cell, tissue and whole organism probably has an important role to play. In keeping with this is the decreased mortality seen in septic shock with the use of insulin the maintenance of blood glucose levels within 4-6 $mmolL^{-1}$ (van den *et al.*, 2001). The role of the K_{ATP} channel in sepsis is unlikely to be limited to the

vasculature and may well also have a fundamental role to play in the function of mitochondria and multi-organ failure.

Chapter Six

Summary

&

Discussion

6.1 Discussion

The most severe manifestation of sepsis-induced cardiovascular dysfunction is septic shock, a condition defined as organ dysfunction/perfusion abnormalities plus hypotension (or a drop in systolic blood pressure >40 mmHg) that has not responded to adequate fluid resuscitation. This results from a combination of excessive vasodilatation, vascular hyporeactivity (i.e. decreased responsiveness to catecholamines) and variable degrees of myocardial depression. Knowledge of the underlying mechanisms of shock will enable a more focused therapeutic strategy.

One such target is the K_{ATP} channel, an ion channel critical in the cardiovascular adaptive response to stress. Pharmacological opening of these channels is already used therapeutically to treat angina pectoris (e.g. nicorandil) while inhibitors (e.g. glyburide) are used in type II diabetes (Seino & Miki, 2003; Rodrigo & Standen, 2005). Excessive activation of the vascular channel is now recognised as a major cause of hypotension and vascular hyporesponsiveness to catecholamines in septic shock (Sorrentino, 1999; Landry, 2001; Warrillow et al., 2006). This has led some researchers to advocate therapeutic blockade of these channels (Warrillow et al., 2006) and this may indeed underlie the mechanism of vasopressin in refractory shock (Barrett et al., 2007). However, outside the vasculature, channel opening may actually represent a protective mechanism against cellular damage (Kaneko, 2005; Otani, 2003).

The aim of my thesis was to examine the role of the K_{ATP} channel in the context of sepsis, with particular reference to the actin cytoskeleton, nitric oxide and the

metabolic state of the tissue. I demonstrated altered K_{ATP} channel pharmacology in both an *in vitro* and *in vivo* model of sepsis, similar to that seen in published *in vitro* models (Sorrentino, 1999; O'Brien, 2001; Wilson & Clapp, 2002). I have demonstrated that it is possible to study the actin cytoskeleton in a semi-quantitative fashion. The development of the method to semi-quantify the actin cytoskeleton in tissue means that other scientists can evaluate and develop their techniques from this. By attempting to solve some of the problems with confocal microscopy of tissue (thickness of tissue sections, immunohistochemistry protocols, image acquisition and analysis protocols) others will either decide that this is an inappropriate technique to answer this question or develop further. The confocal method I finally developed was more reproducible than some of my earlier attempts, with an assessment of a more representative sample. Equally, I developed an objective and reproducible method of image analysis, trying to make it semi-quantifiable. I also developed a novel biochemical technique for the separation of F and G actin in vascular smooth muscle tissue and semi-quantified this using Western blot. I performed measurement of adenine nucleotides in vascular smooth muscle tissue and to my knowledge, this is the first time this has been undertaken.

My data demonstrated that there was not a clear relationship between structure and function in the *in vitro* model of sepsis and that cytoskeletal disruption does not cause the altered pharmacology of the vascular K_{ATP} channel in sepsis. Additionally, a direct effect of nitric oxide on the K_{ATP} channel does not explain the changes observed. Finally, substantial changes in the cellular ATP:ADP:AMP ratio in the tissue does not underlie K_{ATP} channel dysfunction.

6.2 Implications for the vascular biology of sepsis

Confocal microscopy may be the wrong tool with which to quantify the actin cytoskeleton in tissue, partly because of the density and structure of the tissue. Confocal microscopy would be a powerful tool in the assessment of actin stress fibre rearrangement in VSMCs. This could be combined with patch clamp techniques, thereby analysing and correlating the structure and electrophysiology of VSMCs. For instance, one could examine the arrangement of actin, manipulate proteins (e.g. syntaxin 1a) and look at calcium flux and membrane electrophysiology. However, one of the strengths of my methods was that doing microscopy on tissue meant that I was able to utilise a well established method for assessing the function of vascular tissue in sepsis, namely the organ bath assessment of tension. This is clearly the most direct and clinically relevant assessment of vascular tissue. I do believe that Western blotting is a useful technique for assessing the actin cytoskeleton in tissue and I have developed a novel technique for the separation of F and G actin. However, I believe that Western blotting is, at best, a semi-quantifiable technique. If there had been a dramatic (>50 %) change in levels of F actin in vascular smooth muscle in my model of sepsis, I believe that my methods would have picked up such a change.

The inability to replicate altered K_{ATP} channel pharmacology using Deta NO provides important information about the *in vitro* model. It would be interesting to repeat the experiments using L-arginine (Wilson, 2001) or cGMP analogues and inhibitors (Han et al., 2002). Measurement of nitrated proteins in the tissue, in

addition to nitrite, would be very interesting, and would indicate if the NO released by Deta NO had pathological consequences.

The K_{ATP} channel is opened excessively in models of sepsis (Hall et al., 1996; Sorrentino et al., 1999; Chen et al. 2000). However, the actual pharmacology of the channel is also altered, in that it can no longer be closed by inhibitors acting via the SUR, but can be closed by inhibitors acting via the ion channel pore (O'Brien et al., 2005) and the effects of KCOs are potentiated (O'Brien et al., 2001). KCOs increase the open probability of the channel by creating a conformational change in the SUR. This conformational change requires the presence of Mg^{++}ADP being bound to the NBF. Glibenclamide and other sulphonylureas inhibit binding of KCOs to the SUR (Dickinson, 1997; Hambrock, 1998; Loffler-Walz, 1998; Schwanstecher, 1998) by causing a conformational change in the SUR and by preventing binding of Mg^{++}ADP to the NBFs. This then allows the inhibitory effect of ADP on the K_{ir} to tip the balance of the K_{ATP} channel to the closed state (Bryan, 1999). The inhibitory effect of ADP on the K_{ir} requires the presence of the 10 residues on the N-terminus of the K_{ir} 6.2, as the deletion of this eliminates the ability of tolbutamide to exert its inhibitory effect (Bryan, 1999). ATP inhibits the channel by binding to the interface between two Kir subunits within the tetramer, interacting with the C-terminus of one subunit and the N-terminus of another (Antcliff, 2005).

This SUR subunit may well be the region of the K_{ATP} channel affected in sepsis secondary to either nitration (Giannopolou, 2000), nitrosylation (Danne-Dolle, 2000), cytoskeletal disruption (Terzic & Kurachi) or other mechanisms such as

alteration of the Transmembrane Binding Domain (TMD) 1-5 M2 link or the TMD1-5 N-terminus link.

Closure of the K_{ATP} channel in sepsis has been a research and therapeutic goal for over a decade. However, our current understanding of sepsis, shock and MOF suggests that maintenance of microvascular flow and organ perfusion may be critical. Microvascular flow is reduced in patients with sepsis (De Backer et al., 2002). Organ hypoperfusion and subsequent tissue hypoxia may play a role in the development of multiorgan failure (Bateman & Walley, 2005). Microvascular flow recovers rapidly in survivors of sepsis when compared to non-survivors (Bateman & Walley, 2005). Therefore, there may be a role for using therapeutic interventions to open the K_{ATP} channel in sepsis to improve microvascular flow and prevent organ failure. This could be therapeutically achieved by insulin, which opens K_{ATP} channels in the myocardium, preventing damage from ischaemia (LaDisa et al., 2004). In support of this is the finding that the loss of the K_{ATP} channel decreases survival in Kir6.1 knockout mice in an LPS model of sepsis (Kane et al., 2006). This makes it clear that the response that the K_{ATP} channel confers in sepsis has a distinct survival advantage, at least in animals (Kane et al., 2006). The involvement of K_{ATP} channels in the vascular disturbances of sepsis was also questioned in a recent blinded, placebo-controlled study in shocked patients where glyburide had no effect on blood pressure or norepinephrine requirements (Warrillow et al., 2006). This is at odds with historical *in vivo* literature, but probably reflects the failure of SUR inhibitors at standard therapeutic concentrations to block the open channel during periods of metabolic stress, such as sepsis. Therefore, understanding what opens the channel

may well be critical for future progress in critical care patients with sepsis, shock and MOF.

Crucially, I believe the role that insulin plays, as well as the mitochondrial K_{ATP} channel, are fundamental to our future understanding and should be investigated further, to better understand and better target our clinical and therapeutic strategies.

Insulin is known to enhance K_{ATP} channel function in both neurons (Spanswick *et al.*, 2000) and rat skeletal muscle (Tricarico *et al.*, 1997), resulting from a decreased sensitivity to ATP (Tricarico *et al.*, 1997). It is possible that insulin somehow regulates the mitochondrial K_{ATP} channels and thereby maintaining mitochondrial and organ integrity, and preventing the organ from entering a state of bioenergetic/metabolic shut-down. The majority of the evidence for preventing cell death is based on studies using cardiomyocytes, whereas promotion of apoptosis comes from other tissues, namely neuronal (Yu *et al.*, 1997) and pancreas. However, the evidence is conflicting, with some research showing that insulin keeps the K_{ATP} channel open, and that this is associated with increased survival (LaDisa *et al.*, 2004; Tricarico *et al.*, 1997; van den *et al.*, 2001), whilst others show that opening of K_{ATP} channels in mitochondria is associated with apoptosis (Holmuhamedov *et al.*, 1998). Further research is needed to examine if the protective effects of insulin reducing multiorgan failure in sepsis are secondary to its effects on the mitochondrial K_{ATP} channels of the organs at risk. This could be investigated in animal models of sepsis, with *ex vivo* assessment of mitochondrial K_{ATP} channels. Additionally, the timing of insulin may be critical,

with infusions early in sepsis, prior to the development of organ failure being potentially important.

6.3 Summary and Conclusion

Sepsis has a very high mortality rate and yet we still do not have a clear understanding of the pathophysiological processes involved. Vascular hyporeactivity is an important component of sepsis and we are only beginning to gain an understanding of its aetiology. In addition to many other mechanisms, K_{ATP} channels play a fundamental role in vascular hyporeactivity in long-term sepsis. The precise mechanism of their activation has yet to be elucidated. Excessive activation of the K_{ATP} channel is implicated in a number of crucial mechanisms including vascular hyporeactivity, hypotension, insulin resistance and mitochondrial dysfunction. However, as discussed previously, K_{ATP} channel opening may also afford a degree of protection. Realistically, the K_{ATP} channel is only one of the many mechanisms underlying vascular hyporeactivity in sepsis and therefore targeting it therapeutically is unlikely to be the "silver bullet" for septic shock. However, a greater understanding of the pathophysiology underlying its activation can only bring us closer to the day when we can significantly reduce the mortality from sepsis.

6.4 Future Directions

My research would be strengthened by the following experiments:

1. Confocal microscopy to examine the actin cytoskeleton at the single cell level in a tissue-culture model of sepsis.

2. Electrophysiological studies in VSMCs, including examining the role of the syntaxin family of proteins.
3. Repetition of ATP, ADP and AMP measurement in an *in vitro* model of sepsis.
4. Examination of actin cytoskeleton in mesenteric artery to complement my experiments, especially with a validated control, which does not interfere with actin proteins.
5. Examination of the effects of sepsis on the mitochondrial K_{ATP} channel.
6. Further exploration of the NO/cGMP pathway, downstream of NO, and its effects on the K_{ATP} channel in sepsis, including calcineurin, PKC and PKA.
7. Examination of insulin's role in an *in vivo* and *in vitro* model of sepsis, specifically in the organ bath model, to explore the effects on channel pharmacology.
8. Examination of renal, hepatic and cardiac metabolism/ O_2 tension in an *in vivo* model of sepsis, with modulation of K_{ATP} channel pharmacology ± insulin.
9. Specific examination of mitochondrial function in the above experiments (6).
10. Specific examination of 7 and 8 above in a Kir6.1 mouse knockout model.

Bibliography

Aguilar-Bryan, L. and J. Bryan (1999). "Molecular biology of adenosine triphosphate-sensitive potassium channels." **20**(2): 101-135.

Aguilar-Bryan, L., C. G. Nichols, et al. (1995). "Cloning of the beta cell high-affinity sulfonylurea receptor: a regulator of insulin secretion." **268**(5209): 423-426.

Ahluwalia, J., A. Tinker, et al. (2004). "The large-conductance Ca2+-activated K+ channel is essential for innate immunity." Nature **427**(6977): 853-8.

Akira, S. (2003). "Toll-like Receptor Signaling." **278**(40): 38105-38108.

Amann, K. J. and T. D. Pollard (2000). "Cellular regulation of actin network assembly." **10**(20): R728-R730.

Angus, D. C., M. C. Birmingham, et al. (2000). "E5 murine monoclonal antiendotoxin antibody in gram-negative sepsis: a randomized controlled trial. E5 Study Investigators." **283**(13): 1723-1730.

Annane, D., E. Bellissant, et al. (2005). "Septic shock." Lancet **365**(9453): 63-78.

Annane, D., V. Sebille, et al. (2002). "Effect of treatment with low doses of hydrocortisone and fludrocortisone on mortality in patients with septic shock." **288**(7): 862-871.

Antcliff, J. F., S. Haider, et al. (2005). "Functional analysis of a structural model of the ATP-binding site of the KATP channel Kir6.2 subunit." Embo J **24**(2): 229-39.

Arcaroli, J., M. B. Fessler, et al. (2005). "Genetic polymorphisms and sepsis." Shock **24**(4): 300-12.

Ardehali, H. and B. O'Rourke (2005). "Mitochondrial K(ATP) channels in cell

survival and death." J Mol Cell Cardiol **39**(1): 7-16.

Aslan, M., T. M. Ryan, et al. (2003). "Nitric oxide-dependent generation of reactive species in sickle cell disease. Actin tyrosine induces defective cytoskeletal polymerization." **278**(6): 4194-4204.

Barrett, L., M. Singer & L. Clapp. (2007). Vasopressin: Mechanisms of action on the vasculature in health and in septic shock. Crit Care Med **35**(1): 33-40.

Banan, A., J. Z. Fields, et al. (2000). "Nitric oxide and its metabolites mediate ethanol-induced microtubule disruption and intestinal barrier dysfunction." **294**(3): 997-1008.

Bankers-Fulbright et al. (1998). Sulfonylureas inhibit cytokine-induced eosinophil survival and activation. J Immunol **160** (11): 5546-53.

Bateman, R. M. & K. R. Walley (2005). Microvascular resuscitation as a therapeutic goal in severe sepsis. Crit Care **9** (Suppl 4): S27 – 32.

Bellissant, E. and D. Annane (2000). "Effect of hydrocortisone on phenylephrine--mean arterial pressure dose-response relationship in septic shock." **68**(3): 293-303.

Bernard, G. R., J. L. Vincent, et al. (2001). "Efficacy and safety of recombinant human activated protein C for severe sepsis." N Engl J Med **344**(10): 699-709.

Blunck, R., O. Scheel, et al. (2001). "New insights into endotoxin-induced activation of macrophages: involvement of a K+ channel in transmembrane signaling." J Immunol **166**(2): 1009-15.

Bochud, P. Y. and T. Calandra (2003). "Pathogenesis of sepsis: new concepts and implications for future treatment." **326**(7383): 262-266.

Boekstegers, P., S. Weidenhofer, et al. (1991). "Peripheral oxygen availability within

skeletal muscle in sepsis and septic shock: comparison to limited infection and cardiogenic shock." **19**(5): 317-323.

Bone, R. C., C. J. Fisher, Jr., et al. (1989). "Sepsis syndrome: a valid clinical entity. Methylprednisolone Severe Sepsis Study Group." Crit Care Med **17**(5): 389-93.

Boveris, A., S. Alvarez, et al. (2002). "The role of mitochondrial nitric oxide synthase in inflammation and septic shock." Free Radic Biol Med **33**(9): 1186-93.

Brady, P. A., A. E. Alekseev, et al. (1996). "A disrupter of actin microfilaments impairs sulfonylurea-inhibitory gating of cardiac KATP channels." **271**(6 Pt 2): H2710-H2716.

Brayden, J. E. (2002). "Functional roles of KATP channels in vascular smooth muscle." **29**(4): 312-316.

Brealey, D., M. Brand, et al. (2002). "Association between mitochondrial dysfunction and severity and outcome of septic shock." **360**(9328): 219-223.

Brealey, D., S. Karyampudi, et al. (2004). "Mitochondrial dysfunction in a long-term rodent model of sepsis and organ failure." Am J Physiol Regul Integr Comp Physiol **286**(3): R491-7.

Brookes et al. (1999). The assumption that nitric oxide inhibits mitochondrial ATP synthesis is correct. FEBS Lett. **446** (2-3): 261-3.

Brown, G.C (1995). Nitric oxide regulates mitochondrial respiration and cell functions by inhibiting cytochrome oxidase. FEBS Lett. **369** (2-3): 136-9.

Brown, G.C (1997). Nitric oxide inhibition of cytochrome oxidase and mitochondrial respiration: implications for inflammatory, neurodegenerative and ischaemic

pathologies. Mol Cell Biochem. **174**(1-2): 189-92.

Brun-Buisson, C., P. Meshaka, et al. (2004). "EPISEPSIS: a reappraisal of the epidemiology and outcome of severe sepsis in French intensive care units." Intensive Care Med **30**(4): 580-8.

Bryan, J. and L. Aguilar-Bryan (1999). "Sulfonylurea receptors: ABC transporters that regulate ATP-sensitive K(+) channels." **1461**(2): 285-303.

Buckley, J. F., M. Singer, et al. (2006). "Role of KATP channels in sepsis." Cardiovasc Res **72**(2): 220-30.

Cartwright, N., S. K. McMaster, et al. (2007). "Elucidation of toll-like receptor and adapter protein signaling in vascular dysfunction induced by gram-positive Staphylococcus aureus or gram-negative Escherichia coli." Shock **27**(1): 40-7.

Chakravortty, D., N. Koide, et al. (2000). "Cytoskeletal alterations in lipopolysaccharide-induced bovine vascular endothelial cell injury and its prevention by sodium arsenite." **7**(2): 218-225.

Chakravortty, D. and K. S. Nanda Kumar (2000). "Bacterial lipopolysaccharide induces cytoskeletal rearrangement in small intestinal lamina propria fibroblasts: actin assembly is essential for lipopolysaccharide signaling."

1500(1): 125-136.

Chen, S. J., C. C. Wu, et al. (2000). "Abnormal activation of K(+) channels in aortic smooth muscle of rats with endotoxic shock: electrophysiological and functional evidence." **131**(2): 213-222.

Chen, S. J., C. C. Wu, et al. (2000). "Hyperpolarization contributes to vascular hyporeactivity in rats with lipopolysaccharide-induced endotoxic shock."

68(6): 659-668.

Chen, S. J., C. C. Wu, et al. (1999). "Role of nitric oxide and K+-channels in vascular hyporeactivity induced by endotoxin." **359**(6): 493-499.

Chutkow, W. A. et al. (2002). Episodic coronary artery vasospasm and hypertension develop in the absence of Sur2 K(ATP) channels. J Clin Invest. **110** (2): 203-8.

Cipolla, M. J, N. I. Gokina and G. Osol (2002). Pressure-induced actin polymerization in vascular smooth muscle as a mechanism underlying myogenic behavior. FASEB J. **16**(1):72-6.

Clapp, L. H. and A. Tinker (1998). "Potassium channels in the vasculature." **7**(1): 91-98.

Clementi et al (1998). Persistent inhibition of cell respiration by nitric oxide: crucial role of S-nitrosylation of mitochondrial complex I and protective action of glutathione. Proc Natl Acad Sci U S A. **95** (13): 7631-6.

Czaika, G., Y. Gingras, et al. (2000). "Induction of the ATP-sensitive potassium (uK(ATP)-1) channel by endotoxemia." **23**(6): 967-969.

d'Emmanuele di Villa Bianca, R., L. Lippolis, et al. (2003). "Dexamethasone improves vascular hyporeactivity induced by LPS in vivo by modulating ATP-sensitive potassium channels activity." British Journal of Pharmacology **140**(1): 91-96.

Dahl B., F.V. Schiodt et al. (2003). Plasma concentration of Gc-globulin is associated with organ dysfunction and sepsis after injury. Crit Care Med. **31** (1):152-6.

Dalle-Donne, I., A. Milzani, et al. (2000). "S-NO-actin: S-nitrosylation kinetics and the effect on isolated vascular smooth muscle." **21**(2): 171-181.

Danner, R. L., R. J. Elin, et al. (1991). "Endotoxemia in human septic shock." **99**(1): 169-175.

Das, B. and C. Sarkar (2003). "Selective mitochondrial KATP channel activation by nicorandil and 3-pyridyl pinacidil results in antiarrhythmic effect in an anesthetized rabbit model of myocardial ischemia/reperfusion." **25**(2): 97-110.

De Backer et al. (2002). Microvascular blood flow is altered in patients with sepsis. Am J Respir Med Crit Care Med. **166** (1): 98-104.

Dellinger, R.P. et al. (2008). Surviving Sepsis Campaign: international guidelines for management of severe sepsis and septic shock: 2008. Crit Care Med. **36** (1): 296-327.

Dickinson, K. E., C. C. Bryson, et al. (1997). "Nucleotide regulation and characteristics of potassium channel opener binding to skeletal muscle membranes." **52**(3): 473-481.

Eliasson, L., X. Ma, et al. (2003). "SUR1 regulates PKA-independent cAMP-induced granule priming in mouse pancreatic B-cells." **121**(3): 181-197.

Erukhimov, J. A. et al. (2000). Actin-containing sera from patients with adult respiratory distress syndrome are toxic to sheep pulmonary endothelial cells. Am J Respir Crit Care Med. **162** (1): 288-94.

Eskandari, M. K., G. Bolgos, et al. (1992). "Anti-tumor necrosis factor antibody therapy fails to prevent lethality after cecal ligation and puncture or endotoxemia." J Immunol **148**(9): 2724-30.

Evans, T., A. Carpenter et al 1993. Evidence of increased nitric oxide production in patients with the sepsis syndrome. Circ Shock **41**(2): 77-81.

Fall, P. J. and H. M. Szerlip (2005). "Lactic acidosis: from sour milk to septic shock." J Intensive Care Med **20**(5): 255-71.

Fiordaliso, F., A. Leri et al. (2001). Hyperglycemia activates p53 and p53-regulated genes leading to myocyte cell death. Diabetes **50**(10): 2363-75.

Frost, M. T., Q. Wang, et al. (2005). "Hypoxia accelerates nitric oxide-dependent inhibition of mitochondrial complex I in activated macrophages." Am J Physiol Regul Integr Comp Physiol **288**(2): R394-400.

Fujita, A. and Y. Kurachi (2000). "Molecular aspects of ATP-sensitive K+ channels in the cardiovascular system and K+ channel openers." **85**(1): 39-53.

Gao, F., E. Gao et al. (2002). Nitric oxide mediates the antiapoptotic effect of insulin in myocardial ischemia-reperfusion: the roles of PI3-kinase, Akt, and endothelial nitric oxide synthase phosphorylation. Circulation **105**(12): 1497-502.

Garland, J. G. and G. A. McPherson (1992). "Evidence that nitric oxide does not mediate the hyperpolarization and relaxation to acetylcholine in the rat small mesenteric artery." Br J Pharmacol **105**(2): 429-35.

Garvey, E., Oplinger, J., Furfine, E et al. (1997). 1400W is a slow, Tight Binding, and Highly selective Inhibitor of Inducible Nitric-oxide Synthase *in Vitro* and *in Vivo*. J Biol Chem **272(8):** 4959-4963.

Gerard, C., C. Bruyns, et al. (1993). "Interleukin 10 reduces the release of tumor necrosis factor and prevents lethality in experimental endotoxemia." J Exp Med **177**(2): 547-50.

Giannopoulou, E., P. Katsoris et al. (2002). Nitration of cytoskeletal proteins in the chicken embryo chorioallantoic membrane. Arch Biochem Biophys **400**(2): 188-

98.

Gokina, N. I. and G. Osol (2002). "Actin cytoskeletal modulation of pressure-induced depolarization and Ca(2+) influx in cerebral arteries." **282**(4): H1410-H1420.

Goldblum, S. E., X. Ding, et al. (1993). "Bacterial lipopolysaccharide induces actin reorganization, intercellular gap formation, and endothelial barrier dysfunction in pulmonary vascular endothelial cells: concurrent F-actin depolymerization and new actin synthesis." **157**(1): 13-23.

Gribble, F. M., S. J. Tucker, et al. (1997). "The essential role of the Walker A motifs of SUR1 in K-ATP channel activation by Mg-ADP and diazoxide." **16**(6): 1145-1152.

Griffin, E. C., N. Aiyar, et al. (1992). "Effect of endotoxicosis on plasma and tissue levels of calcitonin gene-related peptide." **38**(1): 50-54.

Griffiths, C and J. Garthwaite (2001). The shaping of nitric oxide signals by a cellular sink. J Physiol. **536**(Pt 3): 855-62.

Gross, G. J. and J. A. Auchampach (1992). Blockade of ATP-sensitive potassium channels prevents myocardial preconditioning in dogs. Circ Res. **70**(2): 223-33.

Halestrap A. P (1994). Regulation of mitochondrial metabolism through changes in matrix volume. Biochem Soc Trans. **22** (2):522-9.

Hall, S., S. Turcato, et al. (1996). "Abnormal activation of K+ channels underlies relaxation to bacterial lipopolysaccharide in rat aorta." **224**(1): 184-190.

Hambrock, A., C. Loffler-Walz, et al. (1998). "Mg2+ and ATP dependence of K(ATP) channel modulator binding to the recombinant sulphonylurea receptor, SUR2B." British Journal of Pharmacology **125**(3): 577-583.

Hanley, P. J. and J. Daut (2005). "K(ATP) channels and preconditioning: a re-

examination of the role of mitochondrial K(ATP) channels and an overview of alternative mechanisms." J Mol Cell Cardiol **39**(1): 17-50.

Hart, D. W., D. L. Chinkes, et al. (2003). "Increased tissue oxygen extraction and acidosis with progressive severity of sepsis." J Surg Res **112**(1): 49-58.

Haslberger, A., C. Romanin, et al. (1992). "Membrane potential modulates release of tumor necrosis factor in lipopolysaccharide-stimulated mouse macrophages." Mol Biol Cell **3**(4): 451-60.

Hayabuchi, Y., N. W. Davies, et al. (2001). "Angiotensin II inhibits rat arterial KATP channels by inhibiting steady-state protein kinase A activity and activating protein kinase Ce." **530**(Pt 2): 193-205.

Hernanz et al. (2004). Relationship between circulating levels of calcitonin gene-related peptide, nitric oxide metabolites and hemodynamic changes in human septic shock. Regul Pept. **65**(2): 115-21.

Holmuhamedov et al (1998). Mitochondrial ATP-sensitive K+ channels modulate cardiac mitochondrial function. Am J Physiol. **275**(5 Pt 2): H1567-76.

Hotchkiss, R. S. and I. E. Karl (2003). "The pathophysiology and treatment of sepsis." **348**(2): 138-150.

Hotchkiss, R. S., I. E. Karl, et al. (1992). "Inhibition of NO synthesis in septic shock." **339**(8790): 434-435.

Humphrey, S. J., M. P. Smith, et al. (1996). "Cardiovascular effects of the K-ATP channel blocker U-37883A and structurally related morpholinoguanidines." Methods Find Exp Clin Pharmacol **18**(4): 247-60.

Huttemeier, P. C., E. F. Ritter, et al. (1993). "Calcitonin gene-related peptide mediates hypotension and tachycardia in endotoxic rats." **265**(2 Pt 2): H767-H769.

Inagaki, N., T. Gonoi, et al. (1996). "A family of sulfonylurea receptors determines the pharmacological properties of ATP-sensitive K+ channels." **16**(5): 1011-1017.

Inagaki, N., T. Gonoi, et al. (1995). "Reconstitution of IKATP: an inward rectifier subunit plus the sulfonylurea receptor." Science **270**(5239): 1166-70.

Inagaki, N., J. Inazawa, et al. (1995). "cDNA sequence, gene structure, and chromosomal localization of the human ATP-sensitive potassium channel, uKATP-1, gene (KCNJ8)." Genomics **30**(1): 102-4.

Inagaki, N., Y. Tsuura, et al. (1995). "Cloning and functional characterization of a novel ATP-sensitive potassium channel ubiquitously expressed in rat tissues, including pancreatic islets, pituitary, skeletal muscle, and heart." **270**(11): 5691-5694.

Inoue, M et al (1991). An ATP-driven Cl- pump regulates Cl- concentrations in rat hippocampal neurons. Neurosci Lett. **134** (1): 75-8.

Isomoto, S., C. Kondo, et al. (1996). "A novel sulfonylurea receptor forms with BIR (Kir6.2) a smooth muscle type ATP-sensitive K+ channel." **271**(40): 24321-24324.

Jaburek, M. et al. (1998). State-dependent inhibition of the mitochondrial KATP channel by glyburide and 5-hydroxydecanoate. J Biol Chem. **273**(22): 13578-82.

Janmey, P. A. (1998). "The cytoskeleton and cell signaling: component localization and mechanical coupling." **78**(3): 763-781.

Jonassen, A. K. et al. (2001). Myocardial protection by insulin at reperfusion requires early administration and is mediated via Akt and p70s6 kinase cell-survival

signaling. Circ Res. **89**(12): 1191-8.

Julou-Schaeffer, G., G. A. Gray, et al. (1990). "Loss of vascular responsiveness induced by endotoxin involves L-arginine pathway." **259**(4 Pt 2): H1038-H1043.

Kane, G. C. et al. (2006). Gene knockout of the KCNJ8-encoded Kir6.1 K(ATP) channel imparts fatal susceptibility to endotoxemia. FASEB J. **20**(13): 2271-80.

Kaneko, T., K. Yokoyama, et al. (2005). "Late preconditioning with isoflurane in cultured rat cortical neurones." Br J Anaesth **95**(5): 662-8.

Kantrow, S. P., D. E. Taylor, et al. (1997). "Oxidative metabolism in rat hepatocytes and mitochondria during sepsis." **345**(2): 278-288.

Kobayashi, Y., M. Honda, et al. (1998). "Immunohistological study in sixteen children with acute tubulointerstitial nephritis." Clin Nephrol **50**(1): 14-20.

LaDisa, J. F., Jr., J. G. Krolikowski, et al. (2004). "Cardioprotection by glucose-insulin-potassium: dependence on KATP channel opening and blood glucose concentration before ischemia." **287**(2): H601-H607.

Landry, D. W., H. R. Levin, et al. (1997). "Vasopressin deficiency contributes to the vasodilation of septic shock." **95**(5): 1122-1125.

Landry, D. W. and J. A. Oliver (1992). "The ATP-sensitive K+ channel mediates hypotension in endotoxemia and hypoxic lactic acidosis in dog." **89**(6): 2071-2074.

Landry, D. W. and J. A. Oliver (2001). "The pathogenesis of vasodilatory shock." **345**(8): 588-595.

Lee, P. S., A. B. Waxman et al. (2007). Plasma gelsolin is a marker and therapeutic

agent in animal sepsis. Crit Care Med. **35**(3): 849-55.

Leturcq, D. J., A. M. Moriarty, et al. (1996). "Antibodies against CD14 protect primates from endotoxin-induced shock." **98**(7): 1533-1538.

Levi, M., H. ten Cate, et al. (1993). "Pathogenesis of disseminated intravascular coagulation in sepsis." Jama **270**(8): 975-9.

Liu, S. F. and A. B. Malik (2006). "NF-{kappa}B activation as a pathological mechanism of septic shock and inflammation." Am J Physiol Lung Cell Mol Physiol %R 10.1152/ajplung.00477.2005 **290**(4): L622-645.

Loffler-Walz, C. and U. Quast (1998). "Disruption of the actin cytoskeleton abolishes high affinity 3H-glibenclamide binding in rat aortic rings." **357**(2): 183-185.

Lowry, M. A., J. I. Goldberg, et al. (1998). "Induction of nitric oxide (NO) synthesis in murine macrophages requires potassium channel activity." Clin Exp Immunol **111**(3): 597-603.

Matsuo, M. et al. (2005). KATP channel interaction with adenine nucleotides. J Mol Cell Cardiol. **38**(6): 907-16.

McKenna, T. M. (1990). "Prolonged exposure of rat aorta to low levels of endotoxin in vitro results in impaired contractility. Association with vascular cytokine release." **86**(1): 160-168.

Messaris, E (2007). Actin-binding plasma gelsolin: a potential future ally in the fight against sepsis. Crit Care Med. **35** (3): 970-1.

Miki, T., M. Suzuki et al. (2002). Mouse model of Prinzmetal angina by disruption of the inward rectifier Kir6.1. Nat Med. **8**(5): 466-72.

Miki, T. and S. Seino (2005). "Roles of KATP channels as metabolic sensors in acute metabolic changes." J Mol Cell Cardiol **38**(6): 917-25.

Mirshamsi, S., H. A. Laidlaw, et al. (2005). "Activation of hypothalamic ATP-sensitive K+ channels by the aminoguanidine carboxylate BVT.12777." J Neuroendocrinol **17**(4): 246-54.

Misler, S. et al. (1989). Metabolite-regulated ATP-sensitive K+ channel in human pancreatic islet cells. Diabetes. **38** (4): 422-7.

Mistry, D. K. and C. J. Garland (1998). "Nitric oxide (NO)-induced activation of large conductance Ca2+-dependent K+ channels (BK(Ca)) in smooth muscle cells isolated from the rat mesenteric artery." **124**(6): 1131-1140.

Miyoshi, H. and Y. Nakaya (1994). "Endotoxin-induced nonendothelial nitric oxide activates the Ca(2+)-activated K+ channel in cultured vascular smooth muscle cells." **26**(11): 1487-1495.

Miyoshi, H., Y. Nakaya, et al. (1994). "Nonendothelial-derived nitric oxide activates the ATP-sensitive K+ channel of vascular smooth muscle cells." **345**(1): 47- 49.

Miyoshi, Y. and Y. Nakaya (1991). "Angiotensin II blocks ATP-sensitive K+ channels in porcine coronary artery smooth muscle cells." **181**(2): 700-706.

Miyoshi, Y., Y. Nakaya, et al. (1992). "Endothelin blocks ATP-sensitive K+ channels and depolarizes smooth muscle cells of porcine coronary artery." **70**(3): 612-616.

Mounzer, K. C., M. Moncure (1999). Relationship of admission plasma gelsolin levels to clinical outcomes in patients after major trauma. Am J Respir Crit Care Med. **160** (5 Pt 1): 1673-81.

Muller, M., O. Scheel, et al. (2003). "The role of membrane-bound LBP, endotoxin aggregates, and the MaxiK channel in LPS-induced cell activation." J Endotoxin Res **9**(3): 181-6.

Nameda, Y., H. Miyoshi, et al. (1996). "Endotoxin-induced L-arginine pathway produces nitric oxide and modulates the Ca2+-activated K+ channel in cultured human dermal papilla cells." J Invest Dermatol **106**(2): 342-5.

Nelson, M. T., Y. Huang, et al. (1990). "Arterial dilations in response to calcitonin gene-related peptide involve activation of K+ channels." **344**(6268): 770-773.

Nelson, M. T. and J. M. Quayle (1995). "Physiological roles and properties of potassium channels in arterial smooth muscle." **268**(4 Pt 1): C799-C822.

Nevins, A. K., D. C. Thurmond (2003). "Glucose regulates the cortical actin network through modulation of Cdc42 cycling to stimulate insulin secretion." **285**(3): C698-C710.

Noma, A. (1983). "ATP-regulated K+ channels in cardiac muscle." **305**(5930): 147-148.

Numaguchi, K., S. Eguchi, et al. (1999). "Mechanotransduction of rat aortic vascular smooth muscle cells requires RhoA and intact actin filaments." **85**(1): 5-11.

O'Brien, A. J., G. Thakur, et al. (2005). "The pore-forming subunit of the K(ATP) channel is an important molecular target for LPS-induced vascular hyporeactivity in vitro." Br J Pharmacol **144**(3): 367-75.

O'Brien, A. J., A. J. Wilson, et al. (2001). "Temporal variation in endotoxin-induced vascular hyporeactivity in a rat mesenteric artery organ culture model." **133**(3): 351-360.

Ochoa, J. B., A. O. Udekwu, et al. (1991). "Nitrogen oxide levels in patients after trauma and during sepsis." **214**(5): 621-626.

Oettinger, W., D. Berger, et al. (1987). "The clinical significance of prostaglandins and

thromboxane as mediators of septic shock." **65**(2): 61-68.

Ohashi, M., F. Faraci, et al. (2005). "Peroxynitrite hyperpolarizes smooth muscle and relaxes internal carotid artery in rabbit via ATP-sensitive K+ channels." Am J Physiol Heart Circ Physiol **289**(5): H2244-50.

Otani, H., T. Okada, et al. (2003). "Combined pharmacological preconditioning with a G-protein-coupled receptor agonist, a mitochondrial KATP channel opener and a nitric oxide donor mimics ischaemic preconditioning." **30**(9): 684-693.

Padkin, A., C. Goldfrad, et al. (2003). "Epidemiology of severe sepsis occurring in the first 24 hrs in intensive care units in England, Wales, and Northern Ireland." Crit Care Med **31**(9): 2332-8.

Peck, J. W., M. Oberst, et al. (2002). "The RhoA-binding protein, rhophilin-2, regulates actin cytoskeleton organization." **277**(46): 43924-43932.

Petrak, R. A., R. A. Balk, et al. (1989). "Prostaglandins, cyclo-oxygenase inhibitors, and thromboxane synthetase inhibitors in the pathogenesis of multiple systems organ failure." **5**(2): 303-314.

Petros, A., D. Bennett, et al. (1991). "Effect of nitric oxide synthase inhibitors on hypotension in patients with septic shock." **338**(8782-8783): 1557-1558.

Petros, A., G. Lamb, et al. (1994). "Effects of a nitric oxide synthase inhibitor in humans with septic shock." **28**(1): 34-39.

Pollack, M. M. et al. (1985). Distributions of cardiopulmonary variables in pediatric survivors and nonsurvivors of septic shock. Crit Care Med. **13** (6): 454-9.

Quayle, J. M., A. D. Bonev, et al. (1994). "Calcitonin gene-related peptide activated ATP-sensitive K+ currents in rabbit arterial smooth muscle via protein kinase

A." **475**(1): 9-13.

Quayle, J. M., M. T. Nelson, et al. (1997). "ATP-sensitive and inwardly rectifying potassium channels in smooth muscle." **77**(4): 1165-1232.

Quinn et al. (2003). Do anionic phospholipids serve as cofactors or second messengers for the regulation of activity of cloned ATP-sensitive K+ channels? Circ Res. **93**(7): 646-55.

Quinn et al. (2004). Multisite phosphorylation mechanism for protein kinase A activation of the smooth muscle ATP-sensitive K+ channel. Circ Res. **94**(10): 1359-66.

Rees, D. D., J. E. Monkhouse et al. (1998). Nitric oxide and the haemodynamic profile of endotoxin shock in the conscious mouse. Br J Pharmacol. **124**(3): 540-6.

Reddy, R. C., G. H. Chen, et al. (2001). "Selective inhibition of COX-2 improves early survival in murine endotoxemia but not in bacterial peritonitis." **281**(3): L537-L543.

Revelly, J. P., L. Tappy, et al. (2005). "Lactate and glucose metabolism in severe sepsis and cardiogenic shock." Crit Care Med **33**(10): 2235-40.

Rodrigo, G. C. and N. B. Standen (2005). "ATP-sensitive potassium channels." Curr Pharm Des **11**(15): 1915-40.

Rosser, D. M., R. P. Stidwill, et al. (1996). "Cardiorespiratory and tissue oxygen dose response to rat endotoxemia." **271**(3 Pt 2): H891-H895.

Russell, J. A., K. R. Walley, et al. (2008). "Vasopressin versus norepinephrine infusion in patients with septic shock." N Engl J Med **358**(9): 877-87.

Saidi, R.F., K. Jaeger et al. (1997). Bacteroides fragilis toxin rearranges the actin

cytoskeleton of HT29/C1 cells without direct proteolysis of actin or decrease in F-actin content. Cell Motil Cytoskeleton. **37**(2): 159-65.

Salzman, A. L., A. Vromen, et al. (1997). "K(ATP)-channel inhibition improves hemodynamics and cellular energetics in hemorrhagic shock." Am J Physiol **272**(2 Pt 2): H688-94.

Sandau, K. B., F. Gantner, et al. (2001). "Nitric oxide-induced F-actin disassembly is mediated via cGMP, cAMP, and protein kinase A activation in rat mesangial cells." **271**(2): 329-336.

Sasu, S., D. LaVerda, et al. (2001). "Chlamydia pneumoniae and chlamydial heat shock protein 60 stimulate proliferation of human vascular smooth muscle cells via toll-like receptor 4 and p44/p42 mitogen-activated protein kinase activation." **89**(3): 244-250.

Shimoni, Y., H. S. Ewart, D. Severson (1999). Insulin stimulation of rat ventricular K+ currents depends on the integrity of the cytoskeleton. J Physiol. **1**;514(Pt 3): 735-45.

Schneider, F., C. Schott, et al. (1992). "L-arginine induces relaxation of small mesenteric arteries from endotoxin-treated rats." **211**(2): 269-272.

Schwanstecher, M., C. Sieverding, et al. (1998). "Potassium channel openers require ATP to bind to and act through sulfonylurea receptors." **17**(19): 5529-5535.

Schweizer, M., C. Richter et al. (1994). Nitric oxide potently and reversibly deenergizes mitochondria at low oxygen tension. Biochem Biophys Res Commun. **204**(1): 169-75.

Schwiebert, E. M., J. W. Mills, et al. (1994). "Actin-based cytoskeleton regulates a

chloride channel and cell volume in a renal cortical collecting duct cell line." **269**(10): 7081-7089.

Seino, S. and T. Miki (2003). "Physiological and pathophysiological roles of ATP-sensitive K+ channels." Prog Biophys Mol Biol **81**(2): 133-76.

Shelley, O., T. Murphy, et al. (2003). "Interaction between the innate and adaptive immune systems is required to survive sepsis and control inflammation after injury." Shock **20**(2): 123-9.

Shi, N. Q., B. Ye, et al. (2005). "Function and distribution of the SUR isoforms and splice variants." J Mol Cell Cardiol **39**(1): 51-60.

Shieh, C. C., M. Coghlan, et al. (2000). "Potassium channels: molecular defects, diseases, and therapeutic opportunities." Pharmacol Rev **52**(4): 557-94.

Shinbo, A. and T. Iijima (1997). "Potentiation by nitric oxide of the ATP-sensitive K+ current induced by K+ channel openers in guinea-pig ventricular cells." British Journal of Pharmacology **120**(8): 1568-1574.

Shyng, S., T. Ferrigni, et al. (1997). "Regulation of KATP channel activity by diazoxide and MgADP. Distinct functions of the two nucleotide binding folds of the sulfonylurea receptor." **110**(6): 643-654.

Shyng, S. and C. G. Nichols (1997). "Octameric stoichiometry of the KATP channel complex." **110**(6): 655-664.

Singer, M. and D. Brealey (1999). "Mitochondrial dysfunction in sepsis." **66**: 149-166.

Singer, M., F. Coluzzi, et al. (2005). "Reversal of life-threatening, drug-related potassium-channel syndrome by glibenclamide." Lancet **365**(9474): 1873-5.

Sommer, D., S. Coleman, et al. (2002). "Differential susceptibilities of serine/threonine phosphatases to oxidative and nitrosative stress." Arch Biochem Biophys **404**(2): 271-8.

Sorrentino, R., d. d'Emmanuele, V, et al. (1999). "Involvement of ATP-sensitive potassium channels in a model of a delayed vascular hyporeactivity induced by lipopolysaccharide in rats." **127**(6): 1447-1453.

Sprung, C. L., D. Annane et al. (2008). Hydrocortisone therapy for patients with septic shock. N Engl J Med. **358** (2): 111-24.

Strege, P. R., A. N. Holm, et al. (2003). "Cytoskeletal modulation of sodium current in human jejunal circular smooth muscle cells." **284**(1): C60-C66.

Szewczyk, A., A. Czyz et al. (1996). ATP-regulated K+ channel in mitochondria: pharmacology and function. J Bioenerg Biomembr. **28** (2): 147-52.

Takakuwa, T., S. Endo, et al. (1994). "PAF acetylhydrolase and arachidonic acid metabolite levels in patients with sepsis." **84**(3): 283-290.

Takashi, E., Y. Wang, Ahsraf, M. (1999). Activation of mitochondrial K(ATP) channel elicits late preconditioning against myocardial infarction via protein kinase C signaling pathway. Circ Res. **85**(12):1146-53.

Terzic, A. and Y. Kurachi (1996). "Actin microfilament disrupters enhance K(ATP) channel opening in patches from guinea-pig cardiomyocytes." **492 (Pt 2)**: 395-404.

Thiemermann, C. (1994). "The role of the L-arginine: nitric oxide pathway in circulatory shock." **28**: 45-79.

Thiemermann, C. (1997). "Nitric oxide and septic shock." **29**(2): 159-166.

Thiemermann, C. and J. Vane (1990). "Inhibition of nitric oxide synthesis reduces the hypotension induced by bacterial lipopolysaccharides in the rat in vivo." **182**(3): 591-595.

Thierfelder, S., B. Doepner, et al. (1994). "ATP-sensitive K+ channels in heart muscle cells first open and subsequently close at maintained anoxia." FEBS Lett **351**(3): 365-9.

Tracey, K. J., B. Beutler, et al. (1986). "Shock and tissue injury induced by recombinant human cachectin." Science **234**(4775): 470-4.

Tricarico, D., R. Mallamaci, et al. (1997). "Modulation of ATP-sensitive K+ channel by insulin in rat skeletal muscle fibers." **232**(2): 536-539.

Tsiotou, A. G., G. H. Sakorafas, et al. (2005). "Septic shock; current pathogenetic concepts from a clinical perspective." Med Sci Monit **11**(3): RA76-85.

Tsuchiya, M., K. Tsuchiya, et al. (2002). "Vasopressin inhibits sarcolemmal ATP-sensitive K+ channels via V1 receptors activation in the guinea pig heart." Circ J **66**(3): 277-82.

Tsuneyoshi, I., Y. Kanmura, et al. (1996). "Lipoteichoic acid from Staphylococcus aureus depresses contractile function of human arteries in vitro due to the induction of nitric oxide synthase." **82**(5): 948-953.

Tsuura, Y et al. (1994). Nitric oxide opens ATP-sensitive K+ channels through suppression of phosphofructokinase activity and inhibits glucose-induced insulin release in pancreatic beta cells. J Gen Physiol. **104** (6): 1079-98.

Tucker, S. J., F. M. Gribble, et al. (1997). "Truncation of Kir6.2 produces ATP-sensitive K+ channels in the absence of the sulphonylurea receptor." **387**(6629):

179-183.

Tunctan, B., S. Altug, et al. (2003). "Effects of cyclooxygenase inhibitors on nitric oxide production and survival in a mice model of sepsis." **48**(1): 37-48.

Vallance, P. and N. Chan (2001). "Endothelial function and nitric oxide: clinical relevance." Heart **85**(3): 342-50.

VanderMeer, T. J., H. Wang, et al. (1995). "Endotoxemia causes ileal mucosal acidosis in the absence of mucosal hypoxia in a normodynamic porcine model of septic shock." Crit Care Med **23**(7): 1217-26.

Vanelli, G., S. N. Hussain, et al. (1995). "Glibenclamide, a blocker of ATP-sensitive potassium channels, reverses endotoxin-induced hypotension in pig." **80**(1): 167-170.

Wakatsuki, T., Y. Nakaya, et al. (1992). "Vasopressin modulates K(+)-channel activities of cultured smooth muscle cells from porcine coronary artery." **263**(2 Pt 2): H491-H496.

Warrillow, S., M. Egi and R. Bellomo (2006). Randomized, double-blind, placebo-controlled crossover pilot study of a potassium channel blocker in patients with septic shock. Crit Care Med. **34**(4):980-5.

Wang J. E., M. K. Dahle et al. 2003. Peptidoglycan and lipoteichoic acid in gram-positive bacterial sepsis: receptors, signal transduction, biological effects, and synergism. Shock. **20**(5):402-14.

Wei, E. P., H. A. Kontos, et al. (1998). "Antioxidants inhibit ATP-sensitive potassium

channels in cerebral arterioles." Stroke **29**(4): 817-22; discussion 823.

Wilson, A. J. and L. H. Clapp (2002). "The molecular site of action of K(ATP) channel inhibitors determines their ability to inhibit iNOS-mediated relaxation in rat aorta." **56**(1): 154-163.

Wilson, A. J., R. I. Jabr, et al. (2000). "Calcium modulation of vascular smooth muscle ATP-sensitive K(+) channels: role of protein phosphatase-2B." **87**(11): 1019-1025.

Wu, C. C., S. J. Chen, et al. (2004). "NO and KATP channels underlie endotoxin-induced smooth muscle hyperpolarization in rat mesenteric resistance arteries." **142**(3): 479-484.

Wu, C. C., M. H. Liao, et al. (1999). "Tetramethylpyradizine prevents inducible NO synthase expression and improves survival in rodent models of endotoxic shock." **360**(4): 435-444.

Wu, C. C., C. Thiemermann, et al. (1995). "Glibenclamide-induced inhibition of the expression of inducible nitric oxide synthase in cultured macrophages and in the anaesthetized rat." **114**(6): 1273-1281.

Yamada, M., S. Isomoto, et al. (1997). "Sulphonylurea receptor 2B and Kir6.1 form a sulphonylurea-sensitive but ATP-insensitive K+ channel." **499 (Pt 3)**: 715- 720.

Yaqub, S., V. Solhaug, et al. (2003). "A human whole blood model of LPS-mediated suppression of T cell activation." **9**(3): BR120-BR126.

Yen, M. H., S. J. Chen, et al. (1995). "Comparison of responses to aminoguanidine and N omega-nitro-L-arginine methyl ester in the rat aorta." **22**(9): 641-645.

Yokoshiki, H., Y. Katsube, et al. (1997). "Disruption of actin cytoskeleton attenuates sulfonylurea inhibition of cardiac ATP-sensitive K+ channels." **434**(2): 203-

205.

Yu S. P., C. H. Yeh et al. (1997). Mediation of neuronal apoptosis by enhancement of outward potassium current. Science **278**(5335):114-7.